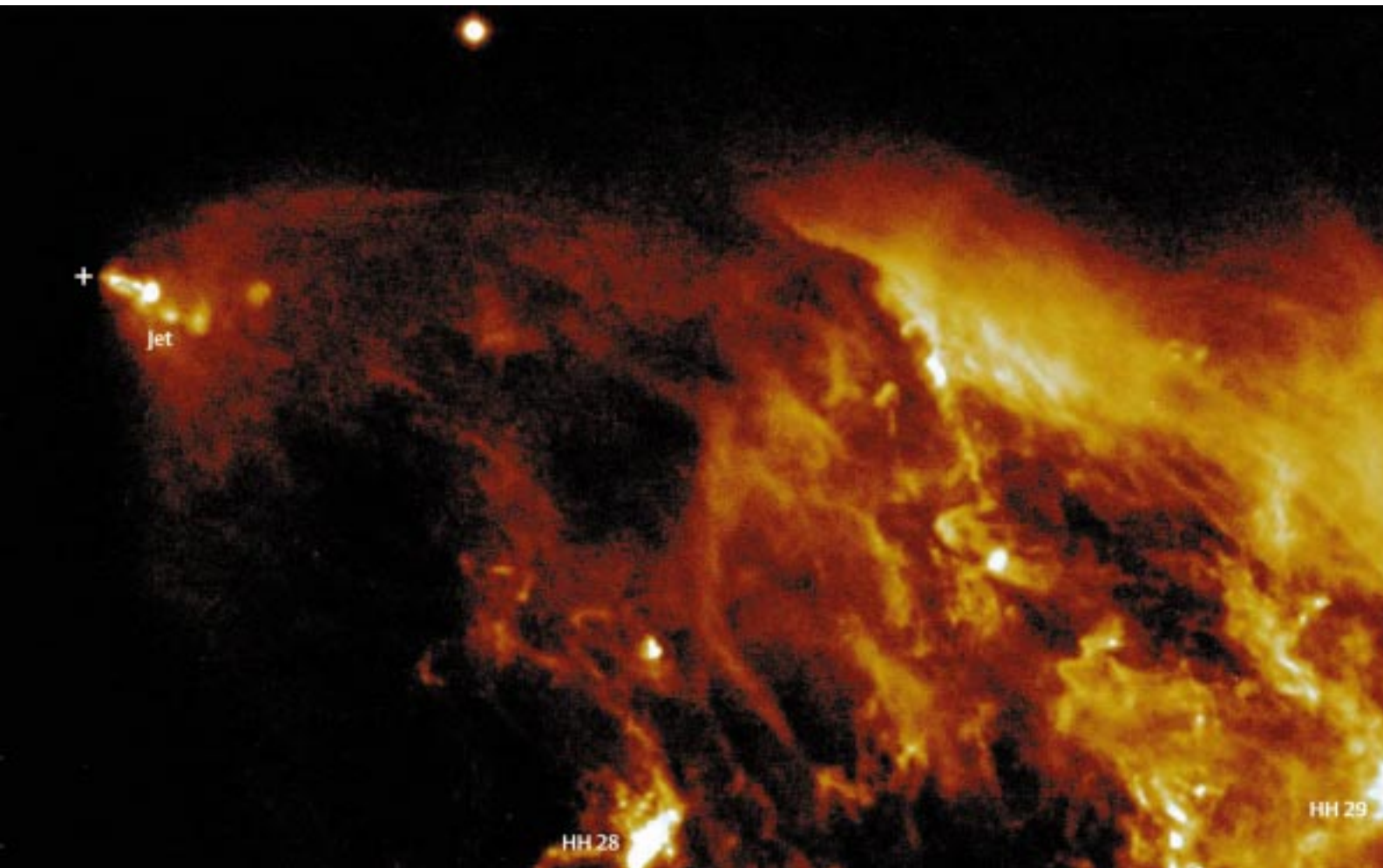# Max-Planck-Institut für Astronomie

Heidelberg-Königstuhl

Annual Report 1997

Cover Picture:
A newborn star (cross), deeply embedded into the dusty molecular cloud out of which it was born. It is not visible in the optical range, but can be observed only in the infrared light. It emits a bright, ionized gaseous jet in polar direction, illuminates an extended reflection nebulosity, and excites the line emission of the Herbig-Haro objects HH 28 and HH 29. See page 23–29.

Max-Planck-Institut für Astronomie

Heidelberg-Königstuhl

Annual Report 1997

Max-Planck-Institut für Astronomie/Max Planck Institute of Astronomy

Managing Directors:
Prof. Dr. Steven Beckwith (until 31.8.1998), Prof. Dr. Immo Appenzeller (since 1.8.1998 onwards)

Academic Members, Governing Body, Directors:
Prof. Dr. Immo Appenzeller (from 1.8.1998 onwards, temporary),
Prof. Dr. Steven Beckwith, (on sabbatical leave from 1.9.1998 onwards),
Prof. Dr. Hans Elsässer (until 31.3.1997),
Prof. Dr. Hans-Walter Rix (from 1.1.1999 onwards).

Scientific Oversight Committee:
Prof. R. Bender, München; Prof. R.-J. Dettmar, Bochum; Prof. G. Hasinger, Potsdam; Prof. P. Léna, Meudon; Prof. M. Moles Villlamate, Madrid, Prof. F. Pacini, Firenze; Prof. K.-H. Schmidt, Potsdam; Prof. P.A. Strittmatter, Tuscon; Prof. S.D.M. White, Garching; Prof. L. Woltjer, St. Michel Obs.

The MPIA currently has a staff of approximately 160, including 43 scientists 37 junior and visiting scientists, together with 80 technical and administrative staff. Students of the Faculty of Physics and Astronomy of the University of Heidelberg work on dissertations at degree and doctorate level in the Institute. Apprentices are constantly undergoing training in the Institute's workshop.

Address: MPI für Astronomie, Königstuhl 17, D-69117 Heidelberg
Telefon: 0049-6221-5280, Fax: 0049-6221-528246
E-mail: Name@mpia-hd.mpg.de, Anonymous ftp: ftp.mpia-hd.mpg.de
Homepage: http://www.mpia-hd.mpg.de
Isophot Datacenter : phthelp@mpia-hd.mpg.de

Calar-Alto-Observatorium
Address: Centro Astronomico Hispano Aleman,
Calle Jesus Durbán Remón 2/2,   E-04004 Almería, Spanien
Telefon: 0034-50-230988, -632500, Fax: 0034-50-632504,
E-mail: Name@caha.es

I   Contents

I General

The MPIA's Research Goals – Yesterday, Today and Tomorrow

In 1967, the Senate of the Max-Planck-Gesellschaft/ Max Planck Society decided to establish the Max-Planck-Institut für Astronomie/Max Planck Institute of Astronomy in Heidelberg with the aim of restoring astronomical research in Germany to a leading global position after the major setbacks it had suffered due to two World Wars. Two years later, the Institute commenced its work in temporary accommodation on the Königstuhl, under the direction of Hans Elsässer. The Institute moved into its new building in 1975 (Figure I.1). A long-term goal which was passed on to the newly established MPIA was to build up and operate two high-performance observatories, one in the northern hemisphere and one in the southern hemisphere. In 1970, after an intensive search for a location, the choice for the northern hemisphere was made in favour of Calar Alto mountain (height: 2168 metres) in the province of Almería, southern Spain. This European location offers good climatic and meteorological conditions for astronomical observations. 1972 saw the establishment of the »Deutsch-Spanischen Astronomischen Zentrums/German-Spanish Astronomical Centre« (DSAZ), known in short as the Calar Alto Observatory.

The complex technological problems associated with the planning and construction of the telescopes were sol-

Fig. I.1: The Max Planck Institute of Astronomy, Heidelberg-Königstuhl. In the right foreground is the astronomical laboratory with its two domes, in the background the Land observatory. (Lossen aerial photography, RPKA 10/4209a)

ved in cooperation with the Carl Zeiss company at Oberkochen and other companies. In this way, a large number of companies have acquired know-how which has helped them to secure leading positions on the world market.

Between 1975 and 1984, the 1.2-metre reflector financed by the Deutsche Forschungsgemeinschaft/ German Research Association as well as the 2.2-metre and 3.5-metre telescopes started operation on Calar Alto (Figure I.2). The 80-centimetre Schmidt telescope was transferred from the Hamburg Observatory. There is also a Spanish 1.5-metre telescope on the site which does not belong to the DSAZ: the Observatorio Nacional de Madrid is in charge of this instrument. The original plans to construct a southern observatory on the Gamsberg in Namibia could not be implemented for political reasons. The 2.2-metre telescope which was intended for this purpose has been loaned to the European Southern Observatory for 25 years. Since 1984, it has been in operation on La Silla Mountain in Chile, where 25% of its observation time is available to the astronomers of the MPIA.

One aspect of the MPIA's present task is the operation of the Calar Alto Observatory. This includes the constant optimisation of the telescopes' capabilities: now that the ALFA adaptive optical system has been commissioned, the 3.5-metre telescope is once again at the forefront of technological development (Chapter II.1).

Other aspects include the development of new measuring instruments in Heidelberg, the preparation of observation programmes and the evaluation of the data obtained from the telescopes. A substantial part of the Institute's work is devoted to building new instruments for the telescopes (Chapter III). The MPIA is equipped with ultra-modern precision mechanics and electronics workshops for this purpose. The Calar Alto Observatory provides the MPIA with one of the two European observatories with the highest performance. Research concentrates on the »classical« visible region of the spectrum and on the infrared region.

In addition to these tasks, the MPIA has been engaged in extra-terrestrial research ever since it was established. This was associated with an early start on infrared astronomy which has played a particularly important part in the Institute's later development as a whole. Nowadays, the MPIA has a substantial involvement in the ISO project (Infrared Space Observatory, Figure I.3) of the

European Space Agency ESA (Chapter II.3): ISOPHOT, one of four measuring instruments on the ISO, was developed under the coordinating leadership of the Institute.

Participation in international observatories and projects is also of very major importance. For example, the Institute has been working for some years on one of the largest telescopes in the northern hemisphere, UKIRT (United Kingdom Infrared Telescope), the British 3.9-metre telescope in Hawaii, and also on MAX (Mid-Infrared Array eXpandable), the IR camera built at the MPIA, and on an associated tip-tilt secondary mirror. In return for these activities, the Heidelberg astronomers receive a fixed proportion of the observation time on this telescope.

The MPIA is coordinating the development of the high-resolution CONICA infrared camera for the ESO's Very Large Telescope (VLT, Figure I.4), which will become the world's largest telescope, on the Paranal in Chile. A decision has already been taken to participate in the development and construction of MIDI, an interferometry instrument for the VLT (Chapter III). Above and beyond this, as from the year 2002, the MPIA will be substantially involved in the Large Binocular Telescope (LBT, Figure I.5), another of the new generation of telescopes. The LBT is currently being built by an American-Italian-German consortium on Mount Graham in Arizona, USA. It will be the most powerful telescope in the northern hemisphere. In conjunction with the MPI

Fig. I.3: The ISO satellite was 5.4 metres tall and weighed 2.4 tonnes. The telescope and the aperture system were cooled down to 1.8 Kelvin with helium gas, which evaporated from a tank containing 2300 litres of superfluid helium.

für extraterrestrische Physik/MPI of Extra-Terrestrial Physics in Garching, the MPI für Radioastronomie/MPI of Radio Astronomy in Bonn, the Astrophysikalisches Institut Potsdam/Potsdam Astrophysical Institute and the Landessternwarte Heidelberg, the MPIA will probably have a 25% share in the costs and use of the LBT.

Aided by this wide and varied range of instruments, the MPIA will be able to go on making a major contribution towards astronomical research in the 21st century.

Thanks to its location in Heidelberg, the MPIA has the opportunity of working in a particularly active astronomical environment: there has constantly been a rich variety of cooperation with the Landessternwarte, the Astronomisches Rechen-Institut, the University's Institute of Theoretical Astrophysics or the Cosmophysics Department of the MPI für Kernphysik / MPI of Nuclear Physics. One particularly striking and effective aspect of this cooperation comprises the Sonderforschungsbereiche/special research areas established over periods of many years: number 328 (»Evolution of Galaxies«, 1987–1998) and number 1700 (»Galaxies in the Young Universe«, from 1999 onwards), in which all the Heidelberg Institutes mentioned above are involved, with major proportions of their resources.

The Institute's tasks also include informing an extensive public audience about the results of astronomical research. Accordingly, members of the Institute give lectures in schools, adult education centres and planetariums, and they appear at press conferences or on radio and television programmes, especially when there are astronomical events which attract major attention from the public. Numerous groups of visitors come to the MPIA on the Königstuhl and to the Calar Alto Observatory. Since 1976, the premises of the MPIA have been the setting for a regular one-week teacher training course held in the autumn, which is very popular among teachers of physics and mathematics in Baden-Württemberg.

The lively interest with which a wide sector of the population follows our work was evident in the enormous crowds attending the »Open Day« on 12 October 1997, when a total of 12500 visitors came to the Königstuhl: only the narrowness of the access roads limited the number of visitors. Finally, the monthly journal *Sterne und Weltraum* (*Stars and Space*), co-founded by Hans Elsässer in 1962, is published at the MPIA. This journal is aimed at the general public and it offers a lively forum both for specialist astronomers and for the large body of amateur astronomers and interested layman.

Some Important Questions

The central question of all cosmological and astronomical research deals with the creation and development both of the universe as a whole, and of the stars, the galaxies, the sun and its planets. The MPIA's research pro-

gram is oriented around this question. In the field of galactic research, the Institute concentrates on the formation of stars in large interstellar clouds made of gas and dust. In the field of extra-galactic astronomy, the focus is on the question of the large-scale structure of the cosmos, the search for the protogalaxies and research into active galaxies and quasars. These are remote stellar systems with an enormous radiation power. The observing astronomers are supported by a theoretical group, which uses sophisticated computer simulations to recreate processes in the universe extending over tens of thousands or millions of years. In this way, the MPIA achieves a fruitful synthesis of observation and theory.

Galactic Research

One important aspect of galactic research at the MPIA is the formation of stars. The very first phases of this process unfold in the interior of the dust clouds, which mean that they remain hidden from our view in visible light. However, infrared radiation is capable of penetrating the dust, which is why this wavelength range is preferable for studying the early stages of the birth of stars.

The newly born star is surrounded by a dense equatorial dust disk in which the material can condense either to form more stars or to form planets. After a few million years, the disk finally disintegrates. This is also how astronomers imagine the birth of our solar system, 4.5 thousand million years ago. Empirical evidence for the actual existence of the protoplanetary disks began to be assembled more intensively during the 1980's, thanks in particular to a great deal of work carried out at the MPIA. Nowadays, the following questions are at the forefront of this Institute's activities: how many of the young stars form a disk around themselves, and for how long can it exist? Which factors decide whether one or more stars - or on the other hand planets - will form in a dust disk of this sort? Over what period do the disks disintegrate?

One interesting phenomenon whose causes are related to the dust disks is that of the collimated gas jets which shoot out into space at high speed, perpendicularly to the disk. These jets, whose cause has still to be clarified, are among the bipolar flows - short-lived but fundamental phenomena in the birth of stars - which have been studied intensively and with great success at the MPIA since the start of the 1980's (Chapter IV.1). In every

case, the equatorial dust disk mentioned above forms the plane of symmetry to the flows and the bright gas clouds. The MPIA's astronomers are seeking answers to some important questions such as: how are the particles accelerated? How long does the bipolar phase last? Does every newly born star generate flows of this sort, and what role does this phenomenon play in the development of young stars?

The later stages of stars are also being investigated at the MPIA. Stars which are substantially more massive than the sun explode as Type II supernovae at the end of their lives. What happens in the last ten thousand years before the explosion? We are now familiar with a class of stars which are probably in this pre-supernova stage: the Luminous Blue Variables. Evidently they too are already casting off parts of their outer shell as they create a gas cloud around themselves. One of these nebulae has been examined at the MPIA – it contained a bipolar structure whose cause has still not been clarified.

Extragalactic Research

It is a cosmologist's dream to be able to look back into the era of the universe when the first galaxies were being formed. However, the protogalaxies are so remote, and
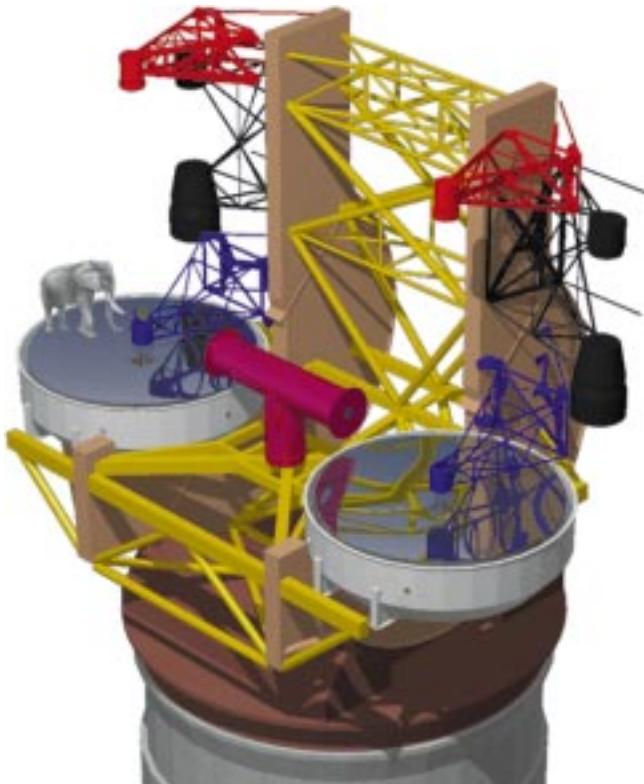

Fig. I.5: Design diagram of the Large Binocular Telescope. It will carry two primary mirrors with a diameter of 8.4 metres, whose beams can be made to interfere. The fully-grown elephant serves to give an idea of size.

the light from them is consequently so faint, that it has so far been impossible to discover them. In order to attain this goal, astronomers must use sensitive detectors working at the limits of the most powerful telescopes, and they also need to develop ingenious search strategies. Since the mid-1990's, the CADIS (Calar Alto Deep Imaging Survey) observation programme has been running on the 2.2- and 3.5-metre telescope at Calar Alto, with the aim of searching for the first galaxies in the universe (Chapter II.2). This programme is intended to run for at least five years and it is currently one of the MPIA's key projects.

The question as to the evolution of galaxies is also closely linked to the question of the nature of quasars. These are compact regions in the centre of certain galaxies. From a region which is probably not very much larger than our planetary system, they are able to radiate several tens of thousands of times more energy than all the stars in the surrounding galaxy taken together. According to the theory which is current today, a massive Black Hole is located at the centre of a quasar; this sucks in the surrounding matter, and the observed radiation is released. The investigation of quasars and of the galaxies at whose centres they are located (the mother galaxies) has been one of the MPIA's fields of work for many years now.

Another focus of extragalactic research at the MPIA is the investigation of jets from galaxies: this phenomenon shows remarkable similarities to the bipolar flows from stars, but it is on a substantially larger scale. In this case, one or two collimated jets of particles emanate from a central source – a quasar or a radio galaxy – to end in large clouds (or lobes, as they are known), where they dissipate. In the interior of the jets, electrically charged particles (electrons and possibly positrons) are moving in strong magnetic fields at almost the speed of light. Since the 1980's, the MPIA has been making major contributions to the issue of how the particles are accelerated in the jet, although this issue has still not been finally clarified. (Chapter IV.2).

Researchers at the MPIA also deal with normal spiral galaxies, of the same type as our Milky Way system. The arms of the spiral play a decisive part in the birth of stars, and therefore in the development of galaxies. However, many fundamental aspects of this phenomenon have still not been understood. How do the spiral arms come into being, and for how long do they remain stable? In addition to this, some spiral galaxies, probably including our own Milky Way, possess a bar-shaped structure which runs through the central region, with the spiral arms starting at its ends. Under what conditions are the bars created, and why do they not form in all spiral galaxies? At the MPIA, these questions are investigated with the help of computer models which are used to interpret observations (Chapter IV.2).

Although the spiral structure is the most striking feature of the spiral galaxies, it has become increasingly

clear since the middle of the 1970's that – in addition to the shining stars and the interstellar matter – there is also a dark component which perhaps contributes ten times as much to the total mass of the spiral galaxies as the stars and the interstellar medium. This Dark Matter is only noticeable because of its gravitational effect. According to present models, it is supposed to be located in an extended halo surrounding the galaxy in the shape of a sphere.

The puzzle of Dark Matter is currently one of the central subjects of astrophysics. With the help of the MAGIC infrared camera, a programme is running on the 2.2 metre telescope at Calar Alto to search for celestial bodies of extremely weak luminosity in the halos of spiral galaxies. At the same time, the theoretical group of the MPIA is carrying out numerical calculations which may provide insight into the spatial distribution and nature of the matter (Chapter IV.2).

The Solar System

The solar system is not among the primary subjects dealt with at the MPIA. Only the zodiacal light has been the subject of detailed studies since the very beginning. The zodiacal light owes its origins to a fine dust component which is distributed throughout the entire planetary system. Thanks to ISOPHOT, it has now become possible to examine this interplanetary dust at wavelengths of about 200 mm for the first time. This allows some conclusions to be drawn about the composition and size of these particles.

However, when important current events have taken place within the solar system, the telescopes on Calar Alto have been able to demonstrate their capabilities time and time again. In 1997, Comet Hale-Bopp was the focus of a great deal of attention on the part of the public. With the Schmidt telescope on Calar Alto, it was possible to obtain detailed photographs showing the rare phenomenon of the striae (Chapter IV.3).

II Highlights

II.1 ALFA – The Atmosphere is Outwitted

The twinkling of the stars is a source of inspiration to poets, but it presents a serious obstacle to astronomers' observations. The flickering is caused by turbulence in the atmosphere, which prevents large earth-bound telescopes from providing pictures with the degree of sharpness that would theoretically be possible. One way out of this dilemma is to use space telescopes, such as the Hubble Space Telescope. However, observatories in orbit around the earth are not only expensive systems, but they are also very difficult to handle.

Since the start of the 1980's, a technology has been developed which makes it possible to correct the image distortions caused by turbulence (known as »seeing« in astronomical jargon) while the observation is still in progress. This method, known as adaptive optics, will be of crucial importance on the large telescopes of the new generation, such as the Very Large Telescope (VLT), or the Large Binocular Telescope (LBT, cf. Chapter I). Interferometry, which is to be operated in conjunction with the VLT, the Keck telescopes and the LBT, will also benefit decisively from adaptive optics. It brings more light to the interference and therefore makes it possible to observe fainter objects.

In collaboration with colleagues at the MPI für extraterrestrische Physik / MPI of Extra-Terrestrial Physics in Garching, astronomers and technical experts at the MPIA have developed and built an adaptive optical system for use at the Calar Alto Observatory. In addition to this, a laser system has been set up which creates an 'artificial star' in the night sky. The adaptive optics system uses this as a bright star for purposes of comparison during the image correction. This system, known as ALFA, was tested successfully for the first time at the end of 1997, and it places the MPIA at the very forefront of research: in the astronomical sector, there are currently only two other instruments of this sort anywhere in the world.

The Principle of Adaptive Optics

In theory, the resolution of a telescope (that is to say, its ability to show separate images of two objects that are located close to one another) depends exclusively on the diameter of the main mirror and the wavelength of the light. In the visible range (wavelength of about 550 nm), a 3.5-metre telescope has a theoretical resolution capaci-
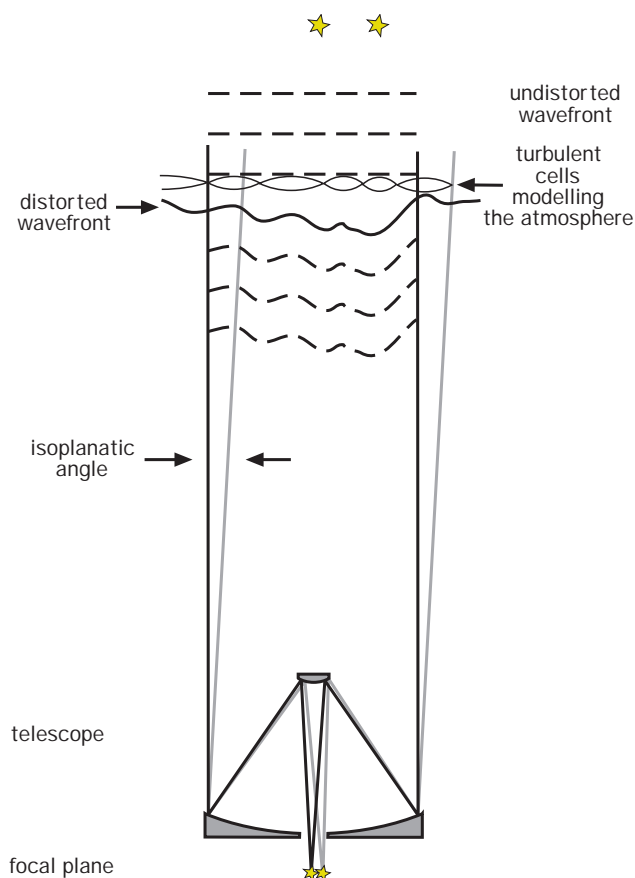
Fig. II.1: Visualization of deformation of the stellar light's plane wave by the turbulent atmosphere.

ty – also known as the diffraction limit – of 0.04 seconds of arc; at 2.2 μm, the figure is 0.16, or four times less. In practice, however, the turbulence of the air blurs the received image so heavily that the typical resolution is only one second of arc. This means that every earthbound telescope, no matter how large it may be, will only attain the same resolution as can already be achieved by any 15 centimetre telescope!

The light from a star may be imagined as a spherical wave which spreads out in space at the speed of light. If a wave of this sort encounters the earth's atmosphere, it is almost perfectly flat, on account of the huge distance from the source (Figure II.1). As it passes through the various layers of the air, however, this wave will experience disturbances which are variable in terms of space
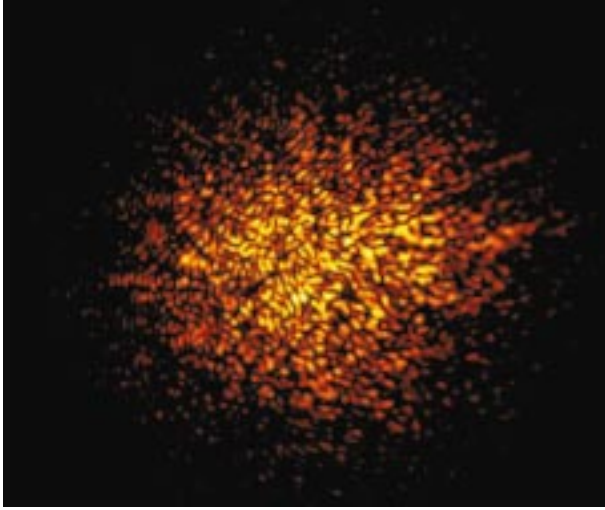
Fig. II.2: The effect of atmospheric turbulence is that a stellar image is broken up into many, randomly divided single images (speckles). The speckles add up under long exposures: the stellar image is smeared into a disc with a mean diameter of one arc-second.

and time. Warm layers of air rise while cold ones fall. There is formation of »air bubbles« or cells with a typical extent of 10 to 20 centimetres and different temperatures, and these mix convectively. Since the refractive index of the air is temperature-dependent, the optical path length and the direction of propagation of the light will change constantly as it passes through the turbulent atmosphere. The air cells act like optical lenses which float about.

The originally flat wave is distorted as it passes through the atmosphere, like a piece of cloth in the wind, so that when it arrives at the telescope, it shows »hills and valleys« with a height of several micrometers. There are two consequences due to this influence which atmospheric turbulence exerts on the wave front. On the one hand, the image of a star is split up into many small images, or so-called speckles (Figure II.2). The number of speckles more or less corresponds to the total number of turbulence cells which the light has traversed. The speckles are distributed over a circular area with a diameter of about one second of arc, in which they dance to and fro in fractions of a second, depending on the turbulent movement. On the other hand, the whole cluster of speckles is slowly drifting forward and backward. On photographs with longer exposures, the superimposition of these two effects leads to a smudged »seeing disk« instead of the diffraction figure which would theoretically be expected.

In principle, the drifting movement of the speckles can be compensated and the »bent« wave can be unbent again to make it straight, by feeding the light on to a mirror which has precisely the opposite pattern to the wave. After it has been reflected, the wave should then be flat again and it should produce the undistorted, diffraction-limited image on the detector.

In order to implement this intention in reality, it is therefore necessary to determine the current distortion of the wave front and to deform the mirror accordingly. The mirror is referred to as 'adaptive' because it is constantly adapting to the form of the wave front.

In practice, an adaptive optical system looks more or less like this (Figure II.3): the light wave coming from the telescope is split into two sub-beams by a beam splitter. While one sub-wave falls on the adaptive mirror and enters the camera from there, the other reaches a so-called wave front sensor. This device analyses the form of the wave, and forwards this information to a computer. The computer uses the data to calculate how the surface of the adaptive mirror must be deformed in order to correct the form of the other sub-wave. (In the case of ALFA, the wave initially falls on the deformable mirror and only reaches the beam splitter afterwards.)

In order for this process to function, it must be possible for the mirror to be adapted so quickly that when the correction takes place, the incoming wave trains are not already being deformed in a different way to the wave train which has just been analysed. Theory shows that about 200 correction steps per second are needed in the visible range, while only about ten are required in the medium infrared range (at a wavelength of ten micrometers).

Fortunately, the absolute deformation of the wave front does not depend on the wavelength. However, completely different relative deformations occur in relation to the actual wavelength at which the observation is being made. In the medium infrared range, at wavelengths of about ten micrometers, the deformation of the wave front only accounts for 30 to 60 per cent of the wavelength. But in the visible range, the disturbance already amounts to about ten times the wavelength. This is why the adaptive mirror in the visible wavelength range must be adapted to the wave front with considerably greater precision than in the infrared range.

In general, it can be seen that the requirements for adaptive optics rise enormously as the wavelengths become shorter. For this reason, systems of this sort are currently only viable in the infrared range, down to a wavelength of about one micrometer.
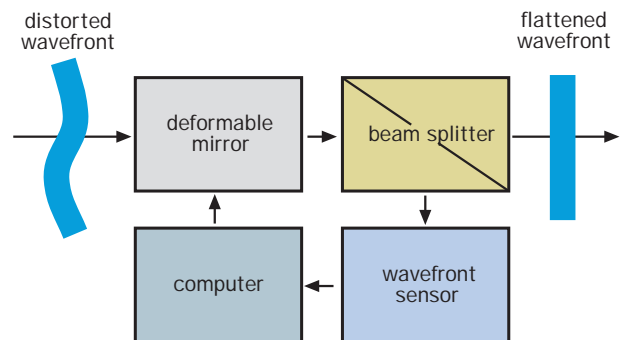
Fig. II.3: The principle of adaptive optics.

astronomical
target

☆reference star

mesospheric
sodium layer

undistorted
wavefront

turbulent
atmosphere

distorted
wavefront

telescope

launch
telescope

transfer optics

589 nm master oscillator

ampli-
fier

pump laser

corrected
wavefront

deformable
mirror

dichroic beam splitter

wavefront
sensor

distorted
wavefront

camera
spectrograph

Tip-tilt
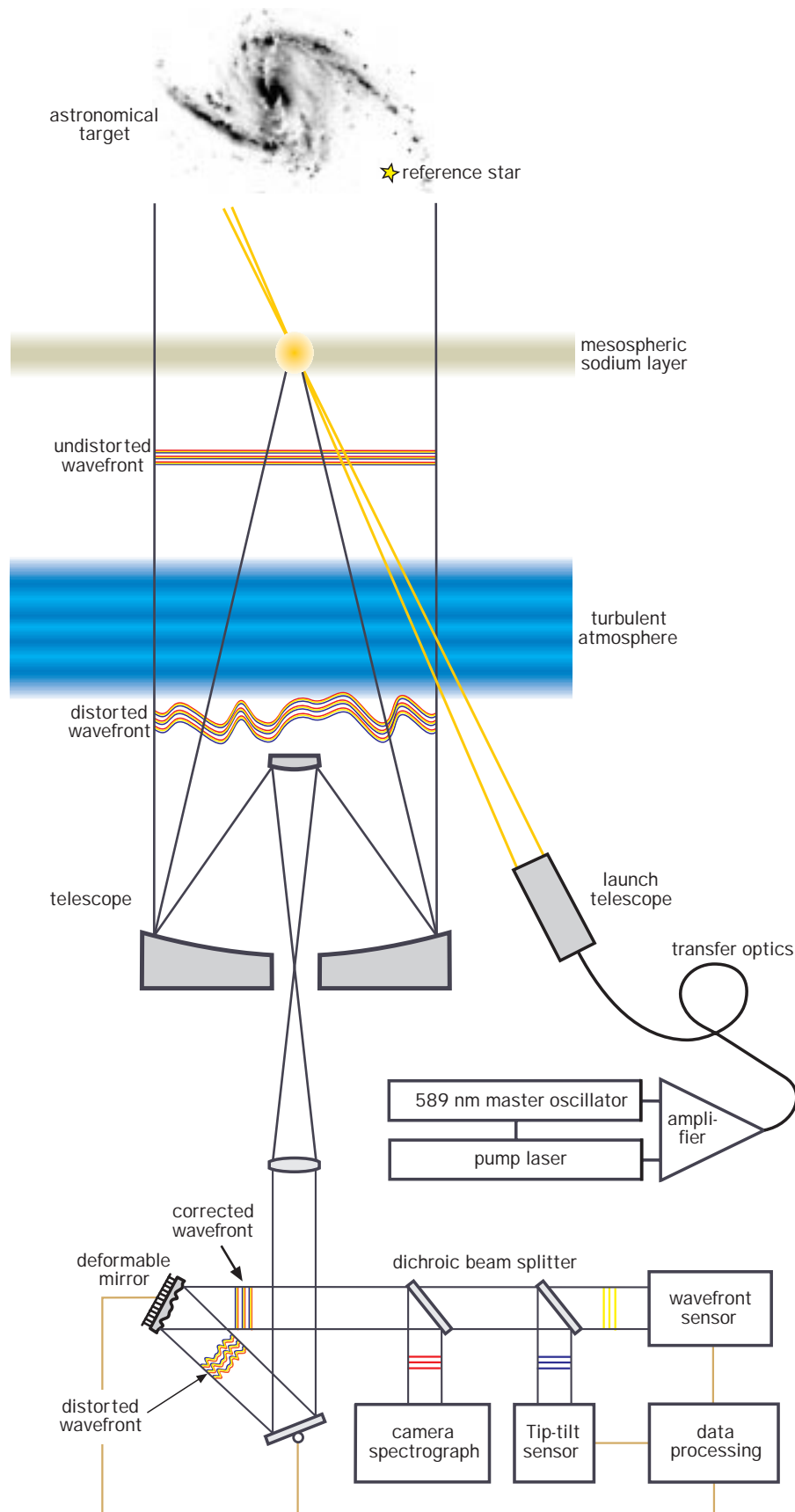sensor

data
processing

Fig. II.4: The principle of adaptive optics in ALFA with laser guide star.

ALFA at the Calar Alto Observatory

An adaptive optical system therefore requires three main components: a wave front sensor, a fast computer and an adaptive mirror. There are basically various ways of implementing the optical components. ALFA was designed for the near infrared wavelength of about two micrometers, and it operates in two steps (Figure II.4). First of all, a tip-tilt mirror compensates the drift movement of the speckle, and then the deformable mirror corrects the form of the wave front. Both mirrors require a sensor which analyses the star image in a rapid time
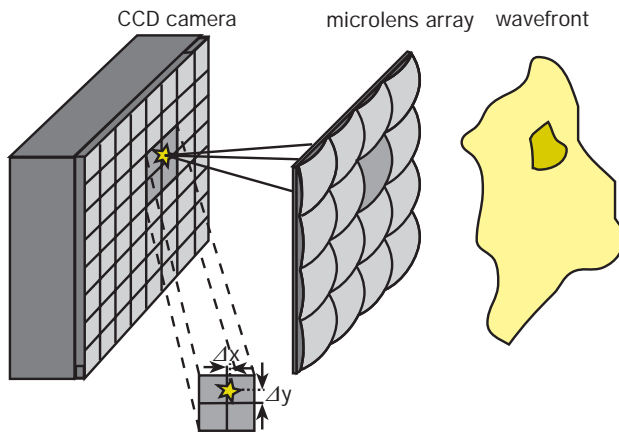

Fig. II.5: The principle of the Shack-Hartmann wavefront sensor, in which a lenticular array forms an image of the stellar image on a CCD.
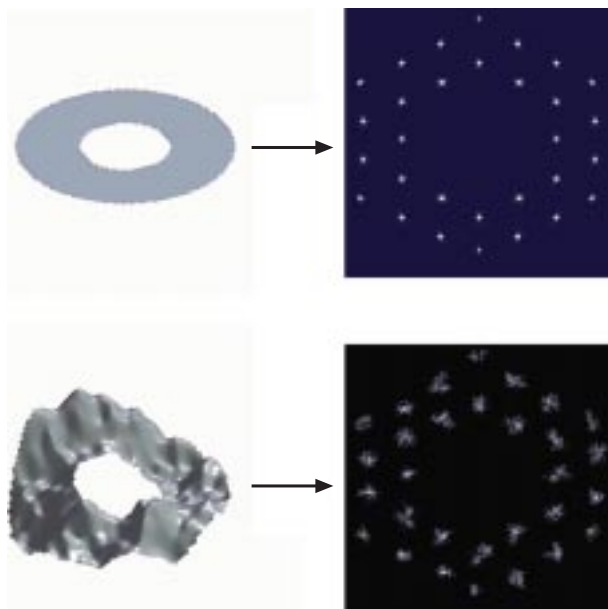

Fig. II.6: A computer simulation showing how the lenticular array in the Shack-Hartmann wavefront sensor generates varying image patterns. A plane wave (left) causes a uniform pattern, a disturbed wavefront results in a distorted pattern. The imaged pattern makes it possible to reconstruct the form of the wavefront deflection.
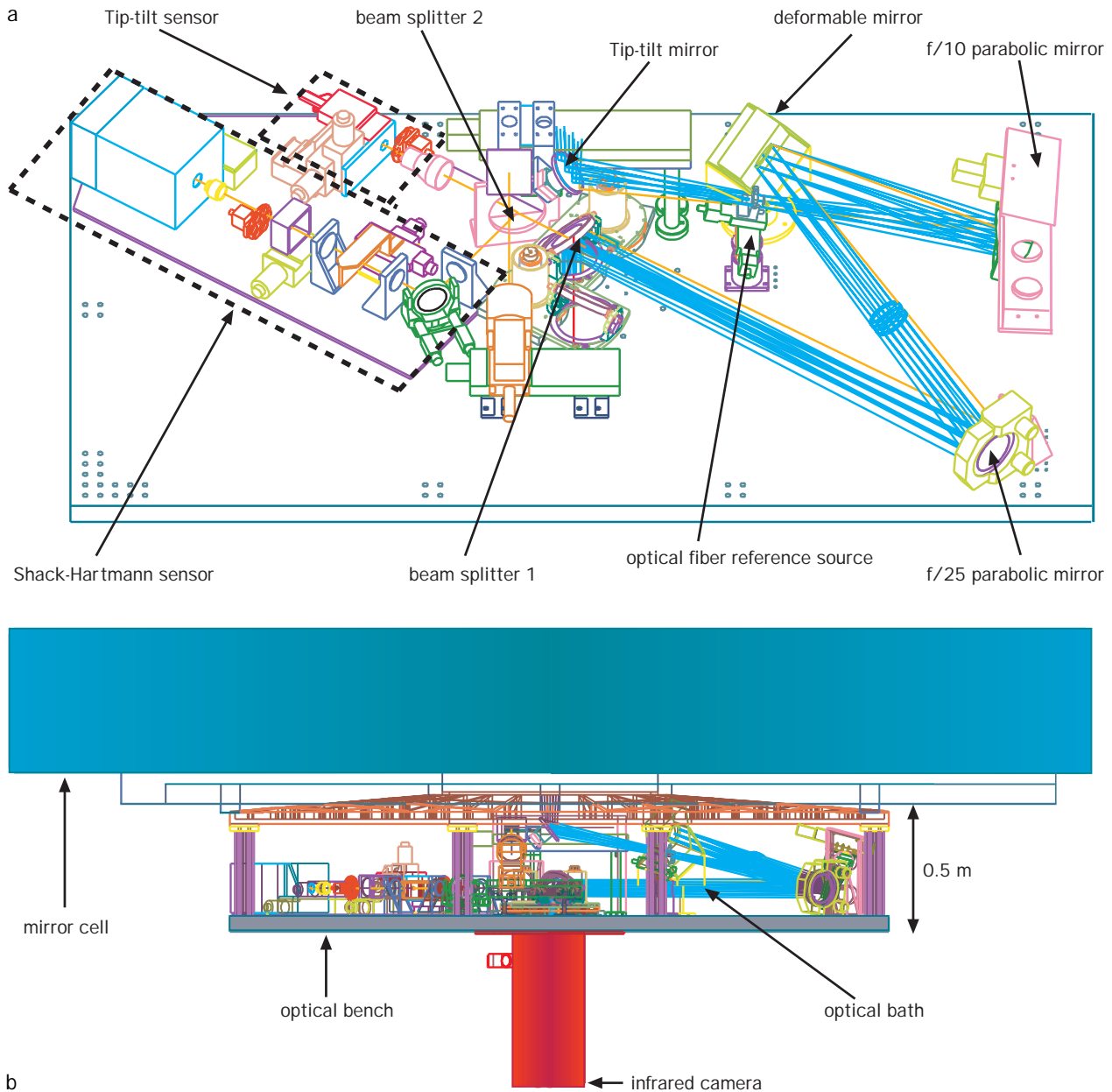
sequence and forwards the measurement data to a control computer.

As the beam of light comes from the telescope, it encounters a beam splitter which diverts the visible component of the light into a camera. This camera registers the image position 30 to 100 times per second, and forwards the information to the computer. The infrared component of the light reaches the tip-tilt mirror which can be swivelled around two axes that are perpendicular to one another. The computer now controls the mirror precisely so that the image cast by the star will stand still. This tip-tilt system is capable of improving the resolution by 0.3 seconds of arc at a wavelength of two micrometers. However, it still does not supply any diffraction limited images. In order to achieve this, the second correction on the deformable adaptive mirror is required.

A so-called piezo-mirror was selected from a variety of options as the adaptive mirror for ALFA. This consists of a plate of glass which is two millimetres thick, with a reflective coating, and so-called piezo-actuators are fitted on its rear side. These are essentially piezo-crystals which expand or contract when an electrical voltage is applied. This makes them ideal as small and fast-acting adjusting elements. In ALFA, the adaptive mirror has a diameter of 70 millimetres, and it is fitted with 97 piezo-actuators which distort it in the area of the contact points. It is operated at a maximum frequency of 1200 Hertz.

The information about the shape which the adaptive mirror must adopt in each case is supplied by the wave front analyser, and part of the light gathered by the telescope is fed to this instrument. A so-called Shack-Hartmann sensor was selected for ALFA. This basically comprises a lens grating (arranged in a rectangular or hexagonal grid) which supplies images of the star to a CCD camera (Figure II.5). In the case of an ideal flat wave, the image pattern corresponds to the symmetrical arrangement of the lenses. However, the real distorted wave front generates a correspondingly distorted grid (Figure II.6). A computer which reads out the CCD camera uses the current form of the grid image to calculate the form of the wave front, and it triggers the piezo-actuators in the adaptive mirror in such a way that the distorted wave will be flattened when it is reflected on this mirror. The adaptively corrected image can now enter the astronomical camera.

For various reasons, ALFA extends the effective focal distance of the telescope. For example, on the 3.5-metre telescope, a focal ratio of $f/10$ becomes a focal ratio of $f/25$. The whole device is fitted on the mirror cell of the main mirror in the Cassegrain focus, and it fits into a case which is 2.70 metres long, 1.5 metres wide and 50 centimetres high (Figure II.7).

a

Tip-tilt sensor   beam splitter 2   deformable mirror

Tip-tilt mirror   f/10 parabolic mirror

Shack-Hartmann sensor   beam splitter 1   optical fiber reference source   f/25 parabolic mirror

0.5 m

mirror cell

optical bench   optical bath

b

infrared camera

The Laser Guide Star

ALFA therefore has two sensors which analyse the image of the star. One of them works in conjunction with the tip-tilt mirror and the other works with the adaptive mirror. Due to the losses of light in the optical system and the fast read-out times, the guide stars must be comparatively bright. The tip-tilt sensor requires a star of the 16th magnitude, while the Shack-Hartmann sensor already needs a star of the 11th magnitude. If the light from the celestial body that is to be examined is itself so faint that it cannot be used as a guide star, another star has to be found. However, such a star must not be too far away in the sky, since its light must have passed through the same air turbulence as the light of the object to be observed. With the tip-tilt system and the Shack-Hartmann

Fig. II.7: (a) The optical layout of ALFA, (b) Complete view of ALFA at the four-metre measuring mirror cell of the 3.5-metre telescope.

sensor, a distance of up to 30 seconds of arc can be tolerated. In this range, however, a star of at least the 11th magnitude will only be found in one to two per cent of all cases. For this reason, ALFA generates its own guide star – with the help of a laser.

Since the light from the guide star must have passed through the same air turbulence as the celestial object that is to be observed, the laser guide star should be generated at the greatest possible height. A layer about 10 kilometres thick at a height of some 90 kilometres is suitable for this purpose. Sodium atoms which are depo-

sited in the atmosphere by micro-meteorites can be found here in relatively high concentrations. If a laser beam is focused on this layer of the atmosphere, it will excite the sodium atoms to shine in a cylindrical area, provided that the correct wavelength is selected. Viewed from the telescope, this cylinder looks like a shining star (Figure II.4).
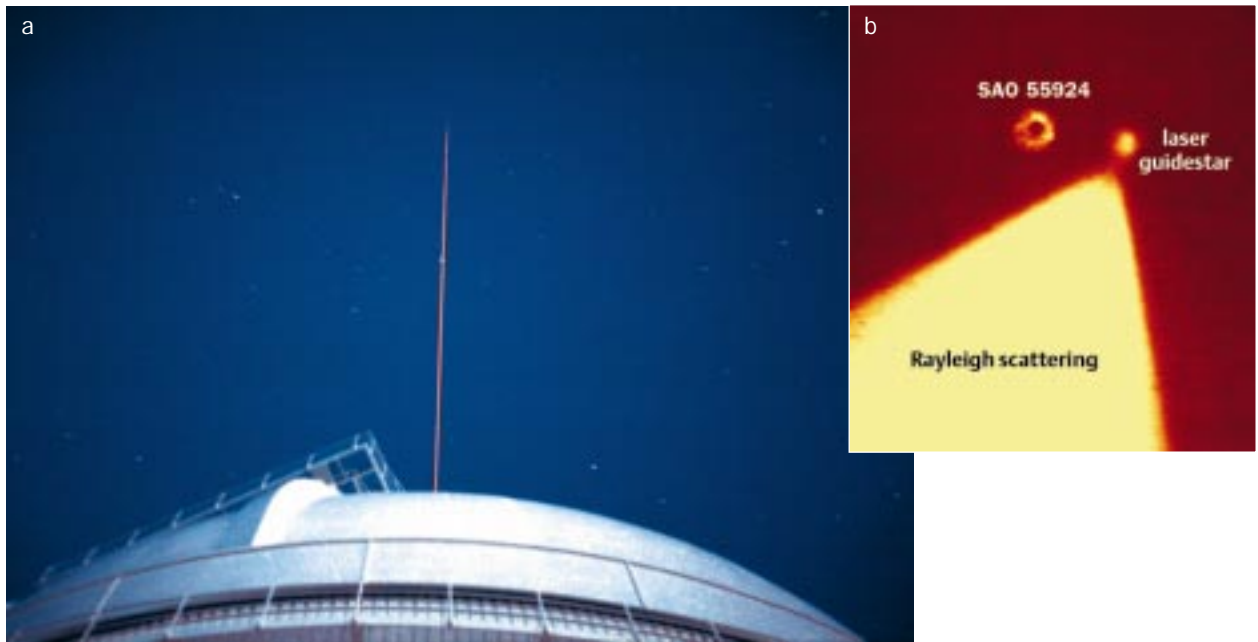
Although this may sound simple in principle, it proves to be a complicated undertaking in practice. The so-called D2 sodium line in the visible range, at a wavelength of 589 nm, has proven to be optimal for this purpose. However, the laser guide star is far from being equally bright all the time, because the concentration of the sodium atoms in the layer fluctuates both in the short term and in a seasonal cycle. Because of this, the brightness can vary by a factor of two, or even more in extreme cases. Moreover, the intensity depends on the distance of the direction of observation from the zenith.

Another critical factor is the radiation power that is deposited in the sodium layer. At first, the brightness of the artificial star rises as the laser power increases, but then at a certain maximum power it goes into saturation – and even if the laser power is increased further, the star does not become brighter. Other essential factors are the laser bandwidth, and the question as to whether a pulsed laser or a continuous wave laser should be used. Even the type of polarisation of the laser light plays a part.

After numerous trials, a decision was made in favour of a variable colour ring laser in continuous wave operation for ALFA. The laser beam has a power of just four watts, and it generates a »star« of the tenth magnitude at a height of 90 kilometres (Figure II.8). The laser system is located in the Coudé laboratory of the 3.5 metre telescope, from where the beam is guided outwards in the opposite direction to the normal »direction of observati-

Fig. II.8: (a) The laser beam emerging from the dome of the 3.5-metre telescope. (b) An artificial star shines in the sky at an altitude of 90 km. The star SAO 55924, practically infinitely remote next to the laser guiding star, is defocused. The Rayleigh cone is created by scattering of laser light in the lower layers of the atmosphere.

on« by the Coudé beam path. Before the beam reaches the main mirror, it is deflected by a mirror to a 50 centimetre projection telescope which is positioned on the side of the mirror cell. There are a total of ten mirrors in the laser beam path, and most of them can be controlled. This allows active tracking of the laser beam.

ALFA in Use

In October 1996, ALFA was tested for the first time on the 3.5 metre telescope at Calar Alto, together with the MAGIC infrared camera. On this occasion, it was possible to achieve a clear separation of the double star 72 Pegasi, whose components are at a distance of 0.53 seconds of arc from one another. The profiles of the star images showed a width of 0.15 seconds of arc, which almost corresponds to the diffraction limit of 0.12 seconds of arc at a wavelength of 2.2 micrometers. 72 Pegasi is such a bright star that it can even be used for the wave front analysis in the Shack-Hartmann sensor.

During the course of 1997, it was possible to obtain further photographs at 2.2 mm which were virtually diffraction-limited (Figure II.9). The artificial star attained a half-width value of three seconds of arc in the sky, which almost corresponded to the expectation of two
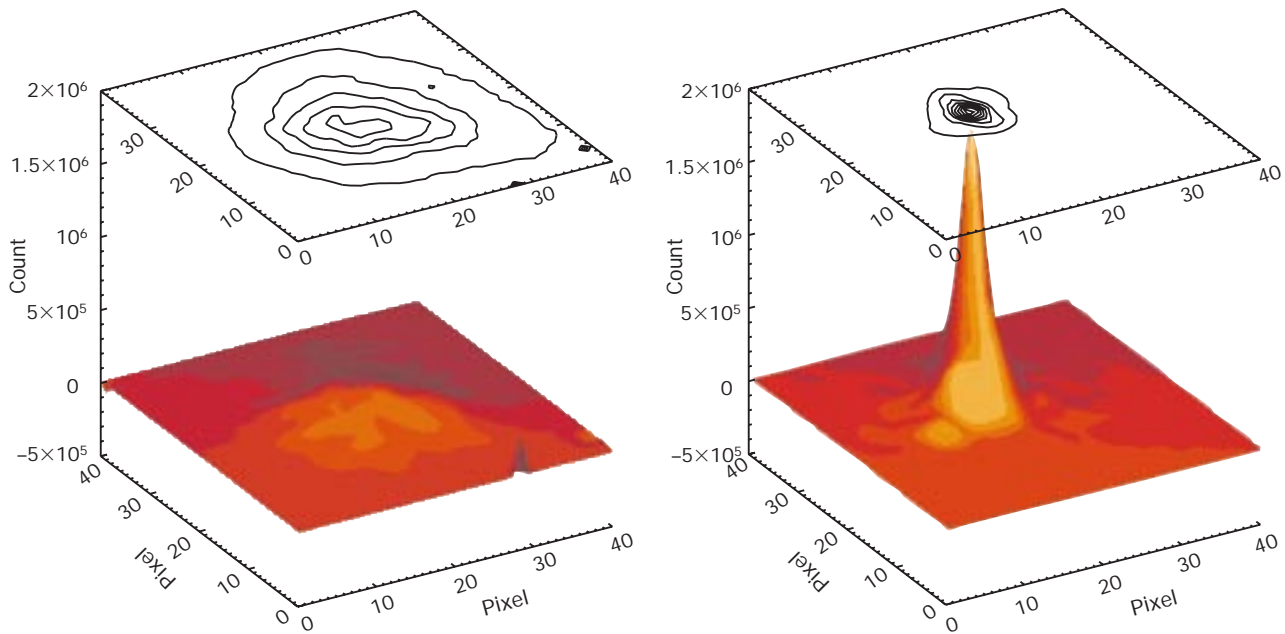
Fig. II.9: The star 14 Peg, recorded in July 1997 with the 3.5-metre telescope at a wavelength of 2.2 mm. Without correction (top), the stellar image has a diameter (full width half maximum) of 0.85 arc-seconds; with ALFA (bottom), the resolution was increased to 0.2 arc-seconds.

.

seconds of arc. This meant that it was about as bright as a star of the 10th magnitude, which would not be detectable by the naked eye. The sensitivity of the wave front sensor was increased by more than two magnitudes during the year, bringing it to 12.3 mag. A new and more sensitive tip-tilt sensor is now operating up to 14.5 mag, and it is planned to increase the sensitivity as far as 15.5 mag.

Since September 1997, ALFA has been working in conjunction with the new high-performance infrared camera OMEGA-Cass (Chapter III). Since May 1998, ALFA will be available with OMEGA-Cass on Calar Alto for observations by all astronomers.

II.2 CADIS – Searching for the Protogalaxies

The first half of the present century saw the most radical change in our conception of the world since the days of Copernicus. Edwin Hubble discovered the movement of the galaxies, thus helping to achieve the breakthrough for Georges Lemaître's theory, according to which the universe was created in a hot »Big Bang«. The Big Bang Theory nowadays forms the foundation of modern cosmology. It implies the idea that the world has a beginning in time, and that it is evolving. In the context of this model of the world, questions about the formation and evolution of the galaxies occupy a central position in cosmological research.

Modern investigations suggest that a thousand million years after the Big Bang, huge gas clouds were already contracting under the influence of gravity and were forming the first galaxies. Several observation programmes aimed at discovering the proto-galaxies have so far failed, due to incorrect strategies and inadequate instrumentation, and consequently many questions still remain unanswered. For example, it is not clear whether today's large galaxies formed as a whole from one cloud, or whether smaller protogalaxies were created first, and then joined together in order to form large galaxies (the building block scenario). How did the evolution continue? Did the galaxies form first, going on to merge into large clusters of galaxies in the course of thousands of millions of years (the bottom-up model)? Or did gas clouds of equal magnitude to the galaxy clusters contract as a whole, to disintegrate at a later stage into smaller fragments from which the galaxies were then formed (the top-down model)?

In order to observe these processes which date back more than ten thousand million years, today's astronomers must work at the limits of the most powerful telescopes and the most sensitive detectors, and they need to develop ingenious strategies. The extremely sophisticated CADIS observation programme (Calar Alto Deep Imaging Survey), planned to last for at least five years, has been running on the 2.2- and 3.5-metre telescopes since the middle of the 1990's; this programme enables the astronomers to search for the first galaxies in the universe.

This undertaking offers prospects of success for a number of reasons:

- More than ten per cent of the available annual observation time on each of the two telescopes is devoted to the CADIS project.
- The use of new focal reducers on the 2.2- and the 3.5-metre telescope has enlarged the image field per photograph to the unusual size of 120 square minutes of arc (Figure II.10).
- Thanks to the use of the new sensitive cameras (Chapter III), a massive increase in the efficiency of the two largest telescopes on Calar Alto has been achieved.
- With the help of computer programs, refined multi-colour photometry enables automatic differentiation of the large number of close galaxies on the one hand, and the small number of suspected protogalaxies on the other.
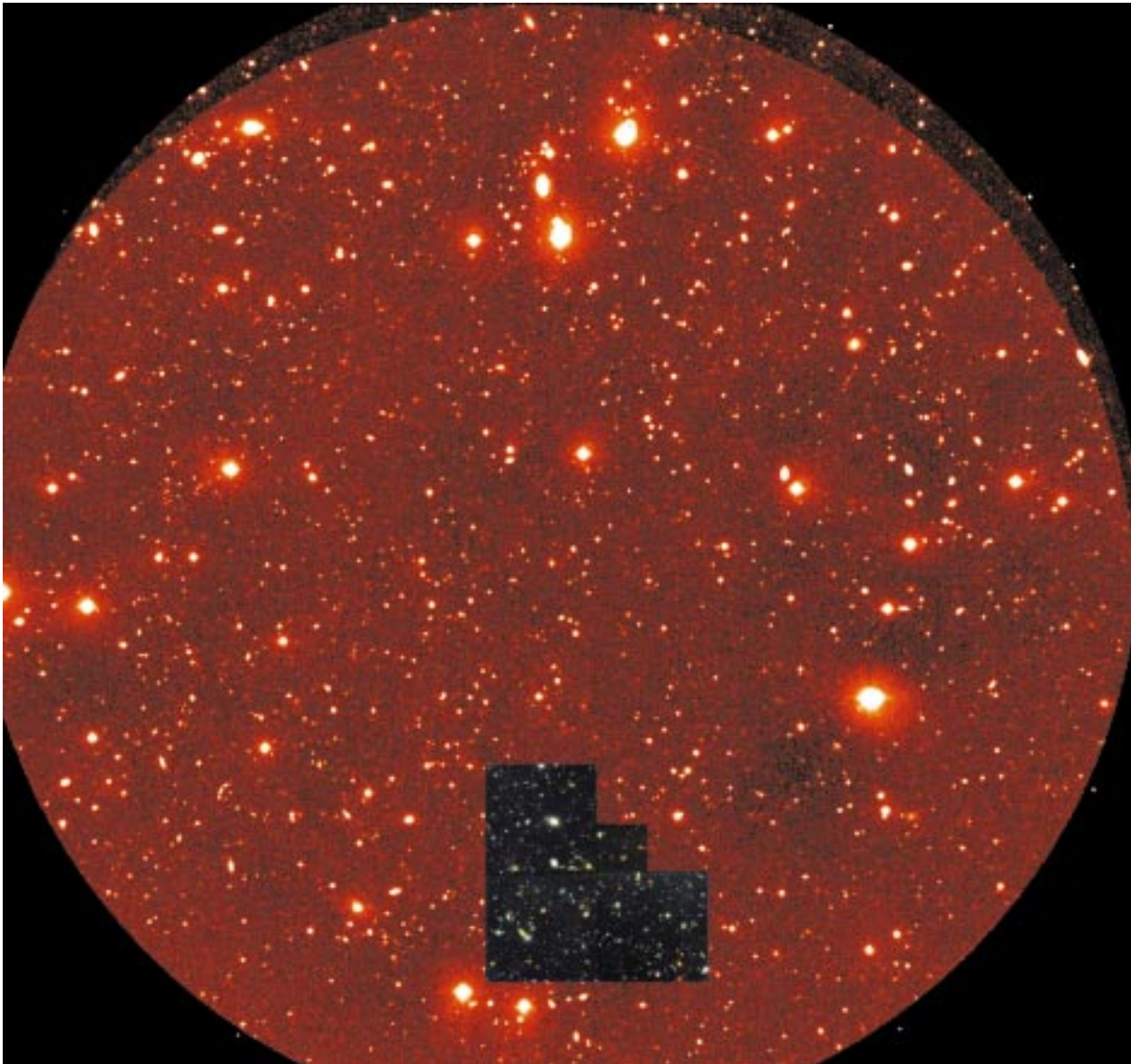
Thanks to CADIS, the MPIA is working at the very forefront of international research, where it has to measure up against the largest observatories on earth, such as the Keck Observatory in Hawaii. Nevertheless, top-class research at the highest level can be carried out with the promise of success, thanks to the ideal instrumentation on Calar Alto, coupled with expedient use of the largest telescopes there.

The main aim of the project is to provide proof of galaxies in the formation phase, at red shifts of $z = 4.7$, 5.7 and 6.6. This red shift range corresponds to a period of 1.2 to 1.8 thousand million years after the Big Bang ($q_0 = 0.1$, $\Omega_0 = 0.2$), when the first galaxies were probably formed.

The Strategy

The CADIS search strategy is based on some simple underlying assumptions. Close galaxies with high rates of star birth contain interstellar gas which, in some cases, is heated up to several thousand degrees, radiating characteristic emission lines. The strongest hydrogen emission line is the so-called Lyman-α-line, which is located in the UV range at a wavelength of 122 nm. The obvious procedure is therefore to observe the sky through a filter which only allows light from the Lyman-α-line to pass through (Figure II.11). In this way, even very remote galaxies should stand out against the background of the sky. Two problems have to be taken into account here.

1) The spectrum of the protogalaxies is shifted towards the red end of the spectrum (long wavelengths). This red shift is a consequence of the expansion of the universe: let us assume that a hydrogen atom in a protogalaxy were to emit a Lyman-α-photon with a wavelength of 122 nm, which reaches the earth today, some 13 thousand million years later. Over the course of this time, the universe – or to be more precise, space itself – has expanded by a factor of about six. Corresponding to this expansion of space, the wavelength of the Lyman a-light beam has also been extended. For this reason, we do not receive it in the UV range at the emitted wave-

Fig. II.10: The sky field seen by the wide-angle camera on the 2.2-metre telescope. The considerably smaller so-called Hubble Deep Field of the Hubble Space Telescope is shown within the white contours for comparison purposes. The Deep Field is an extremely deep exposure, obtained in late 1995.

length $\lambda_0 = 122$ nm, but in the red region of the spectrum at wavelength $\lambda_e = 732$ nm. The red shift parameter is defined as $z = (\lambda_e - \lambda_0)/\lambda_0$. The expansion of space is $R_e/R_0 = 1 + z$. This means that the Lyman-α-line appears at different points in the spectrum depending on the remoteness of the galaxies.

The CADIS project therefore requires filters which are transparent in precisely defined ranges. The astronomers at the MPIA use a Fabry-Pérot filter for this purpose. Essentially, this consists of two mirrored glass plates which only allow light of a specific wavelength to pass through, as a result of multiple reflection and destructive and/or constructive interference; in this case, the pass band depends on the distance of the glass plates from one another. The pass band can therefore be adjusted by changing this distance.

2) There are many more or less close dwarf galaxies which produce the same effect as very distant large gala-

xies, purely on account of their low luminosity. The gas which they contain can also emit intensive linear radiation. For example, hydrogen not only emits at the Lyman-α-line but also at 656 nm (Hα) and 486 nm (Hβ); or, as another example, oxygen emits at 501 nm and 372 nm. Now, if a galaxy is found with an emission at 732 nm, it may either be a Lyman-α-emission at $z = 5$ or a Hα-emission at $z = 0.1$, or else a Hβ-emission at $z = 0.5$, and so on. In order to clear up this multiple ambiguity, the following consideration was adopted: if a galaxy shines intensively in Hα, it generally does so in the oxygen
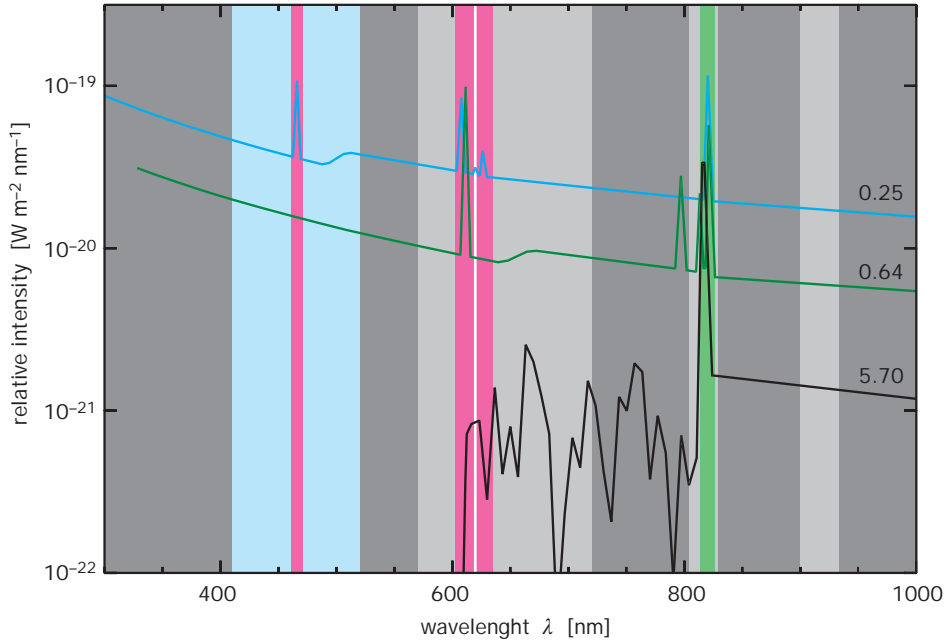
Fig. II.11: Demonstration of the Vetofilter strategy on the CADIS. An emission line shown in the Fabry-Pérot region B (green region), could turn out to be e.g. Hα-emission with $z = 0.25$ (blue spectrum), [OIII] at $z = 0.64$ (green spectrum) or Lyman-α at $z = 5.7$ (black spectrum). Correct identification is ensured through observation with the Vetofilters (red region): the galaxy at $z = 0.25$ shows additional emission lines at wavelengths of 465 nm and 612 nm. The galaxy at $z = 0.64$ reveals itself through the emission line at 612 nm. A galaxy with $z = 5.7$ cannot be detected either in one of the Vetofilters nor in a blue one (blue region), since its radiation below 600 nm is swallowed up by intergalactic hydrogen clouds in the line of sight.

In addition, eight or nine images taken through broad and medium band filters are needed. All in all, each of the eight to ten selected celestial fields are imaged at about 39 wavelengths. For each wavelength, an average of ten images is produced, resulting in about 400 images per celestial field and per red shift interval. CADIS will require a total of more than 3000 individual images.

Protogalaxies

The instrumentation required for this sampling was ready at Calar Alto in May 1996. CAFOS2.2 was used on the 2.2-metre telescope, while the wide field infrared camera OMEGA-Prime and the multi-object spectrograph MOSCA were used on the 3.5-metre telescope (Chapter III). In 1997, the group still had to struggle with some starting-up difficulties. Now, however, all the observations needed to carry out a multicolour analysis are available for a total of four fields. Moreover, in order to optimise the multicolour method, observations have also been carried out on one field of the so-called Canadian French Redshift Survey, in which spectra for 271 objects are available. So far, only two CADIS fields have sufficient observations with the Fabry-Pérot etalon and the narrow-band filters to permit searches for remote galaxies with Lyman-α-emission.

The immense number of CCD images makes it clear that the software is particularly important for the evaluation of the CADIS data, since only a computer can search for the proverbial »needle in a haystack« within a reasonable time (Figure II.12). In accordance with the usual calibration and reduction procedure for CCD photographs, the program first determines the positions of the objects on all the images, and compares these with

lines [OII] at 373 nm and [OIII] at 496 nm as well. This creates a requirement for additional images of the same field of the sky taken through so-called veto filters (Figure II.11), which are transparent in the precise range of these oxygen lines. If a galaxy appears in both filters, it is a low red shift dwarf galaxy. If it can only be recognised in the Fabry-Pérot image, it could be one of the remote galaxies that are being sought. The intensity ratio in the various filter ranges is determined for every galaxy, and a red shift class is assigned to it with an estimated probability.

To search for young galaxies with Lyman-α-emission, the astronomers selected three wavelength ranges at 700 nm, 820 nm and 918 nm, corresponding to red shift values of about $z = 4.75$, $z = 5.74$ and $z = 6.53$. Nine images taken through the Fabry-Pérot filter are required for each range. Over the narrow wavelength range, this makes it possible to achieve a high resolution in the red shift ($\sigma < 0.0005$), corresponding to that of a spectral image. Images taken through three veto filters are added.

one another. As it does so, the computer finds an average of 25000 suspected objects, of which about half have turned out to be deceptive. These illusory objects are created by statistical brightness fluctuations in the celestial background. Several images which have been obtained through the same filter can then be added together in order to improve the quality (statistic) of the image.

In several steps, the program then searches for all those objects which correspond to the criteria described for a remote galaxy with Lyman a-emission. The group began to sense the difficulties of this procedure in 1996, when it had finally isolated nine objects in one of the fields as possible young galaxies at z = 5.7, after several steps. Unfortunately, subsequent spectral examinations brought the sobering realisation that none of these cases actually involved a remote galaxy.

In 1997, a new and improved analysis revealed not a single candidate for a protogalaxy in the so-called 9H field. It was only in the 16H field that the astronomers were able to track down two candidates. From these data, it is possible to calculate the number density of these objects as less than 0.03 per square minute of arc and red shift range. In fact, theoretical models predict a density for the observable protogalaxies of about 0.03 per square minute of arc and red shift range. This means that a maximum of three to four protogalaxies may be expected per CADIS field.

Quasars, Galaxies and Stars

The main task of CADIS is definitely to search for protogalaxies. However, the extensive data material also contains an abundance of other information which is not to be left unused. For example, the observations that are now available represent the largest extragalactic sampling at the 2.1 μm wavelength that has been undertaken anywhere in the world.

In 1997, it emerged that the software can identify quasars with brightnesses of up to the 22nd magnitude, with virtually no errors. Out of 70 selected objects, subsequent spectroscopic observations with MOSCA proved that only one had been wrongly classified. A first evaluation is already showing signs of a small surprise. In the 16H field, there were six quasars in the red shift range between z = 2.3 and z = 3.7, whereas not even one was to be expected here on the basis of previous quasar searches. This could have consequences for our ideas about the evolution of quasars.

It is currently assumed that the volume density of the quasars rose at about z = 4 after the Big Bang, to reach a

Fig. II.12: In a celestial field such as this, the search for primordial galaxies is like the proverbial one for a needle in a hay stack.
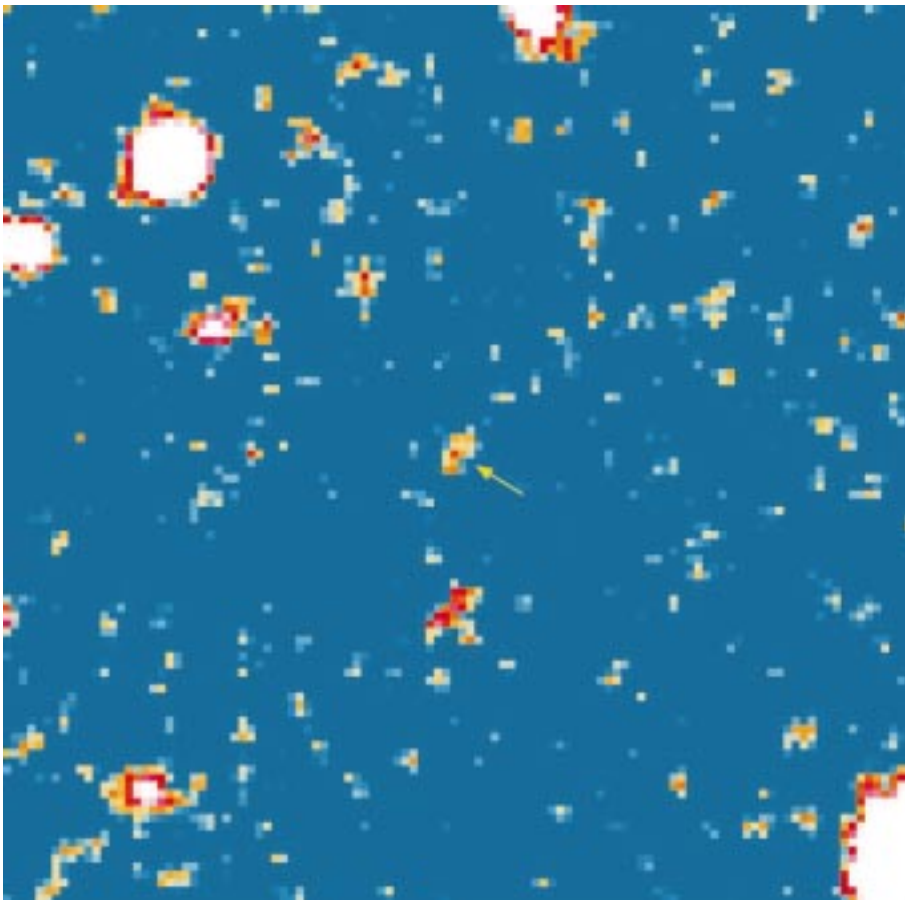
maximum at $z = 2$. The density then fell very sharply as far as $z = 1$. In the more immediate vicinity of the Milky Way ($z = 0$), virtually no more quasars are observed. The cause of this evolution is unknown. The new CADIS values could indicate that the maximum density is displaced at higher red shifts and that the maximum quasar density was already attained at an earlier point after the Big Bang.

The aim of the quasar project is to determine the evolution of quasars in the red shift range between $z = 2$ and $z = 5$. In all the fields together, a total of several hundred objects up to the 23rd magnitude are expected. Of course, there are also hopes of discovering some quasars with even greater red shifts, up to $z = 6$. The current record-holder, with $z = 4.9$, was discovered as long ago as 1991.

Galaxies at medium red shifts with weak emission lines can also be identified with CADIS. Out of the selected objects in the 9H and 16H fields, more than two thirds of which are dwarf galaxies, 40% were at $z = 0.25$, 40% were at $z = 0.65$ and a further 15% were at $z < 1.25$. This resulted in a total density of 2.5 galaxies per square minute of arc and red shift range. This data material will make it possible to determine the luminosity function (number per luminosity interval) of the galaxies with weak emission lines.

The discovery of a large number of extremely red objects (ERO's) was unexpected. The latest discovered population is up to six magnitudes brighter at the 2.2 μm wavelength than in the red region of the spectrum. In the 16H field, six of these objects have been discovered, corresponding to a surface density of 0.06 ERO's per square minute of arc. One of these objects is a star of very low mass, but the majority of the ERO's are probably galaxies at red shifts of $z > 1$ in which there is either a very old red stellar population, or else large quantities of dust are present, causing intense reddening of the starlight. Both types of galaxy would be very interesting.

As well as galaxies and quasars, CADIS can also be used to identify and classify stars. Surprisingly, a good many stars were located above the disk of the Milky Way. This discovery seems to confirm the so-called model of a »thick disk«. According to this model, considerably more stars are located in an area between 1000 and 4000 pc (3200 and 13000 light years) above the galactic disk than would be expected on the basis of simple models of the Milky Way system. If this supposition is confirmed, it will result in far-reaching consequences for theories of the formation and evolution of the Milky Way system.

II.3 ISOPHOT – A Celestial Explorer in the Infrared Range

Infrared Astronomy

Since the start of the 1980's, infrared astronomy has been developing at a breathtaking pace: it has been possible to keep on raising the sensitivity of semiconductor detectors again and again, and the observable range has been constantly extended to include higher wavelengths. At the same time, the size of the detector arrays and the spatial resolution of the images obtained has been continuously increased.

From the earth, infrared astronomy is possible in atmospheric windows at about 2.5 mm and between 3 mm and 5 mm, or between 8 mm and 13 mm. Outside of these windows, molecules in the earth's atmosphere – particularly water and carbon dioxide molecules – absorb the radiation from space. For this reason, infrared astronomy is carried out in observatories at very high altitudes, as well as with telescopes carried by balloons, aircraft and especially satellites.

In particular, cosmic infrared sources comprise dust-rich regions and regions where stars are being formed inside large dust clouds, within which molecules can form. In this connection, astronomy benefits from the fact that the absorption of infrared radiation by dust is considerably weaker than the absorption of visible light. As a result, processes taking place in the interior of the clouds become visible in the infrared range. However, although the cool dust appears entirely black on the opti-

cal photographs, it radiates in the infrared range due to its intrinsic thermal emission. In this way, it serves as an indicator of the formation of stars in other galaxies.

At the same time, numerous chemical elements can also be detected in the infrared range: examples include atomic and singly ionised carbon, and molecules such as water and carbon monoxide. On the one hand, observations of molecule emission lines are used to determine the concentration of those substances and the physical conditions which prevail there, such as density and temperature. On the other hand, the Doppler effect can also be used to determine the state of movement of the gas, for example in the interior of a dust cloud.

ISO, the Infrared Space Observatory

The first complete sampling of the sky at the wavelengths of 12, 25, 60 and 100 mm was accomplished in 1983 with the Infrared Astronomical Satellite, IRAS, built by the Netherlands, Great Britain and the USA. This satellite had a lifetime of ten months. Its successor was the Infrared Space Observatory, ISO, belonging to the European Space Agency, ESA. Unlike its predecessor which carried out a fixed pre-programmed sampling

Fig. II.13: The Orbit of ISO.
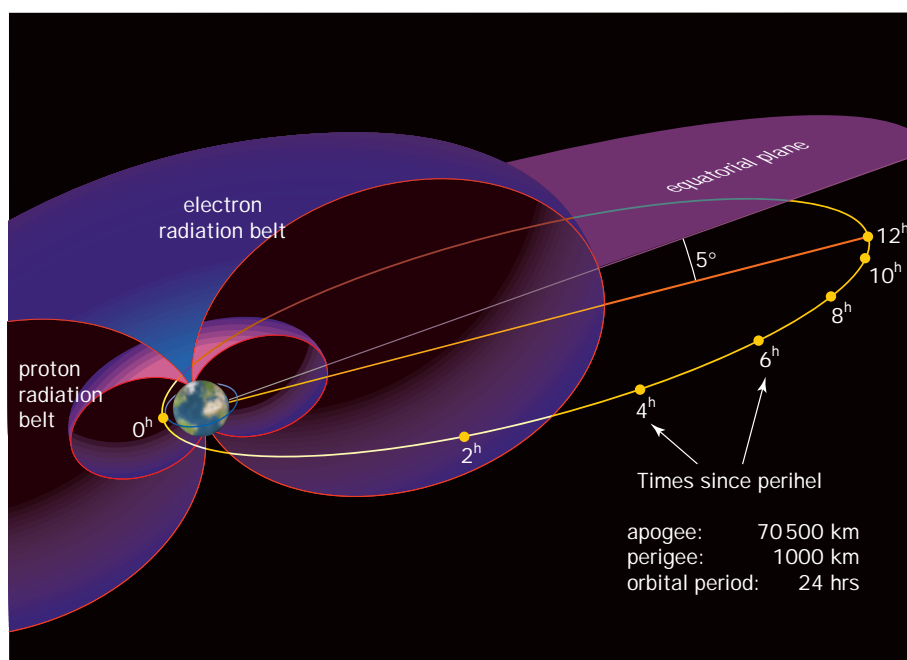
program, ISO observed selected infrared sources under the direct control of the astronomers on earth. The wavelength range was extended as far as 240 mm, the detection sensitivity was raised by a factor of one hundred, and high-resolution spectroscopy and polarimetry of very weak sources were also made possible for the first time in this wavelength range.

ISO was launched from an Ariane 4 on 17.11.1995 into a highly elliptical orbit, on which its distance from earth varied between 1000 and 70000 km within 24 hours (Figure II.13). On every orbit, the observatory traversed the earth's radiation belt. The instrument had to be switched off during this phase. 16.5 hours per day were available for observations.

The experts had originally aimed for a lifetime of 18 to 20 months. When the satellite was switched off in April 1998 because its reserves of coolant were exhausted, it had worked for almost 29 months and during this period, it had carried out approximately 26 000 individual observations. This meant that ISO had far exceeded expectations, turning it into the most successful infrared mission of the 1990's.

ISO had a 60 cm mirror, together with four scientific instruments (Figure II.14): ISOCAM, a camera and polarimeter for the range from 2.5 µm to 17 µm; ISOPHOT, a photopolarimeter, camera and spectrophotometer for 2.5 µm to 240 µm; and SWS and LWS, two spectrometers for the ranges from 2.4 µm to 45 µm and 43

µm to 197 µm. ISOPHOT was built under the direction of the MPIA, in collaboration with the DASA's main contractor, Dornier Satellitensysteme GmbH. The cooled focal plane instrument was built by the Carl Zeiss company. Other contributors included the MPI für Radioastronomie/MPI of Radio Astronomy, Bonn and the MPI für Kernphysik/MPI of Nuclear Physics, Heidelberg. Another German institute with a particular part to play in the ISO was the MPI für extraterrestrische Physik/MPI of Extra-Terrestrial Physics in Garching, which was heavily involved with the construction of the SWS.

The telescope was cooled by 2,140 litres of superfluid helium, so that the instruments operated at a temperature of 1.8 K. This is the only way in which it is possible to detect infrared sources which emit thermal radiation at temperatures as low as 12 Kelvin. In many respects, this called for developments on new technological territory. Almost all the components had to be newly developed, from the detectors and filters and the read-out electronics through to the black paint used on all the reflecting parts in the interior. Completely new features at such extreme temperatures included moving parts to drive filter wheels, gratings and locks with high reliability and low power consumption in the range of a few milliwatts. Success confirmed this concept, which was modified in relation to IRAS: the filter wheels, for example, carried out more than one million steps without any problems.

Fig. II.14: The 5.4-metre long Infrared Space Observatory, ISO, in the assembly hall at Aerospatiale. 2300 litres of superfluid helium cool the entire satellite down to near absolute zero. (Photo: DASA)

ISOPHOT

ISOPHOT, which was developed under the coordinating management of the MPIA, showed its strengths in providing evidence of weak sources at the longest – and hitherto largely unresearched – wavelengths of up to 240 µm (Figure II.15). In particular, the extension of the sensitivity range was made possible by the use of so-called stressed detectors. These are cube-shaped light-sensitive semiconductors made of silicon or germanium, with typical edge lengths of one millimetre. In photodetectors of this sort, the electrical conductivity increases with the number of photons absorbed. By targeted contamination (doping) of the crystals with extraneous atoms, the sensitivity can be extended to higher wavelengths. Above and beyond this, the sensitivity range can be extended to even greater wavelengths if the crystals are built into a small »vice« and are exposed to mechanical pressure. In series of experiments lasting many years at Battelle, Frankfurt, it was finally possible to develop stressed germanium crystals doped with gallium atoms which are sensitive up to a wavelength of 240 µm. These were used for the first time in ISOPHOT.

ISOPHOT could be operated in several modes: photometric measurements were possible over the entire spectral range, and there were 13 aperture sizes and 25
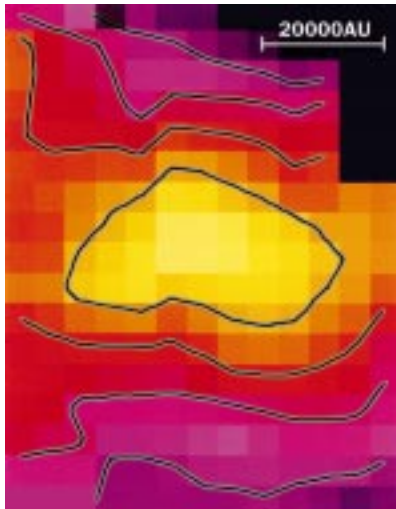
Fig. II.15: Astronomers in Heidelberg used the ISOPHOT to discover a prestellar core with a temperature of 12 Kelvin in the Ophiuchus dark cloud.

filter ranges to choose from. As well as broad-band filters, there were also narrow-band filters to detect emission bands such as those from SiO or polycylic-aromatic hydrocarbons (PAH's), which were suspected to be a major component of the interstellar dust. Two cameras, one with nine sensor elements (C100 camera) and one with four sensor elements (C200 camera) were sensitive to the long-wave range from 60 to 240 mm. Polarimetry was also possible up to the longest wavelengths. A spectrophotometer developed in conjunction with Spanish scientists simultaneously supplied spectra from 2.5 to 5 mm and from 6 to 12 mm at a resolution of $\lambda/\Delta\lambda = 90$. A chopper was available as an option in all the modes.

By way of payment for the development of the instruments, the scientists responsible were each given 6.5% of the usable mission time. For the MPIA, this resulted in a total of 730 hours of pure observation time. ISOPHOT proved to be the most-used instrument on ISO (Figure II.16).
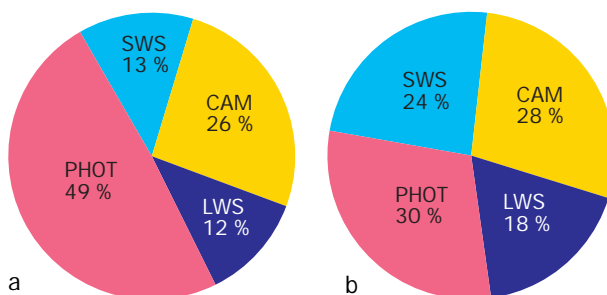

Fig. II.16: ISOPHOT was the most intensively used instrument on board ISO. This is true both for the number of observations (a) and observation time (b).

The ISOPHOT Data Centre

ISO has sent an enormous amount of observation data back to earth, and this has to be carefully calibrated and archived. The respective observer only has the sole right to the data for one year, after which ESA makes them accessible to the public. It is therefore particularly important to have a clearly arranged archive, organised on the basis of objective criteria. This task was accomplished when ESA set up a central archive at its station in Villafranca, Spain, and in addition to this, the four institutes under whose direction the instruments were constructed also built up a data centre. Furthermore, the MPI für extraterrestrische Physik/MPI of Extra-Terrestrial Physics at Garching is also setting up a data archive for the SWS spectrometer in whose construction it participated.

The Heidelberg ISOPHOT Data Centre was installed on the premises of the Astrolaboratory at the MPIA, and it went into full operation in 1997. A total of 8 posts (including doctorate students) were required for this purpose. In collaboration with the ISO Science Operations Center, Madrid, the »PHT Interactive Analysis« (PIA) standard software was developed at the MPIA in order to evaluate the raw data supplied by the satellite.

By the end of 1997, 23 gigabytes of raw data had been stored here on 807 CD-ROM's. Updated versions of the pipeline software are constantly being compiled so that the observation data can be evaluated with ever-increasing precision. The sixth version was already available in 1997, and others will follow. In the near future, the data will cease being stored on CD-ROM, and instead they will be archived on the new DVD (Digital Versatile Disk) medium. DVD's have about ten times the storage capacity of CD-ROM's.

As well as pure archiving, the Heidelberg Data Centre functions in particular as a service facility for visiting scientists. In 1997, 99 astronomers visited the data centre, where they received support with data evaluation over several days (and occasionally over several weeks). The institution is financed until the end of 2001.

Highlights in 1997

ISOPHOT observations were already causing a sensation as long ago as 1996 when, for example, proof was obtained for the first time of carbon dioxide ice particles in regions where stars are being born. CO_2 ice is probably a component of the ice mantles of dust particles. Equally surprising was the discovery of very cool condensation in the interior of dust clouds. The temperature of these probable pre-stellar cores is about 12 to 15 Kelvin.

Due to the unexpectedly long lifetime of the observatory, increased efforts were called for in order to calibrate the data. It should therefore come as no surprise that

the evaluation of the enormous volume of data material is still in the initial stages, and the scientific harvest has only just begun to be reaped. There is no doubt that the observations carried out with ISO will continue to occupy astronomers for a decade, and scientific publications can only be expected to climax after several more years. Below, we present some highlights from the results achieved at the MPIA with ISOPHOT.

Dust in the Coma Galaxy Cluster

The space between the galaxies is largely empty. In galaxy clusters, x-ray telescopes have proven the presence of gas at temperatures of several tens of millions of degrees, with an average density of some 103 atoms per cubic centimetre. This means that the intergalactic gas is distributed more thinly – by a factor of about a thousand - than the diffuse interstellar gas in the galaxies. Arguments have raged over several decades as to whether dust is also present in galaxy clusters.

One argument against this proposition was the presence of hot intergalactic gas, in which dust cannot exist for long. But various vague observed indications spoke in favour of it. The matter was brought to a head by investigations of galaxies and quasars which lie behind galaxy clusters. Here, there were indications that the surface density of observable background galaxies declines towards the central region of a cluster located in the foreground. This could be explained by a homogeneous distribution of dust in the interior of the cluster. The consequence of this would in fact be that the light which passes through the central region is absorbed more heavily than the light in the outer regions. However, previous studies of this sort have not been convincing: they have only led to estimates that the visual extinction in the central region of the Coma cluster must amount to less than 0.3 magnitudes. An investigation of 56 clusters using the IRAS data and eleven clusters in the sub-millimetre range produced no clear evidence in favour of thermal IR emission from diffusely distributed intergalactic dust. A problem which arises here is the irregularly structured emission of the galactic cirrus, caused by dust in our Milky Way.

The question of intergalactic dust is interesting for a variety of reasons. On the one hand, it would contribute to the total mass of the clusters, if only to a small extent. On the other hand, due to its extinction, it would show more remote galaxies as redder and fainter than they actually are. This would have effects on distance determinations, of the sort which are not undertaken using the spectra of the objects, but on the basis of their colour. Moreover, the dust could supply some indication as to the dynamic age of the clusters, since the dust particles are constantly being destroyed by the hot gas, and this accordingly means that they also have to be »topped up« again.

Thanks to ISOPHOT, a new possible approach to this old problem has now been created, enabling us to observe galaxy clusters in the hitherto inaccessible range above 100 mm. In July 1996, a one-hour examination of the Coma galaxy cluster became possible. This cluster, which is rich in galaxies, is located at a distance of 138 Mpc (or about 450 million light years), and in the X-ray range, it shows intensive radiation of intergalacitc gas.

Observations were made in two wavelength ranges around 120 μm and 185 μm with the C200 camera, whose detector consists of a 2 × 2-array stressed Germanium-Gallium crystal. The Coma cluster was scanned along two axes running transversely to one another, and for each scan line, 16 fields were photographed at 3 ×3 square minutes of arc. The two scans crossed over in the central region, at the location of the elliptical galaxy NGC 4874. One of them – the east-west scan – also traversed a second elliptical galaxy with the designation NGC 4889. As expected, it was not possible to detect either of the galaxies, since they do not contain enough cold dust. A bright object was apparent at the end of the east-west scan. This is the IR spiral galaxy IC 4040, which has already been detected with IRAS and is a member of the Coma cluster.

In order to detect possible extended IR radiation from the interior of the cluster, the images had to be carefully calibrated and corrections had to be made for interference effects such as impacts of cosmic radiation particles on the detector. For the subsequent analysis, the IR fluxes of the four detector elements were firstly determined on an individual basis for each image, and then they were averaged, thus providing two one-dimensional flux distributions through the cluster.

Neither of the scans showed any significant increase in IR radiation from the Coma cluster. However, the picture was different after the ratio of intensities at 120 mm and 185 mm was formed in the scans. In this case, an almost symmetrical increase in intensity was recognisable around the central region (Figure II.17). The reason why this IR radiation only became apparent when the ratios were formed is that the dust in the Coma cluster has different radiation properties than the foreground galactic cirrus. Thus, for example, the Coma dust could have a higher temperature. Assuming a radially symmetrical distribution of intensity for the IR radiation, the average from the two scans was formed in favour of a minor statistical error: and when this was done, the effect emerged even more clearly.

It was now assumed that the radiation in the peripheral regions of the cluster originates from the galactic cirrus. This component was subtracted, by linear interpolation of the intensity assigned to it between the peripheral points. This left an excess radiation of approximately 0.1 MJy/sr at 120 μm in the central region, with a diameter of 10 minutes of arc, corresponding to 0.2 Mpc (0.65 million light years). On account of the pre-
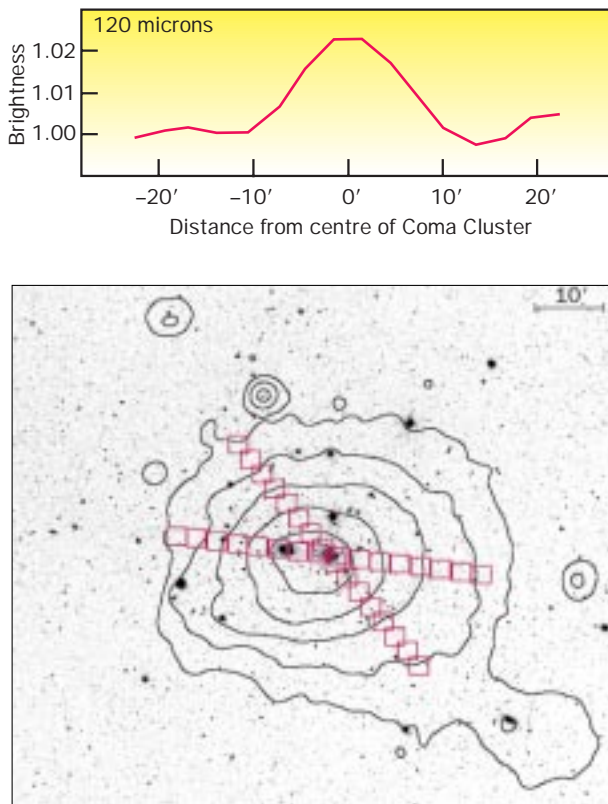
Fig. II.17: Dust in a cluster of galaxies was detected for the first time, using ISOPHOT. Two scans through the Coma cluster (bottom) showed a nearly symmetrical dust distribution around the centre (top).

vious subtraction, this value represents a lower limit for the radiation from the Coma cluster.

It is not possible to derive an unambiguous temperature for the dust from the IR flows measured in the two wavelength ranges. The temperature also depends on the radiation properties of the particles. Using two different assumptions, lower limits for the temperature are obtained of 26 Kelvin or 38 Kelvin respectively. At the same time, an upper temperature limit of 55 or 80 Kelvin respectively can be derived from the fact that the dust was not registered with IRAS at 60 μm. Now, if we assume a homogeneous distribution of the dust and specific radiation properties of the dust particles in the central region with a diameter of 0.2 Mpc, values for its total mass of between 6.2×10^7 and 1.6×10^9 solar masses are obtained.

Observations with ROSAT, the X-ray satellite, yielded a mass of 5×10^{12} solar masses for the hot gas in this region. This means that the average gas/dust ratio in the Coma cluster is between 1.3×10^{-5} and 3.2×10^{-4}. In comparison with the interstellar dust, therefore, the dust in the Coma cluster is depleted by a factor of 20 to 600, and this results in a visual extinction in the central region of between 0.01 and 0.2 magnitudes.

The question of the origin of the dust is now of interest. According to model calculations, it should be vapo-

rised in the interior of the hot gas within a hundred million years. Two possibilities are currently feasible: either the dust is constantly being blown out of the galaxies into intergalactic space by stellar winds, or else it was swept out of the galaxies when two galaxy clusters fused with one another. The second scenario in particular could apply to the Coma cluster, because various observations suggest that this galaxy cluster has a relatively low dynamic age, and that it consists of two interpenetrating or merging clusters whose central galaxies were once NGC 4889 and NGC 4874 respectively.

In order to verify this hypothesis, a project is currently in progress at the MPIA to search for dust in clusters of different types, and of different suspected dynamic ages. If the hypothesis is correct, then no dust should be found in old, relaxed clusters, whereas dynamically young clusters which are apparently merging with one another should show large amounts of dust.

The NGC 6090 Starburst Galaxy

One of the outstanding results of the IRAS mission was the discovery of a class of galaxies which shine considerably more brightly than normal galaxies in the remote infrared range. At wavelengths of about 60 μm, normal spiral galaxies irradiate much less energy than in the blue range. By contrast, the IRAS galaxies are up to one hundred times brighter in the far infrared range than in the blue range. In IR, they can generate more than 10^{12} solar luminosities, meaning that they are among the most luminous celestial bodies of all after the quasars.

The explanation for these IR galaxies is that a phase of increased star formation is taking place within them. In extreme cases, star formation rates of 100 solar masses per year have been determined, which is several tens of times higher than the rate in normal spiral galaxies such as the Milky Way. For this reason, these systems are also called »starburst galaxies«. The large numbers of hot young O and B stars heat up the surrounding dust, which then irradiates the absorbed energy in the infrared range again. In many cases, the starburst is triggered by tidal forces which occur when two galaxies move past one another in close proximity, or even penetrate one another.

NGC 6090 is a starburst galaxy at a distance of 117 megaparsec (or about 380 million light years), which radiates more than 10^{11} solar luminosities in the infrared range; it has also been observed by IRAS. On optical photographs, it can be seen that NGC 6090 consists of two merging galaxies. Their two cores are at a projected distance of 6.4 seconds of arc from one another (corresponding to 12 000 light years). This object has already been examined at 1.3 mm and in the UV range. ISO has now created the additional possibility of examining NGC 6090 from the near to the distant infrared range,

where the galaxy radiates its maximum energy. Thanks to ISOPHOT, NGC 6090 has been studied with the C100 and C200 cameras (60 μm to 200 μm), the photometer (3.6 μm to 200 μm) and the spectrometer (2.5 μm to 11.6 μm) (Figure II.18).

From the spectral progression which was observed, it was possible to calculate that the galaxy is radiating 2.8×10^{11} solar luminosities in the entire range from 3 μm to 240 μm. Half of this alone comes from the range between 40 μm and 120 μm. A simple model can be used to derive a star formation rate of 21 solar masses per year from this. By using the spectrometer, it is also possible to establish unambiguous proof of emission bands from polycyclic-aromatic hydrocarbons (PAH's) (Figure II.19).

Thanks to these measurements, the spectrum in the infrared region was therefore well known. This made it possible to draw comparisons with theoretical models. The general approach of models of this sort consists in the assumption of three dust components: 1) cool cirrus dust which is heated up by the interstellar radiation field; 2) warm dust in the star formation regions; and 3) hot dust in the environment of an active core area, which is generally associated with a Black Hole. The high intensity ratio of I (60μm) / I (25 μm) argues against an active galactic core just as much as observations in the optical range. At the same time, the ISO measurements point to a dust temperature of more than 25 Kelvin, which argues against significant contamination by cirrus dust.

It was ultimately possible to obtain a very good reproduction of the measured spectrum with the help of a model which was developed by colleagues at the MPI für Radioastronomie/MPI of Radio Astronomy in Bonn in 1994, and was then used successfully on the close starburst galaxy M 82. This model takes account of hot stars in population I, which greatly heat up the dust in their surroundings and form so-called Hot Spots, and also of cooler stars in population II, which generate a rat-
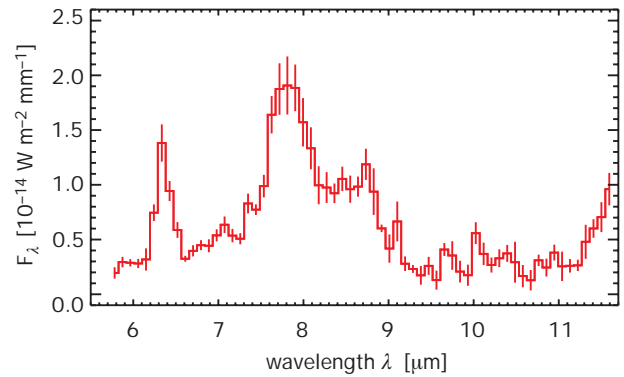

Fig. II.19: The spectrum of NGC 6090 recorded with ISO-PHOT. Emission bands show up at wavelengths of 6.2, 7.7, 8.6 and 11.3 μm, which probably originate from polycyclic aromatic hydrocarbons.

her uniform IR radiation field from the heated dust. Above and beyond this, the model takes account of very small dust particles and of PAH's. The latter are significant on account of their emission bands between 3 μm and 14 μm.

This model gave very good reproduction of the spectral energy distribution of NGC 6090, which had been measured with ISOPHOT. Even so, it could not explain the strong emission above 100 μm. To cope with this, the group at the MPIA added an additional dust component to the model, with an approximate temperature of only 20 Kelvin; in order to explain the observations, the total mass of this component must be approximately 108 solar masses. This component turns out to constitute the lion's share of all the dust in NGC 6090. If a temperature of about 50 Kelvin is assumed for the dust in the star formation areas, this warmer component only contributes 106 solar masses to the total mass of dust.

Although cool dust at temperatures below 20 Kelvin had already been suspected, its presence could not be proven with IRAS, since the sensitivity of this satellite only extended to a wavelength of 100 μm. With ISO, the astronomers now found surprisingly large quantities of dust with temperatures of 12 to 15 Kelvin. Moreover, an

Fig. II.18: The Starburst galaxy NGC 6090, recorded as an optical image (left) and at a wavelength of 60 μm with ISO-PHOT (right).

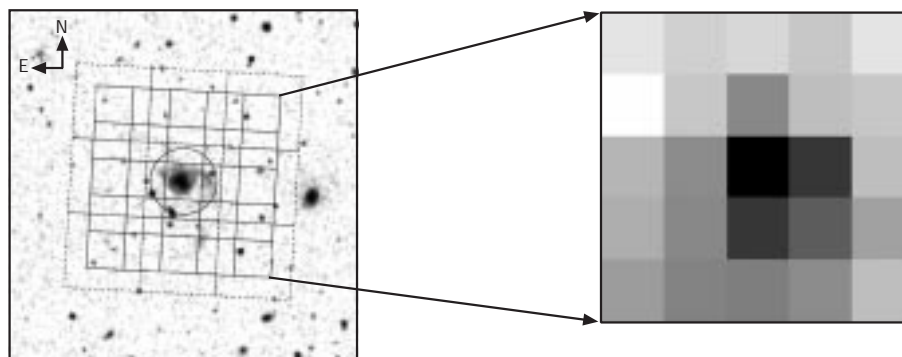initial analysis suggests that the dust particles are relatively large.

Random Sampling in the Far Infrared Range

Since ISO was examining individual objects rather than carrying out a continuous sampling of the sky, the instrument had to be slewed from one celestial position to the next between the separate observations. Although the observation sequence was optimised by means of computer programs so that the minimum of time was lost, longer slews of more than a hundred degrees were still unavoidable every now and then. In order to make some use of this slewing time, it was decided to switch the ISOPHOT's C200 camera on during the slews. This yielded one-dimensional scans across the entire sky in the far infrared range around 200 μm, which had remained unexplored until the ISO mission (Figure II.20). During the slews, the satellite attained a maximum speed of 8 minutes of arc per second. At a read-out frequency for the detector of 8 images per second, the maximum interval between two consecutive detector positions was therefore one minute of arc. During the acceleration phase at the start of each slew and the deceleration phase at the end, the speed was less, which also meant that the distance between two consecutive detector positions was shorter.

This technology was intended to enable the detection of point-shaped sources as well as extended IR sources.

Fig. II.20: Map of all the slews across the sky carried out by ISO during its mission. This normally wasted time was exploited for a random sampling with ISOPHOT at a wavelength of 200 μm.

In this way, it was possible to make additional use of some 550 hours throughout the entire mission, corresponding to five per cent of the observation time.

The evaluation of these data calls for special techniques which were initially tested under the auspices of a so-called minisurvey, in a selected region close to the ecliptical north pole. This field comprises about one hundred square degrees, and it features a low radiation background due to galactic cirrus, as was already known from the IRAS data. By August 1997, the region had been swept by a total of 337 slews with a total length of 1263 degrees, corresponding to 4.22 hours of observation time (Figure II.21).

In the first evaluation phase, the objective was to prove the existence of point sources in the minisurvey (Figure II.22). For this purpose, it was initially necessary to subtract the diffuse background emission coming from the cirrus. This was achieved by eliminating all those signals whose sources are broader than ordinary point sources. By doing this, however, we also lose circular extended objects such as close galaxies or planetary nebulae. In the case of extended cirrus structures such as elongated filaments or condensations, the procedure is not unambiguous. If the image field of the detector happens to cross a filament of this sort perpendicularly to its longitudinal extension, the software may possibly register this structure as a point source; if it passes over the filament diagonally, it will appear to be extended. Improved software should make it possible to differentiate between critical cases of this sort as well.

The data material which is processed in this way also contains signals caused by the impact of cosmic particles. These are narrower than those of real IR sources, and this allows them to be identified. In the minisurvey, all the remaining signals which were only slightly above
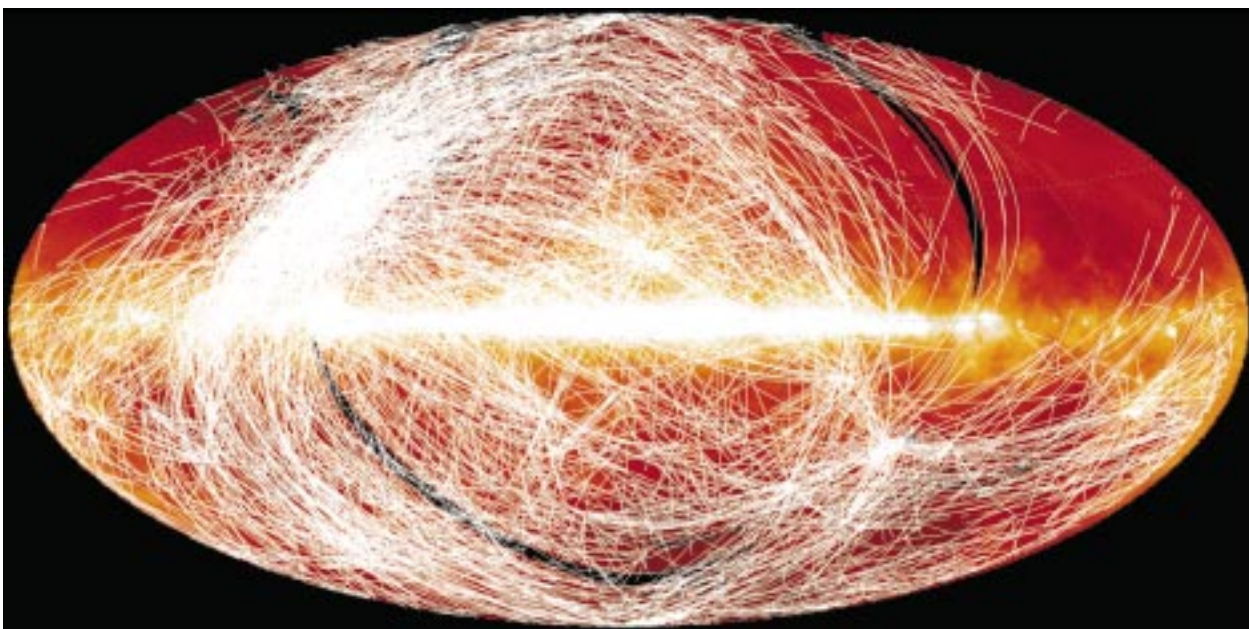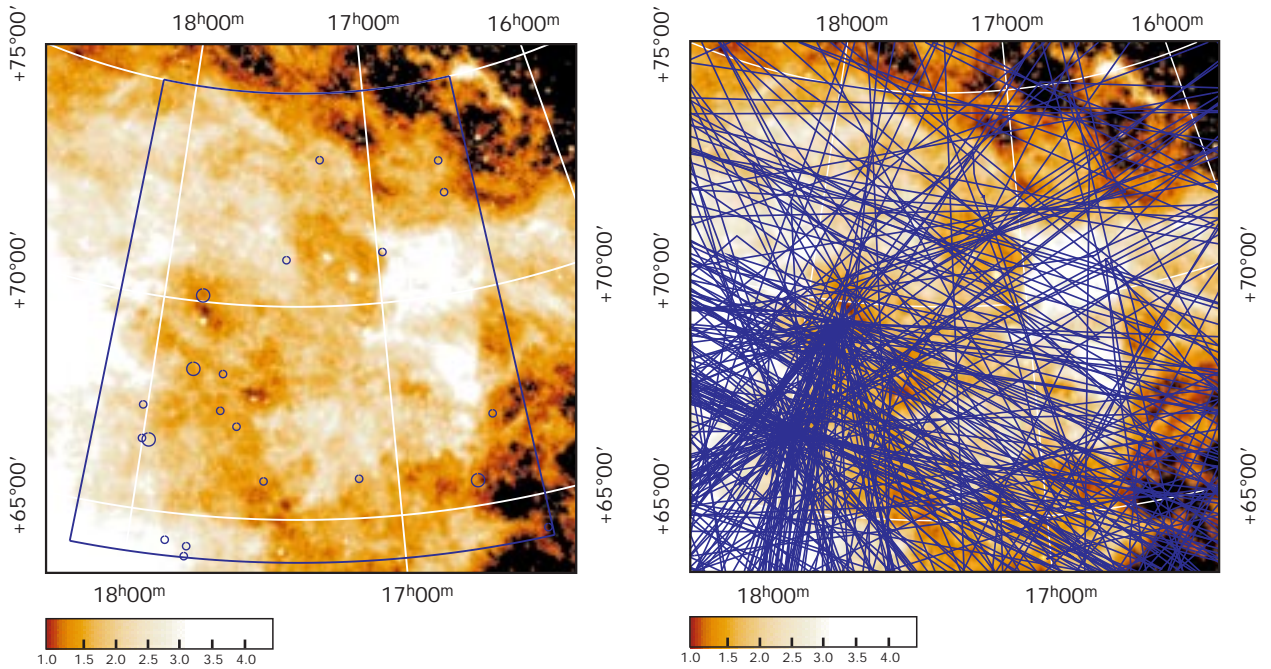
Fig. II.21: (Left) Celestial field in the northern mini-random sampling. (Right) ISO's slews in the same field.

the background noise (two σ) were evaluated as real, which also guaranteed the detection of very weak sources. In order to determine the absolute radiation fluxes of the observed objects, a special procedure was needed which had to solve the following basic problem: during the slew, the image of the object passes in any random direction over the detector, which consists of four imaging elements. For example, this means that a source can be registered by three elements, but it may also be registered by only one element. In the least favourable case, the object only glances the external areas of the detector, so that not even the maximum of the intensity distribution passes over the detector. Now, on the basis of the signals originating from the imaging elements, the software calculates a two-dimensional Gauss distribution, which gives a first approximate description of the intensity profile of the point sources. This has made it possible to determine the absolute values of the intensities within a precision of 30%. The absolute values could only show uncertainties up to a factor of two to three in the least favourable case. In the future, the Gauss fit is due to be replaced by an analytical intensity profile which is better suited to the observation conditions.
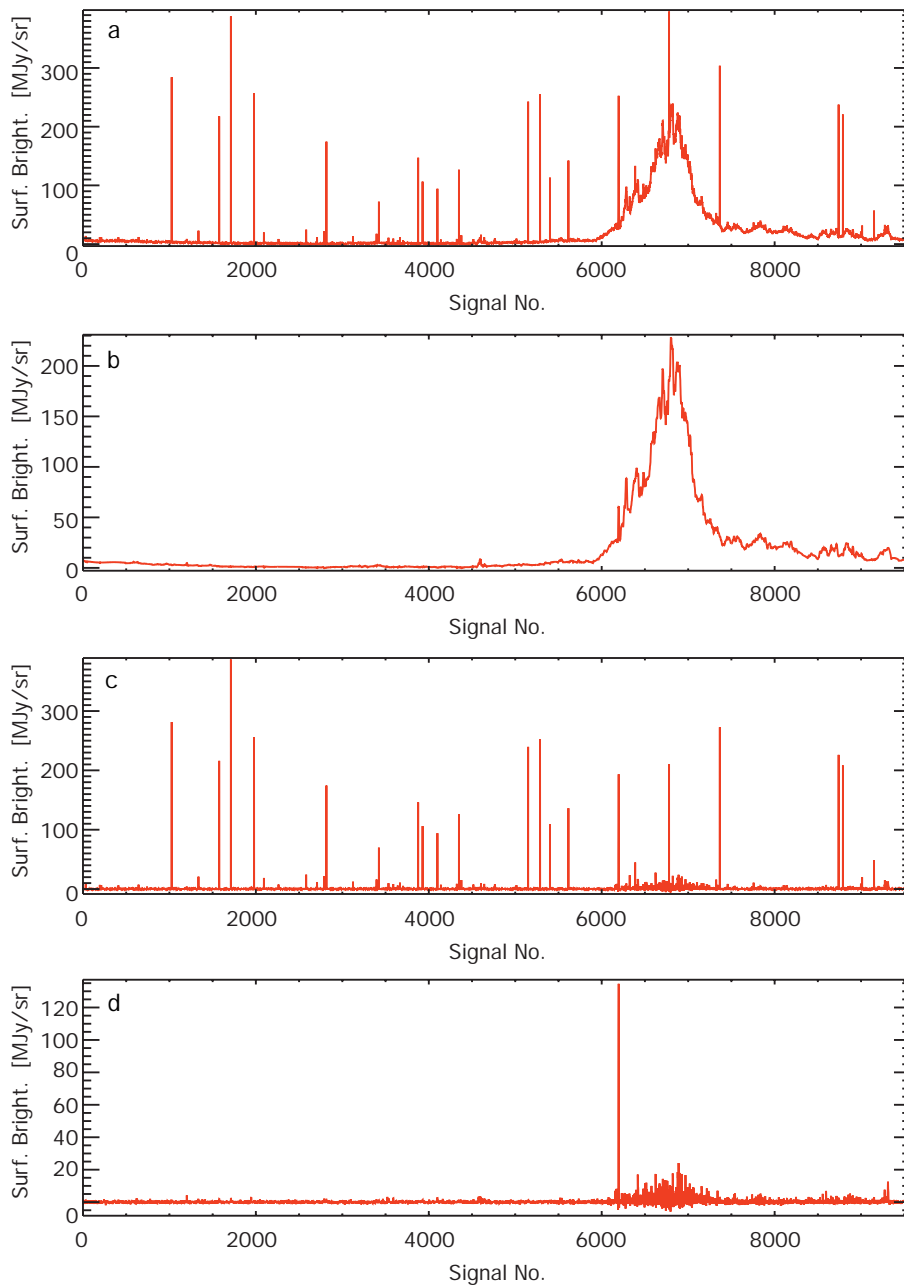
The slews in the minisurvey area which were processed in this way led to the following results: all point sources with a brightness of at least 5 Jy were registered, as also expected by comparison with the IRAS catalogue. Between 2 and 5 Jy, the probability of detection was 90%; below 2 Jy, it dropped to 50% of all IRAS sources.

Among the reasons which explain this is the fact that ISO's track in the sky during the slew is only known with an accuracy of about one minute of arc, so that some expected sources only glanced the edge of the detector field and their signal remained below the detection limit.

All in all, ISO registered 21 IR sources in the area of the minisurvey. A comparison of these objects with optical images showed that they were almost exclusively galaxies, and that only one object is located in the Milky Way: this is the planetary nebula NGC 6543. Another object with the designation IRAS 16384+7313 is probably a bright condensation in the galactic cirrus. Of the 19 galaxies, 8 turned out to be bar spirals, and two were interacting pairs of galaxies. Since spectra of some galaxies already exist, it was possible to show that galaxies with red shifts of up to z = 0.1 can be detected in connection with the random sampling.

The minisurvey then allows extrapolations of the number of IR sources to be expected from the total random sample. Accordingly, it should be possible to detect an average of one source brighter than 2 Jy for every 40 degrees of slew length. This is equivalent to a surface density of 0.5 objects per square degree, which corresponds extremely well to the IRAS catalogue, where 0.5 extragalactic objects per square degree are also listed in the area of the minisurvey. Since a length of 150 000 degrees was swept in the course of the entire ISO mission, corresponding to coverage of approximately 17% of the sky, measurements for the flow at a wavelength of 200 μm should be available for about 4000 galaxies – and in most cases, this will be for the first time.

This database will contribute towards determining the nature of galaxies with intense emission in the far infra-

red range. As well as this catalogue, which consists predominantly of extragalactic point sources, the 200 μm strip cards are now being sampled on the basis of the coldest places in the Milky Way. As a result of this, a second catalogue will be compiled, containing prestellar cores, globules and other galactic objects. This will be of major importance for the observation of star forming regions.

Fig. II.22: Procedure used in the identification of point-sources during the random sampling. (a) The signal obtained along the slew, (b) background recorded with automatic software, (c) difference between the original signal (a) and the background (b). In (c), the spikes caused by the impact of cosmic particles are eliminated. (d) End-result: the only remaining point-source around signal number 6100 could be identified as galaxy NGC 6946.

The spiral galaxy Messier 51 in an image taken with the CCD camera MOSCA (see p.34) at the 3.5-metre telescope on Calar Alto.

III Development of Instruments

One of the essential criteria governing the performance of a telescope is the size of its main mirror. But an equally decisive factor is the choice of the detector which registers an image of the targeted section of the sky or a spectrum of the observed source of light in the focal plane. For about one hundred years, astronomers used photographic plates as the means of recording the image; their emulsion has a quantum yield of less than one per cent, which means that a specific point on the emulsion must be impacted by more than one hundred light particles before it will register one of them.

Since the start of the 1980's, astronomers have had so-called Charge Coupled Devices (CCD's) at their disposal. These are light-sensitive semiconductors which attain quantum yields ranging from 60 to almost 100 per cent, depending on the wavelength (Figure III.1). By using these devices, a 50- to 100-fold increase is made possible in the sensitivity of the detectors, and hence in the efficiency of the telescopes. These miniature plates, just a few square centimetres in size, consist of a large number of light-sensitive pixels (picture elements). The largest CCD's have several million pixels. The light arriving at each individual pixel generates an electrical charge which is stored in the pixel. At the end of each exposure, an electronic system reads out the CCD chip, and a computer converts the charge distribution that has been registered into an optical image. The new detectors also offer some other decisive advantages: the number of charge carriers that are generated is directly proportional to the intensity of the incoming light, and the digital images that are produced are immediately available for further evaluation in the computer.

Nowadays, CCD's are used in commercially available video recorders and even in cameras, but the normal commercial CCD's cannot be used on telescopes. Only chips of the very highest quality are suitable for astronomy. These are produced by companies such as Philips or Rockwell, but detailed tests on their suitability have to be carried out at the MPIA's laboratories before they can be put to use on one of the telescopes.

The instruments themselves – that is, the cameras and the spectrographs in which the detectors are used – are also unavailable through commercial channels: instead, they have to be designed and built individually. In general, the scientist in charge of the project specifies the desired properties of the instrument, and then the prototype is produced in the MPIA's workshops. In a large number of cases, cooperation also takes place with companies, who are not infrequently confronted with entirely new tasks in connection with special orders of this type. The know-how which they acquire in this process strengthens their competitive edge on the world market.

There now follows an overview of the MPIA's more recent measuring instruments.

CAFOS2.2 – Calar Alto Focal Reducer System for the 2.2 Metre Telescope

The large telescopes on Calar Alto have a particularly wide image field with perfect optical quality. In its Ritchey-Chrétien focus, for example, the 2.2-metre telescope has a usable field with a diameter of 67 minutes of arc, corresponding to 33 centimetres. Since CCD's have edge lengths of just a few centimetres, it follows that they can only be used to cover part of the complete image field. A focal reducer system lowers the effective focal distance, and therefore the diameter of a telescope's image field, improving its ability to adapt to the size of the CCD's: it recollimates the beam behind the focal plane, and focuses it in a second focal plane with the help of a camera optic (Figure III.2).
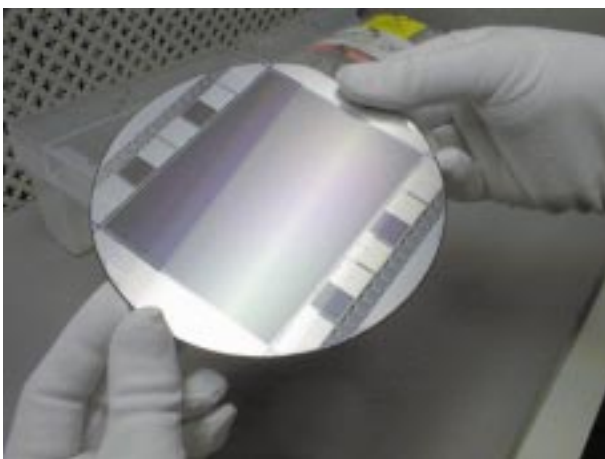

Fig. III.1: Light-sensitive CCDs have largely replaced the photographic plate as a detector in astronomy. The aim is to build ever-larger chips. The picture shows the currently largest CCD, with 7000 × 9000 image elements (format: 8.4 cm × 10.8 cm).
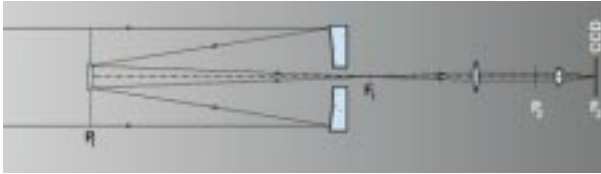
Abb.III.2: The principle of a focal reducer. The converging beam is rendered parallel once again behind the Cassegrain focus (F1), using a collimator. Thus a secondary image of the entrance pupil P1 is formed at P2. This is focused with the camera on the CCD at F2. The effective total focal length f is reduced by the factor f(camera)/f(collimator), so that a large field-of-view is imaged.

The CAFOS2.2 system reduces the effective focal distance of the 2.2-metre telescope from over 17 metres down to 8 metres. This apparatus also makes it possible to use other instruments, such as spectral gratings or prisms. The CAFOS2.2 contains eight so-called »grisms« (derived from the words »gratin« and »prism«). A grism is a prism with the addition of a spectral grating positioned on its rear side. It splits the spectrum of the incoming light throughout the entire visible range of wavelengths from 320 to 950 nanometers. For polarisation investigations, it is also possible to insert a Wollaston prism into the beam path. Another feature is that narrow-band recording is possible thanks to a Fabry-Pérot interferometer. One of its properties is that a very narrow spectral pass range can be adjusted throughout a wide wavelength range. This may be compared with a radio receiver, which can be set to narrow-band radio transmitters throughout a specified frequency range.

CAFOS2.2 excels in the field of direct images and spectral examinations of very faint objects with relatively high spectral resolution. The instrument is used intensively to search for the remotest galaxies in the Calar Alto Deep Imaging Survey, CADIS (Chapter II.2). A control system offers a large number of automatic observation sequences and help routines which free the observer from routine tasks such as series of focusing operations or calibration tests. In the very near future, it is intended to equip the instrument with a largely automated observing mode.

MOSCA – Multi-Object Spectrograph for Calar Alto

MOSCA is a multi-purpose instrument which can be used for direct imaging as well as for spectrographic investigations. This instrument, which went into operation at the end of 1996, is used on the 3.5-metre telescope behind the main mirror bore in the Ritchey-Chrétien focus (Figure III.3 and III.4). MOSCA is a focal reducer which lowers the actual focal distance by a factor of 3.7,

FIG. III.3: The MOSCA infrared camera in operation.

resulting in an effective aperture ratio of f/2.7. This means that it enlarges the image field which can be registered on the CCD chip to 11×11 square minutes of arc, allowing complete imaging of relatively close and large galaxies such as M 51 (see the figure p. 32). The detector currently in use is a CCD with 2048×2048 pixels, which is sensitive through a large wavelength range from 330 nm to 1 micrometer. MOSCA is the counterpart to CAFOS2.2 on the 3.5-metre telescope.

MOSCA is equipped with two filter wheels for direct imaging. One of these contains seven standard filters, while the other can be fitted with as many as ten special filters which the observer can bring along with him to suit his own purposes. A Fabry-Pérot interferometer is also built into the instrument: this can be set as a narrow-band filter (pass width 1.5 to 2 nm) throughout a range from 550 to 950 nm. Six different grating prisms (grisms) with various spectral resolutions are available for spectroscopic investigations.

During 1997, MOSCA was mainly used as a multi-object spectrograph. In this way, simultaneous records can be made of the spectra from several celestial bodies, such as the galaxies in a cluster. For this purpose, a metal plate is inserted in the focal plane of the telescope; slits have already been milled in this plate at precisely measured positions. This pattern of slits corresponds to the
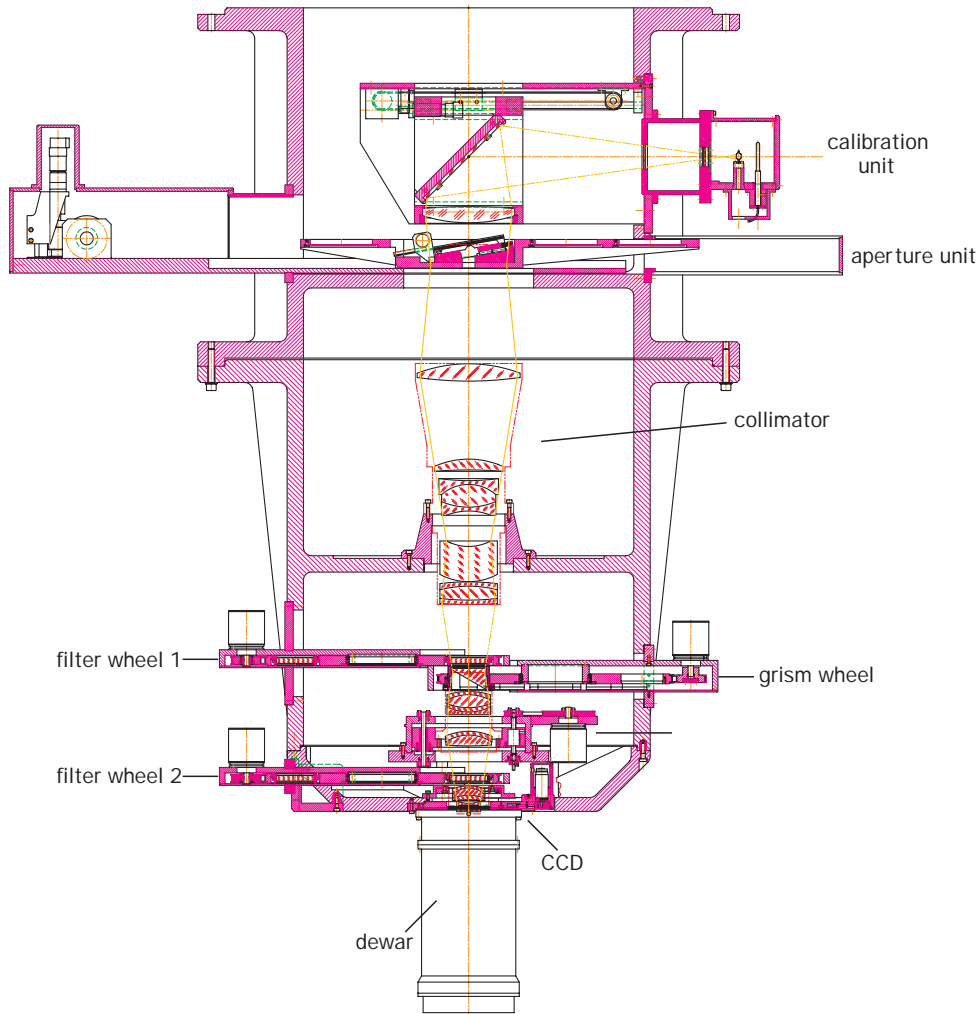
Fig. III.4: MOSCA: schematic diagram.

distribution of galaxies in the focal plane, so that a spectrum from all the celestial objects is obtained simultaneously with one single imaging operation.

The masks can be produced in the MPIA's workshops within a few minutes, to a precision of one micrometer. All users of the instrument, including visiting observers, can have the masks they require produced at the MPIA. Finally, a semi-automatic procedure makes it possible to align the telescope and the mask within 10 to 20 minutes. One example of MOSCA's use was in the search for the remotest galaxies in the Calar Alto Deep Imaging Survey, CADIS (Chapter II.2).

OMEGA-Prime – a Camera for the Near Infrared

OMEGA-Prime (Figure III.5) is the first camera on Calar Alto to be equipped with infrared detectors of a new generation. It began operation in the spring of 1996 on the primary focus of the 3.5 metre telescope. At the heart of the instrument is a chip which was developed in the Rockwell Science Center and at the University of Hawaii, made from a mercury-cadmium-tellurium compound (HdCdTe) with 1024×1024 pixels (Figure III.6). This chip is 16 times larger than its predecessor in the MAGIC camera. Its sensitivity range extends from 1 to 2.5 micrometers, so that it covers the near infrared range. OMEGA-Prime was designed at the MPIA and built in the Infrared Laboratories at Tucson, Arizona.

A filter wheel with 15 positions enables investigations to be made in various wavelength ranges, and excellent image quality throughout the entire field is supplied by a corrector consisting of three optical elements (Figure III.7).

OMEGA-Prime is used in the primary focus of the 3.5-metre telescope, where a large image field of 6.8×6.8 square minutes of arc is obtained. This makes the instrument outstandingly suitable for sampling the sky to locate weak infrared sources such as protogalaxies or brown dwarves, and also for detailed study of star formation regions. OMEGA-Prime was released for general observing operation in the autumn of 1996, and it immediately became the instrument in greatest demand.
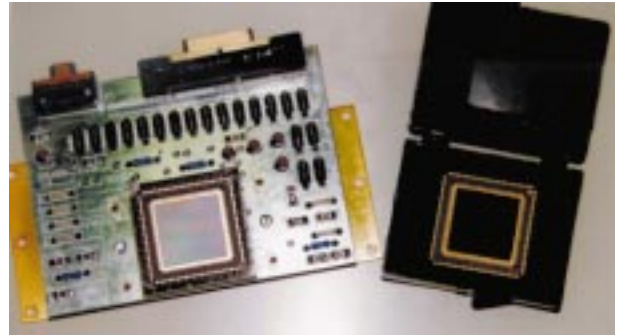
Fig. III.6: OMEGA Prime's CCD unit.
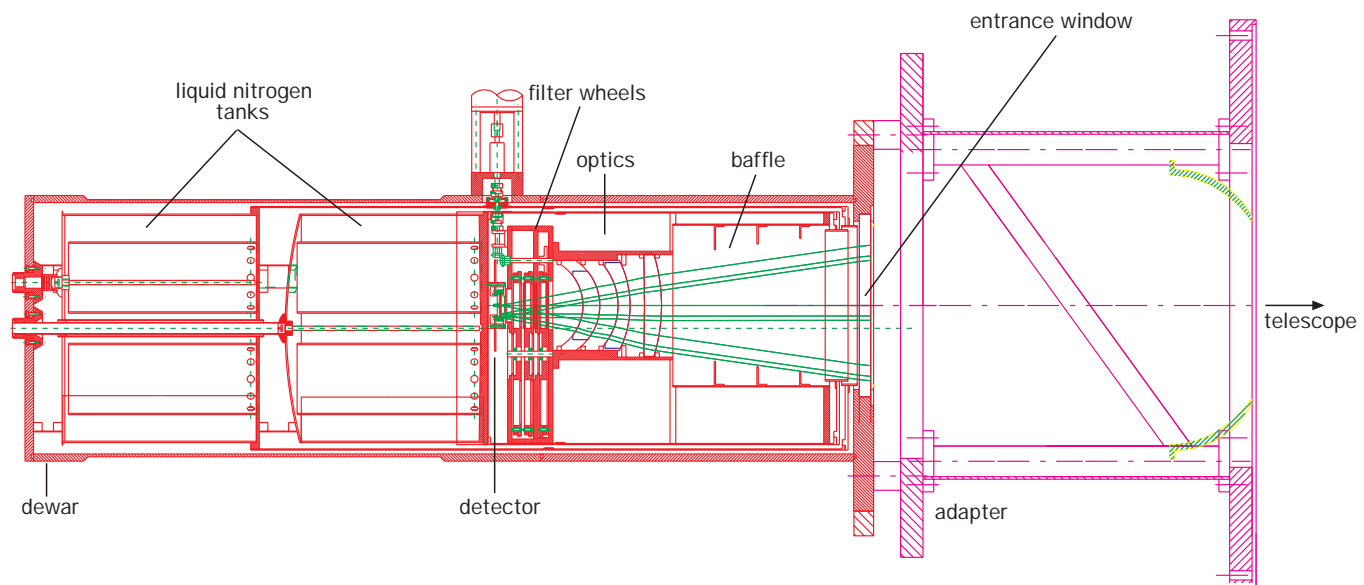
Fig. III.5: The OMEGA Prime camera on a test-rig.

Fig. III.7: OMEGA Prime: schematic diagram.

OMEGA-Cass – Spectrometer and Camera for the Near Infrared

OMEGA-Cass is a further development of Omega-Prime. This instrument (Figure III.8 and III.9) is designed for use in the Cassegrain focus of both the 3.5- and the 2.2-metre telescopes on Calar Alto. As well as direct photography, it can also be used for spectral and polarisation investigations.

The design and construction of OMEGA-Cass was started at the MPIA in the summer of 1996. As in the OMEGA-Prime, an HdCdTe-Array with 1024×1024 pixels operates as the detector, with sensitivity in the wavelength range from 1 to 2.5 micrometers. The imaging scale can be changed by choosing from three different camera optics. In the $f/10$ beam of the 3.5 metre telescope, the scale varies between 0.1, 0.2 and 0.3 seconds of arc per pixel. In conjunction with ALFA, the adaptive optical system, (Chapter II.I), the aperture ratio varies from $f/10$ to $f/25$, yielding values of 0.12, 0.08 and 0.04 seconds of arc per pixel for the imaging scale on the detector.

Two filter wheels can accommodate a total of 18 colour filters which allow imaging in various wavelength ranges. Moreover, OMEGA-Cass offers two possible methods of polarisation analysis. Four filters which

can be rotated in stages of 45 degrees, as well as two Wollaston prisms, supply the linear degree of polarisation for extended sources. Three grisms (grating prisms) give OMEGA-Cass its spectroscopic properties. The spectral resolution $\lambda/\Delta\lambda$ is between 500 and 1000.

At room temperature, every object emits infrared radiation in the sensitivity range of Omega-Cass. This means that the components of the instrument itself would »blind« the detector at room temperature. The instrument has to be cooled in order to prevent this. OMEGA-Cass has two cooling tanks filled with liquid nitrogen, which keep the instrument at the required operating temperature of about 80 Kelvin for more than 36 hours. The external tank cools the outer radiation shield, while the inner tank is in direct thermal contact with the whole internal optomechanical structure.

OMEGA-Cass saw »first light« on the 3.5-metre telescope in August 1997, only 15 months after the start of construction. All three imaging optics are available and the polarisers and grisms are fully integrated. The first tests satisfied all expectations, so OMEGA-Cass is sure to develop into a new »work horse« on the 2.2- and 3.5-metre telescopes.

At the end of 1997, it was suggested that an imaging spectrograph should also be installed in OMEGA-Cass. For this purpose, an array consisting of a large number
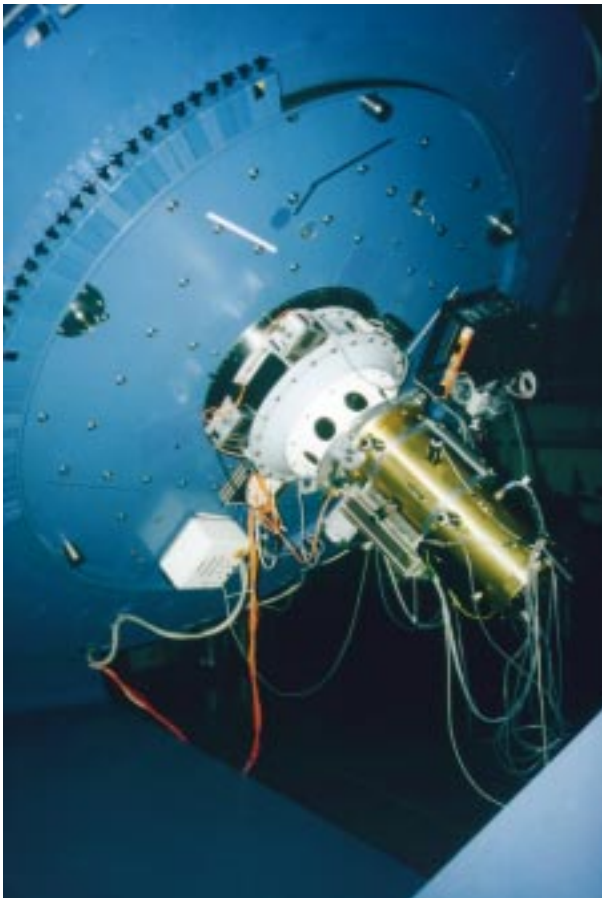

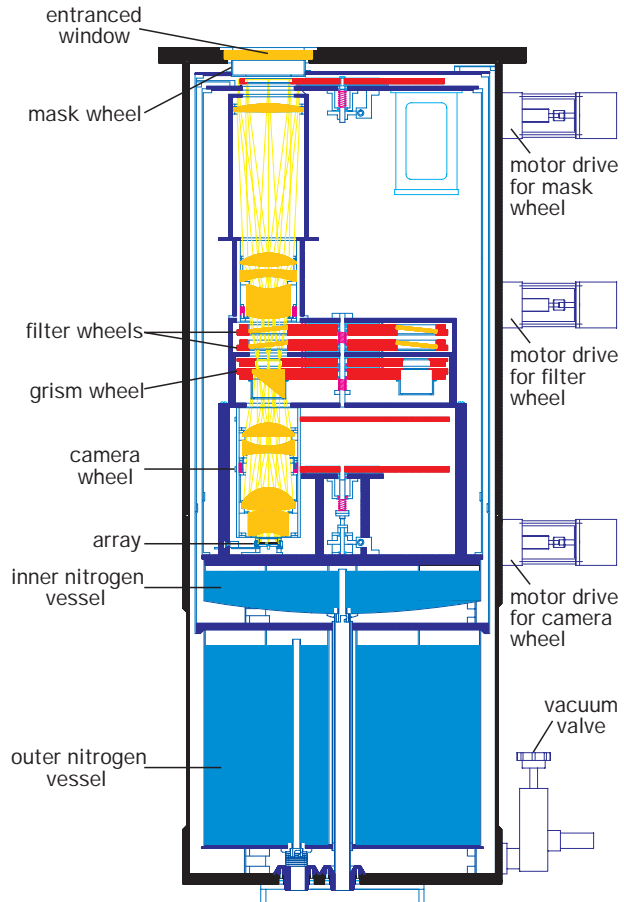
Fig. III.8: OMEGA-Cass at the 3.5-metre telescope.

Fig. III.9: OMEGA-Cass: schematic diagram.

of individual lenses is to be positioned in the focal plane. This will allow a small spectrum to be produced for each of about 100×100 image dots of an area of sky in an image (3D spectroscopy) .

CONICA – Coudé Near-Infrared Camera for the VLT

The European Southern Observatory, ESO, is currently setting up the Very Large Telescope, VLT, on the 2630-metre-high peak of Paranal in Chile's Atacama Desert (Figure I.4). When fully completed, this facility will consist of four large telescopes, each with a mirror of 8.4 metres in diameter, and three smaller auxiliary telescopes with 1.8 metre mirrors. The VLT will then be the observatory with the largest total mirror area anywhere in the world. Each of the four large telescopes has three outputs, which can be fitted with extremely high-performance cameras and spectral equipment. CONICA will operate on the first of the four telescopes, which saw »first light« at the end of May 1998. CONICA is currently being built under the coordinating leadership of the MPIA in collaboration with the MPI für extraterrestrische Physik/MPI of Extra-Terrestrial Physics in Garching. This instrument (Figure III.10 and III.11) is due to start operation in the year 2000. The astronomers at the institutes involved in the construction of CONICA will have 45 nights' observation time with this instrument available to them on the VLT.

The contract which was concluded with ESO in 1991 provided for CONICA to be operated in the Coudé focus (f/50) of the first telescope. However, new arrangements have been made on account of delays to construction work in the Coudé beam path: now, CONICA will operate in the Nasmyth focus (f/15), and will supply diffraction-limited images with resolutions as low as 0.026 seconds of arc in the near infrared range from 1 to 5 micrometers, in conjunction with the NAOS adaptive optical system.

An infrared array with 1024×1024 pixels is used as the detector, and the imaging scale can be adapted to the chosen wavelength. There will be four scales between 0.014 and 0.11 seconds of arc per pixel. For each of these scales, two camera systems are available, operating in the two wavelength ranges from 1 to 2.5 micrometers and from 2 to 5 micrometers. Depending on the selected variant, the image field has an extent of between 14×14 and 56×56 square seconds of arc, and a diameter of 73 seconds of arc at the lowest resolution.

CONICA is a multi-functional instrument in which the following optical elements will be available:

A Fabry-Pérot interferometer is continuously variable in the range between 2 and 2.5 micrometers, and it enables narrow-band recording for all imaging scales. The pass range of about 1 nanometer will then correspond to a spectral resolution of $\lambda/\Delta\lambda = 2000$. A set of 20 standard
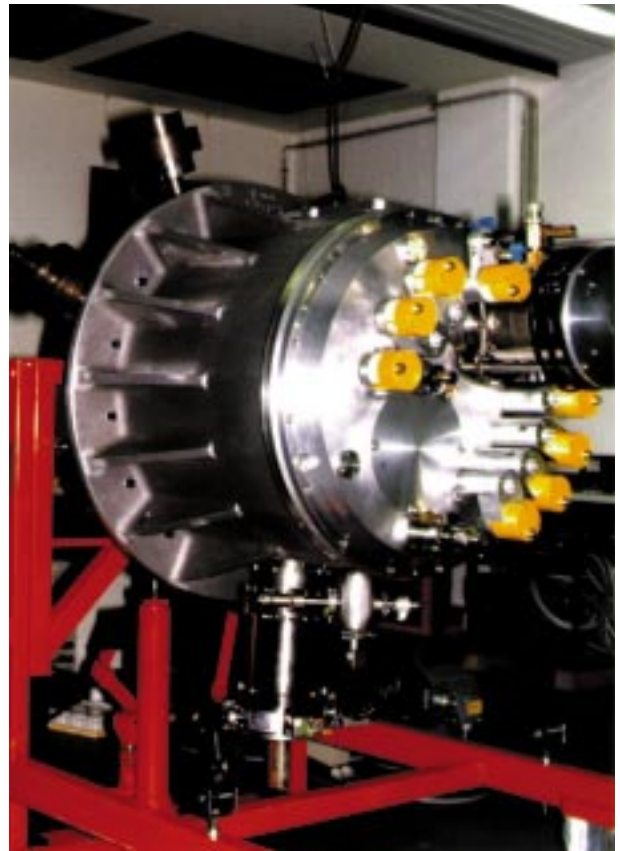
Fig. III.10: The CONICA camera being tested.

colour filters and 15 narrow-band filters is available, and these can be integrated on two filter wheels. Wollaston prisms and polarisation filters make it possible to measure the linear polarisation of extended objects. Furthermore, three grisms provide the possibility of two-dimensional spectral investigations with an average spectral resolution $\lambda/\Delta\lambda$ of between 250 and 1000.

Like all infrared cameras, CONICA also has to be cooled. A two-stage sealed circulating cooling system brings the radiation shield and the internal cooling structure down to a temperature of less than 80 Kelvin. The second stage cools the detector down to the optimal operating temperature of about 35 Kelvin. The cooling of the instrument can be accelerated by means of an additional cooling system which uses liquid nitrogen. A stable operating temperature is attained after less than 24 hours.

The cryostat and the adapters were completed in 1997, and all the optical components were delivered. Extensive cooling tests yielded successful results, and full mechanical integration of the instrument was possible for the first time at the end of 1997. The system for reading out and storing the data was converted to a processor of the new generation which can handle data flows of up to 40 MB per second – which is an important requirement for applications such as speckle interferometry.

adapter

calibration
optics

calibration source

Fabry Pérot
radiation shield

collimator

vacuum
vessel

entrance
window

shutter

detector access

detector

TADC

closed cycle cooler

filter access

encoder

LN cooling system

camera wheels

filter wheels

polarizer wheels

Lyot stop wheel

focal plane assembly

Fig. III.11: CONICA: schematic diagram.

It will be possible to use CONICA for all current areas of research. Pride of place goes to investigations of areas where stars are being formed and to protoplanetary dust disks, the Galactic Centre, the gaseous envelopes around Red Giants, and the se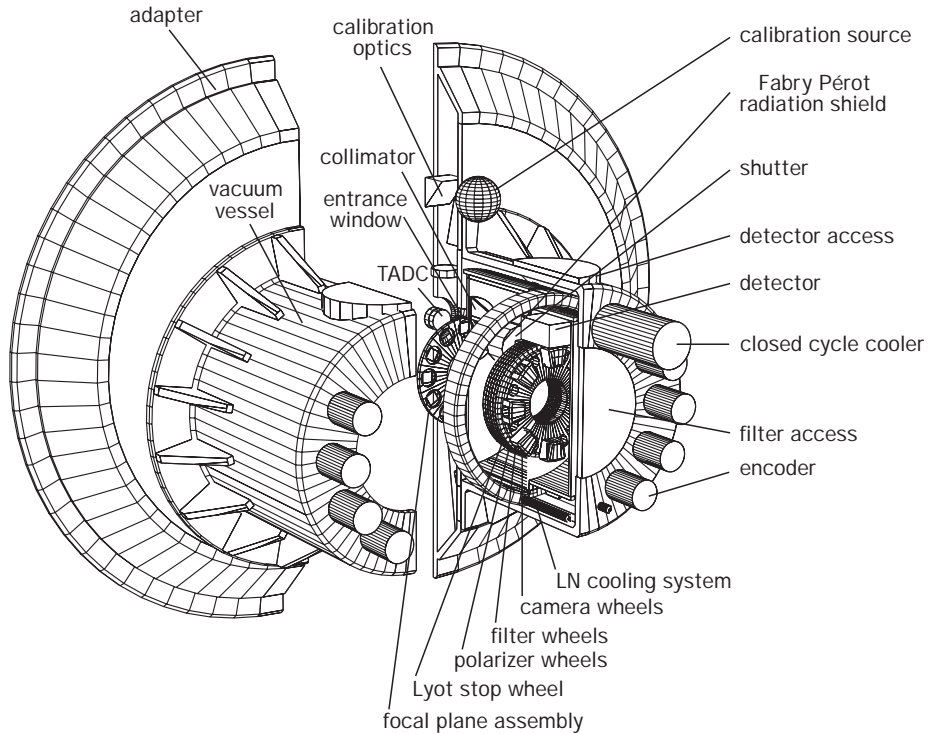arch for extrasolar planets. In the extragalactic field, high priority will be given to observations of the central regions of active galaxies and remote infrared galaxies.

MIDI – Mid-Infrared Interferometry Instrument for the VLT

As from the year 2000, the Very Large Telescope will also operate as an optical interferometer. For this purpose, the beam paths of two or more telescopes will be combined and coherently superimposed in one common image plane. An interferometer of this sort has the spatial resolution of one single telescope with a mirror whose diameter would be equivalent to the basic length of the two telescopes linked by the interferometric coupling. Two of the VLT's telescopes, separated by a distance of 130 metres, will then be capable of achieving a resolution of a few thousandths of a second of arc in the near infrared range.

Three interferometry instruments are envisaged at present: AMBER will combine three or more telescopes at a wavelength of 2.2 micrometers; MIDI is intended to enable interferometry with two telescopes at 10 micro-

meters; and thanks to the so-called Phase Referencing technique, PRIMA should make it possible to produce two-dimensional images in the near-infrared range with only two telescopes.

The MPIA will be undertaking the development and construction of the MIDI instrument. Material costs of approximately 1.5 million DM and additional personnel costs of a comparable amount are estimated for this purpose. The first observations are due to take place in the spring of 2001.

The path lengths of the beams arriving from the two telescopes must correspond precisely to within fractions of a wavelength, equivalent to about one micrometer. Most of the difference in path lengths, which is principally due to geometry, will already have been compensated before the beams enter the instrument. Inside MIDI, the diameter of the beam will be reduced from 80 mm to 10 mm, and the remaining difference in path lengths will be compensated by means of movable piezo-electrically driven mirrors. A beam splitter combines the beams to create the interference image (Figure III.12).

At the same time, however, it must also be possible to measure variations in the brightness of the observed celestial object due to air turbulence or clouds. For this purpose, part of the two beams will be diverted out of the interferometric beam path so that continuous separate measurements of the brightness can be taken.

The thermal background radiation which occurs at a wavelength of 10 micrometers may well present a major problem. For this reason, an »empty« area of the sky in close proximity must be measured at fixed time intervals
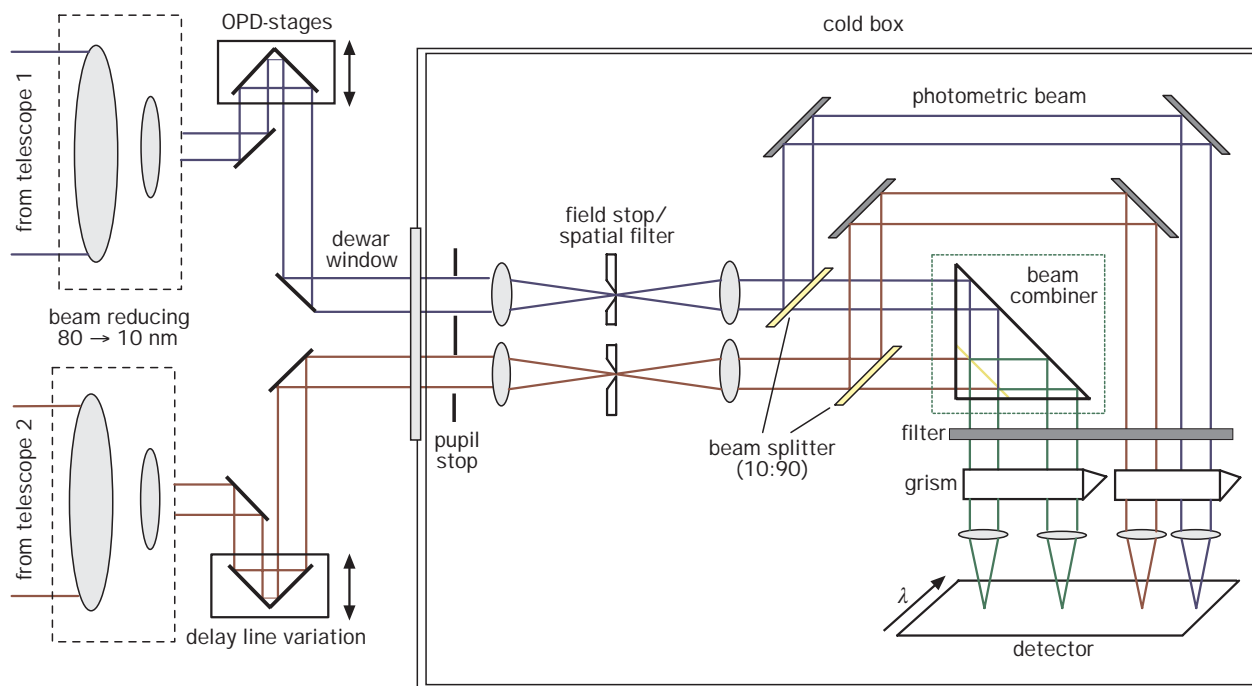
Fig. III.12: MIDI: schematic diagram.

as a brightness comparison. Such »chopping« measurements (as they are known) are also necessary for normal direct imaging, but on the VLT interferometer they require substantially higher outlay, since the VLT telescopes and MIDI must operate together synchronously.

The main areas in which MIDI is to work will probably be the observation of double stars, protoplanetary disks, Brown Dwarves, extrasolar planets and active galaxies.

PACS – IR Camera for FIRST, the Far Infrared Space Telescope

In the year 2007, the European Space Agency (ESA) intends to launch FIRST, the Far-Infrared and Submillimetre Space Telescope (Figure III.13). This is the ESA's fourth major cornerstone mission. FIRST will be provided with a 3 metre mirror and three scientific instruments which are intended to cover a wavelength range from 85 to 900 micrometers. It will therefore link up to the field of radio astronomy at long wavelengths. One focal point of the research programme will be the observation of protostellar dust clouds and protoplanetary dust disks. It will also be possible to detect the infrared radiation from very remote young galaxies in the sub-millimetre range.

The MPIA will be participating in the construction of PACS, one of the measuring instruments. This project is being led by the MPI für extraterrestrische Physik/MPI

Fig. III.13: Computer-generated drawing of the FIRST infrared observatory.

Fig. III.14: The ray-path in PACS.
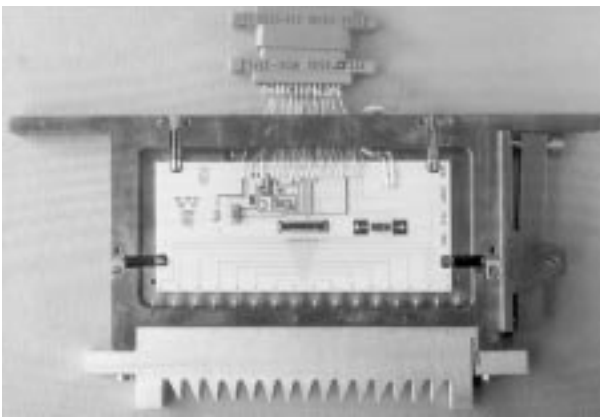
Fig. III.15: PACS test modul. 16 germanium-gallium crystals are mechanically compressed (bottom). The readout electronics can be recognized at the top.

of Extra-Terrestrial Physics in Garching. PACS should make it possible to carry out photometric and spectrometric investigations in the wavelength range between 80 and 210 micrometers (Figure III.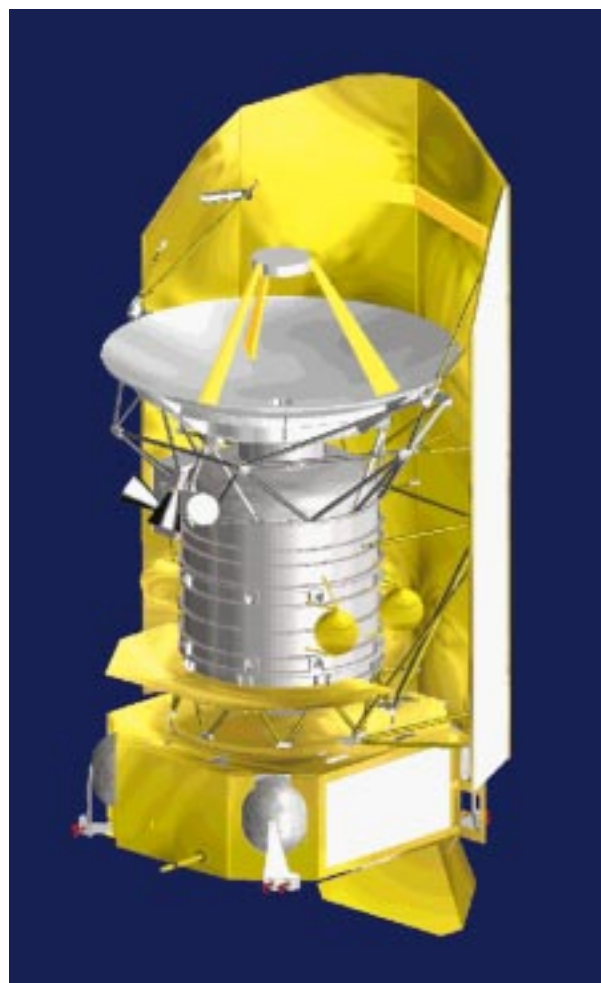14). The MPIA will be making major contributions towards the development of the cameras, the pre-amplifiers, the focal plane choppers and the optomechanics, and also towards building up and operating the data centre. FIRST and PACS will enable an even more productive random sampling of the sky (»Serendipity Survey«) than the one which has recently been carried out with ISO (Chapter II.3).

PACS will have two infrared detector arrays with 16 $\times$ 25 pixels each, consisting respectively of stressed and unstressed germanium-gallium crystals. The »stressing« of crystals is a technique which has been studied in detail at the MPIA during the development of the detectors for ISOPHOT. It has become apparent that the sensitivity of the crystals can be extended to longer wavelengths if they are exposed to a mechanical pressure (Figure III.15). This involves the risk that the crystals could be destroyed. Several series of experiments at the MPIA are intended to examine the mechanical, electrical and optical behaviour of the crystals manufactured by the ANTEC company.

An electronic system is being built at the IMEC company to provide reliable read-outs from the arrays at the target operating temperature of 1.7 Kelvin. For this purpose, it is essential to ensure that the electronics are rated below the maximum values specified for PACS, such as those for the dark current or the development of heat. The MPIA is playing a major part in specifying and developing these cold electronics, and in the acceptance tests.
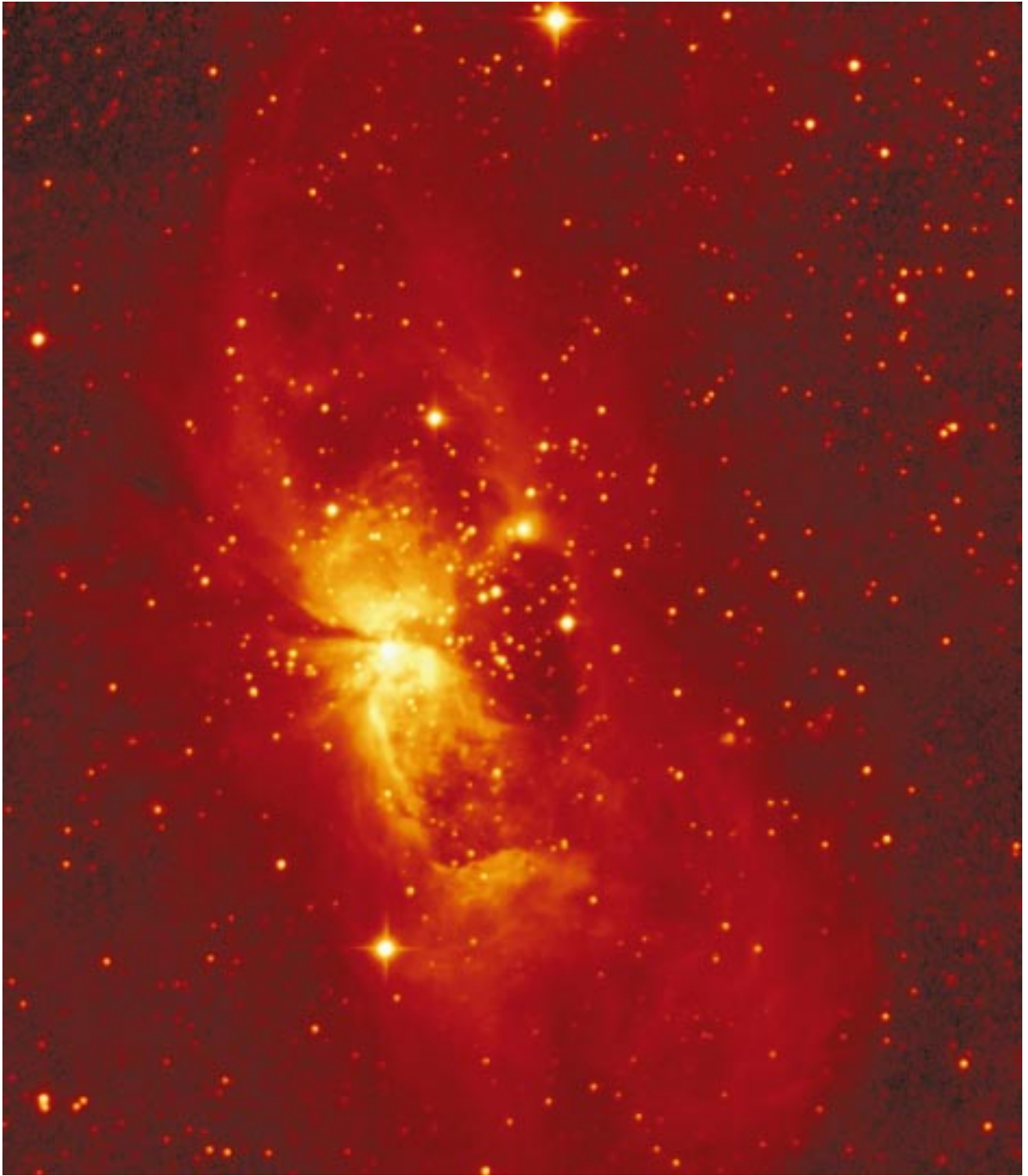
The Bipolar Nebula S 106 in an image taken with the 3.5-metre telescope on Calar Alto at the wavelength 2.1 μm.

IV Scientific Studies

IV.1. Galactic Astronomy

The Bipolar Phase – Jets of Young Stars

Stars are formed within large interstellar clouds of gas and dust: astronomers have been convinced of this for decades. They are also familiar with the large star-forming regions in the Milky Way: in the northern sky these are mainly the Orion dark cloud and the Taurus-Auriga complex. Star formation starts if a cloud exceeds a particular density. Then it becomes unstable and begins to contract under the effect of its own gravity (Figure. IV.1). During contraction, large clouds break up into several smaller condensations. These rotate, and due to the centrifugal force they form, during this process, a disc made of gas and dust which is normal to the axis of rotation, in the centre of which matter continues to condense and heat up. If the temperature rises to several mil-

lion degrees, hydrogen nuclei begin to fuse with each other. This releases energy, and the gas continues to heat up. Now a counter-pressure to gravity builds up, so that the protostar's collapse is halted. The protostar has now become a self-luminous, stable sphere of gas. The star was born.

In line with this idea, the search for the protostars embedded deep in the dense dark clouds started in the Seventies, as soon as the first infrared detectors came into use. Their characteristic feature was supposed to be the indication of matter falling towards them. This indication was searched for long and hard, but in vain. On the other hand, soon one made the surprising discovery that young stars expel gaseous winds with velocities of up to 600 km/s into space. Until the end of the Seventies it was believed that these stellar winds were blown uniformly in all directions (isotropically). Then came the next surprise: young stars generate bipolar flows - more or less strongly collimated winds of particles, which move away from the star in two opposing directions.

At MPIA, the nebula S 106 became the paradigm of such a bipolar structure (see Figure on p. 42). Here it was also possible to establish unambiguously, that the particle winds flow away from the star in the direction of the poles, at right angles to a dense equatorial disc of

Fig. IV.1: : Main phases of star formation. First an interstellar cloud collapses; whilst still contracting, a new star is created at its centre (bottom right). A disc has formed around it after roughly 100 000 years and the bipolar phase starts (top). Planets can later form in the circumstellar disc. After about one thousand million years, a sun-like star has reached its stable burning phase.
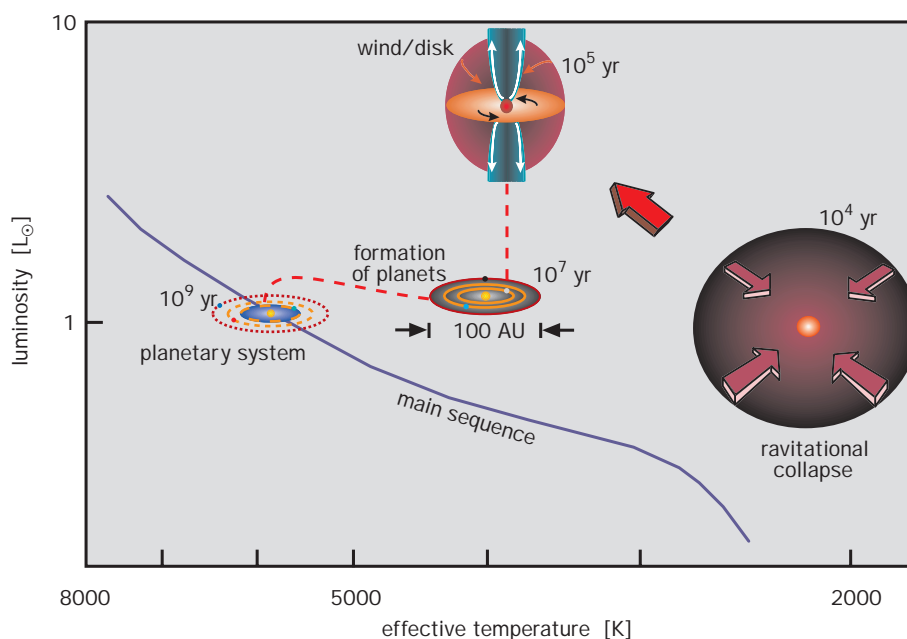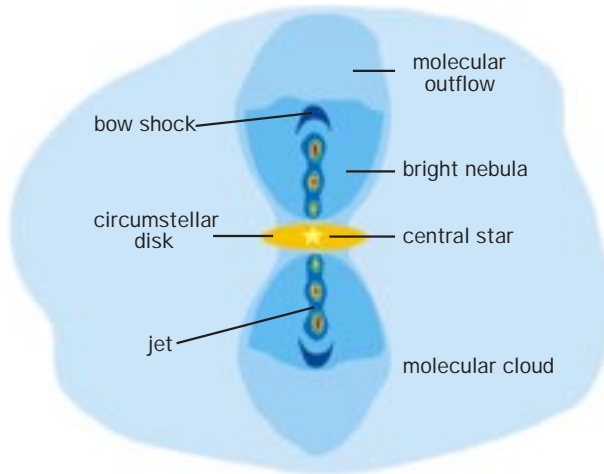
Fig. IV.2: Schematic representation of the surroundings of a young star during the bipolar phase. Two jets shoot out into space at right angles to the circumstellar disc.

dust. These outwardly-directed streamers, concentrated in the polar directions, could therefore definitely coexist with material falling into the centre of the system (accretion), provided that accretion takes place predominantly within the dense equatorial disc. This provided the link with the theory of the protostellar disc. And soon it became clear that the bipolar outward streamers are by no means a curiosity, but rather a fundamental phenomenon which accompanies stellar formation.

The list of surprises continued in the early Eighties with the discovery of the bipolar jets. These are very tightly bundled jets of matter, shooting out of young stars far into their surroundings at velocities of several hundred kilometres per second. Here too, a disc of gas and dust forms the plane of symmetry (Figure IV.2). Luminous gas nodes are ranged within many of these jets like pearls on a string. A large number of these gas streamers end in arc-like structures, considered to be

Fig. IV.3: Two jet systems: HL Tauri (top) and HH 30 (bottom). The false colours show the radiation emitted at different wavelengths. Blue is scattered stellar continuum radiation, green is line radiation produced by hydrogen (Hα) and red by ionised sulphur ([SII]).
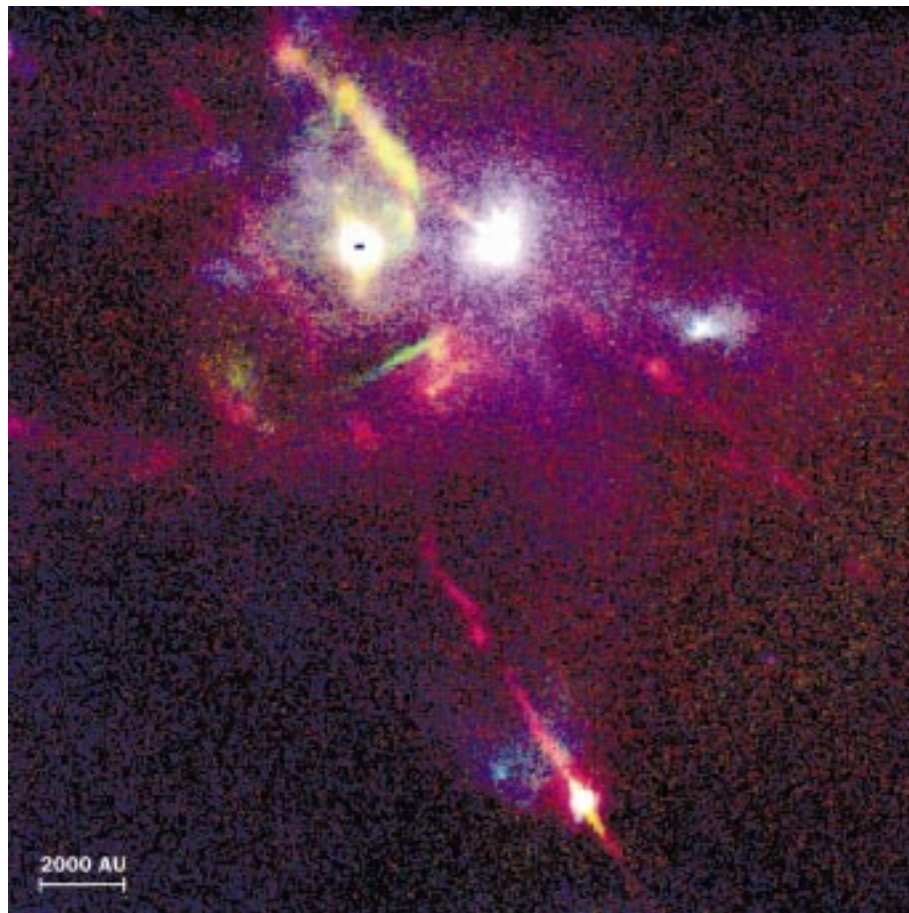
frontal waves. They mark the end of the jet, where the streamer hits the surrounding interstellar medium and drills into it further and further. To that extent they are comparable with the bow wave of a ship in water, or better still with the pressure wave of a supersonic aircraft, since the jet's frontal waves move at many times the speed of sound through the surrounding medium.

In many respects, the jets of young stars exhibit similarities with the jets ejected from the centres of galaxies (Chapter IV.2). However, in extragalactic jets, the streamers probably contain mostly relativistic electrons which give off synchrotron radiation. The stellar jets consist of normal interstellar matter, which is heated up and ionised in shock waves. Electrons and ions recombine in the cooling zones behind the shock front, and emit the observed radiation. It is concentrated in the hydrogen Balmer lines and in the forbidden lines of atomic and singly or doubly ionised oxygen (O, O^+, O^{++}) as well as from singly-ionised sulphur (S^+) and nitrogen (N^+).

The brightest emission regions of such jets were known to astronomers as far back as the Fifties. Since then they have been designated HH objects, after their discoverers Herbig and Haro. But it was only made clear in the Eighties that they are parts of jet systems. In fact, the fundamental investigations of stellar jets go back to studies conducted at MPIA. They have been among the Institute's main research projects since 1983. A large proportion of the jets known today were discovered during these studies, and their detailed investigation, largely conducted at the Calar Alto observatory, has contributed decisively to the deciphering of this phenomenon. It is estimated that 50 stellar jets are known today, of which 15 to 20 can be attributed to MPIA (Figure IV.3).

The jet sources are associated with T Tauri and Herbig Ae/Be stars which are embedded deeply in the dark clouds. The former are stars of roughly solar mass and aged between 10^5 and 10^6 years, whilst the latter are over two solar masses. These stars represent the transition phase between the collapsing protostellar clouds and the fully-evolved main sequence stars. Often they are still located inside the gas and dust cloud from which they evolved, so that they cannot be observed in the visual spectrum.

A few jets are also known in the southern sky, of which the most prominent is HH-46/47 (Figure IV.4). It is being expelled by a young star in the small dark cloud ESO 210-6A. The jet streams towards us from a gap at the front of the cloud, with measured radial velocities of up to 170 km/s, and terminates in the arc-shaped nebula HH-47A. A weak opposite jet can be discerned at the cloud's back side, in which the gas moves away from us. This system too, was investigated in detail at MPIA.

One prominent feature is the node-shaped condensations in the jets, whose formation has not been completely explained up to now. At first it was assumed that standing shocks are involved, as occur for example in
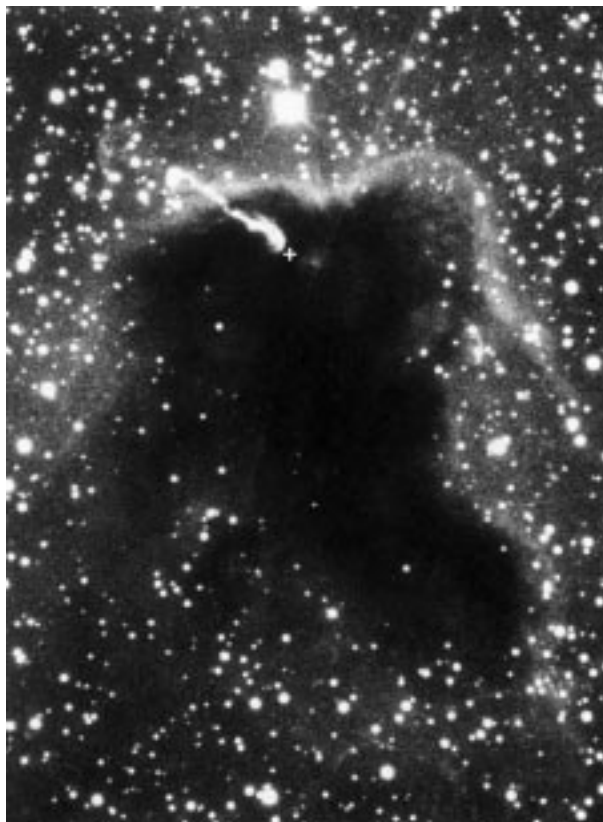
Fig. IV.4: The dark cloud ESO 210-6A in the southern sky, from which a jet is shooting out at the front. A counter-jet is just about visible at the cloud's edge in the opposite direction (Image: B. Bok, Cerro Tololo).

ultrasound beams generated in the laboratory. In this case the nodes should exhibit practically no proper motion at all, but rather be stationary in the stream. The analogy suggested itself since the gas in the stellar jets is moving at up to 20 times the speed of sound.

However, this idea was abandoned once astronomers at MPIA succeeded for the first time, in 1987, in determining the nodes' proper motion, using a study of the jet in the dark cloud L 1551 in the Taurus-Auriga complex (see cover image). It was shown that the nodes are moving, as does the surrounding gas in the jet, at considerable velocities of around 300 km/s away from the star.

Instead, nowadays one tends to assume that many of these condensations result from short-term intensifications of the source's active phases. If that is the case, then eruptions during which a new node is created should occur at intervals of roughly one hundred years.

This idea makes it clear that the jets are very interesting not only in themselves, but furthermore also provide information on the source and even on its evolution over time. Although stellar jets have been studied in great detail since their discovery, 1997 came up with yet another surprise.
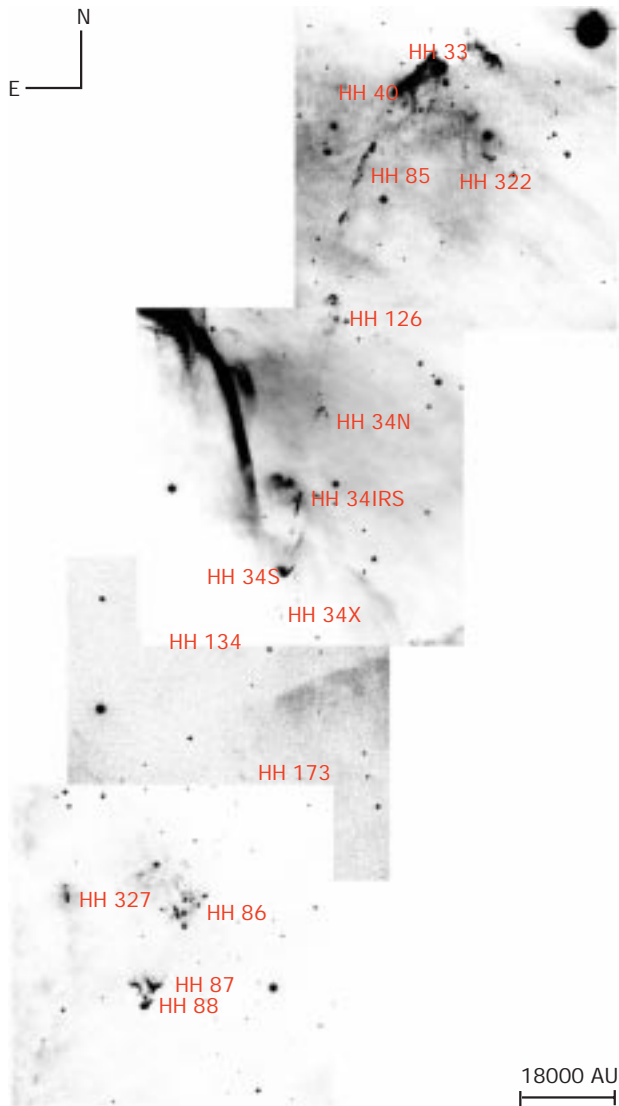
Fig. IV.5: The HH-34 superjet. The star is invisible in the optical spectrum, and is at the position marked HH 34 IRS. The two jets probably terminate at HH 88 and HH 33.

One group of American astronomers became aware that beyond the HH-34 jet's northern and southern bow waves there exists a chain of more HH objects, roughly as an extension of the jets. Thus the idea was mooted that they also belong to this streamer system, which therefore would be considerably more extended than was previously assumed.

During two observing runs at the 2.2-metre MPIA telescope at La Silla and at the 3.5-metre telescope on Calar Alto, the MPIA team focused more specifically on several regions. The group used a well-known method in order to distinguish HH objects from reflection nebulae, which also occur frequently in star formation regions: it recorded a region of the sky once through a filter which only allows through light in the stellar continuum, and again through a narrow-band filter which only transmits light in the region of the two lines of simgly-ionised sulphur ([SII]). Reflection nebulae appear on both images, HH objects however only on the narrow-band filter ones.

Two such images were thus obtained, to the south and the north of the two suspected bow waves HH 34S and HH 34N. The long-exposure [SII] images now showed, in the southern region, several (in part known) HH objects such as HH 86 and HH 173 (Figure IV.5). However, two additional nodes became visible on the line connecting these two objects. Weakly-luminous gas can be discerned further to the south, which appears to link HH 86 with HH 87 and HH 88. The assumption that the jet does not end at HH 34S but extends considerably further, up to HH 88, was supported by radial velocity measurements. The velocities are negative (directed towards the observer), and drop from –150 km/s (jet) down to –14 km/s (HH 87). In HH 88 they are slightly positive, at +17 km/s.

The streamer also seems to continue to the north of the previously-suspected jet termination, HH 34N. It extends over HH 126 and HH 85 all the way to HH 33. Here too, this hypothesis is confirmed by the measured radial velocities of 220 km/s (HH 34N), 137 km/s in HH 85 and 90 to 140 km/s in HH 33. Furthermore, no other object was found, besides the already-known jet source, which could be responsible for the recently discovered streamers and HH objects.

Thus, HH 34's jet is not, as was assumed up to now, 200 arc-seconds long in total, but over 1300 arc-seconds. At a distance of 1500 light-years) and an angle of inclination of the jet's axis against the celestial plane of 24 degrees, this indicates a linear extension of about 10 light-years. The »superjet« HH 34 is, thus, one of the longest known jets anywhere.

Jets already known, were also followed along greater distances than previously suspected in two other starfields. For example: the jet of RNO 43 (Figure IV.6). It extends over altogether more than 1000 arc-seconds, which corresponds to a linear extension of 7.5 light-years. The suspected northern bow wave (HH 245) exhibits a structure reminiscent of a matchstick figure with arms and legs. Such shapes also turn up in computer simulations of jet streams, and support the hypothesis that this is the jet's frontal wave. This system is interesting in its s-shape: about 280 arc-seconds to the north and 170 arc-seconds to the south of the source, which can only be detected in the radio spectrum, the stream is bent by ca. 40 degrees.

In another field surrounding HH 24, a very complex system of altogether eight jets could be made out. They reach lengths of up to 500 arc-seconds, corresponding to 3.6 light-years.

Various conclusions can be drawn from the realisation that the jets are considerably more extended than previously assumed. For one, the jets' dynamic age can be calculated from their lengths and the velocity of the gas: the jets are three to ten times older than first assumed.
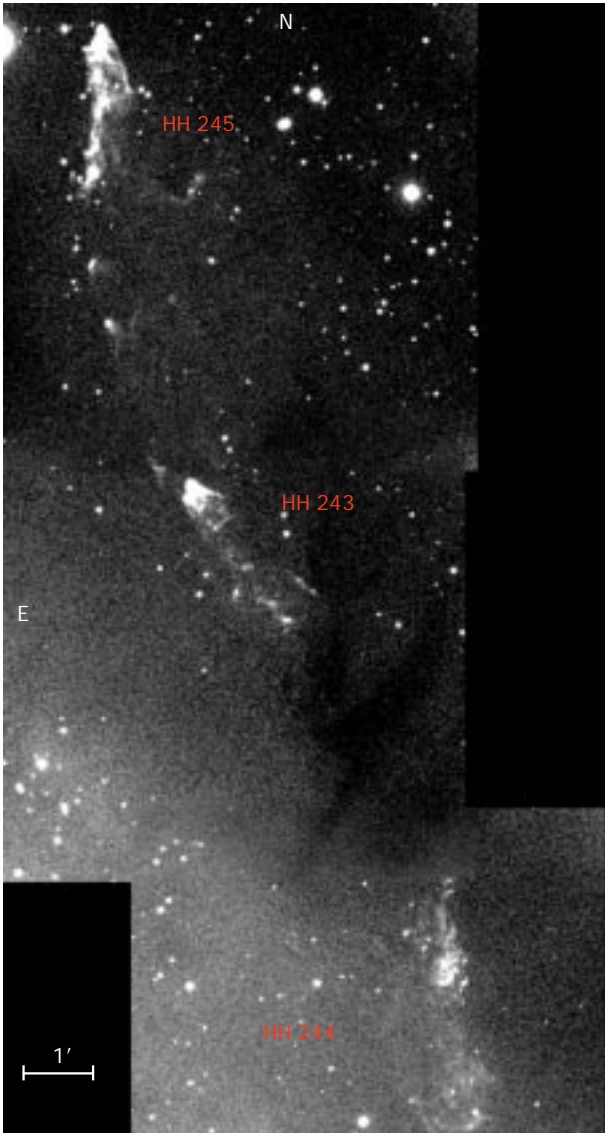
Fig. IV.6: The jet of RNO 43. The two particle beams probably terminate at HH 244 and HH 245.

For example, the HH-34 jet's age is 3000 to 5000 years, that of the RNO-43 jet as much as 11 000 years. The other examined streamers are also around 8000 years old. The mass loss due to the jets is around 10^{-8} solar masses per year. This means that a T Tauri star loses a total of 10^{-4} solar masses during this stage in its evolution.

The total momentum which the streamers transfer to the surrounding medium during their lifetime can also be estimated. Considerably higher values are calculated now than was assumed thus far, namely 0.5 to 10 solar masses $\times$ km/s. These figures can be compared to the momentum which the so-called molecular flows carry. These molecular flows, demonstrated through the linear emissions of their CO molecules in the radio spectrum, are also mostly bipolar and possess roughly the same alignment as the jets, are substantially less collimated and much slower (their radial velocities lie around a few tens of kilometres per second), but carry with them much larger masses of gas. The causal link between these two types of outflows has thus far been unclear. However, since it now appears that the magnitude of the total momentum carried by the molecular flows, namely from 1 to 20 solar masses $\times$ km/s, corresponds to that of the jets, it is possible that the stellar jets drive the molecular flows. Up to now this seemed impossible, since the momentum carried by the jets seemed far too small.

The jets as a group are distinguished by high collimation and marked linearity. However, as already described in connection with the jets of HH 34 and RNO 43, changes in direction are also observed. These may have a variety of causes: density gradients or dense condensations in the interstellar medium, »side-winds« from other jets, flow instabilities or even wobbling (precession) of the jet's source. Precession should be exhibited roughly symmetrically in the two jets of one source. This case would be particularly interesting, since it would provide information on the state of the central stars.

However, precession seems rather unlikely in both HH 34 and RNO 43. Behind the bend in HH-34's jet, the beam appears to widen suddenly – an effect one would expect if the flow is deflected by an obstacle such as a dense cloud. In RNO 43, the deflection occurs abruptly and at a large angle of ca. 40 degrees, so that here too one must regard an external influence, e.g. a condensation in the surrounding medium, as the likeliest cause.

Today it is regarded as certain that the jet sources are T Tauri stars surrounded by a disc of dust, with the jets emerging at right angles to the disc's plane. In one case (HH-30 jet), MPIA researchers managed to follow the jet as close as 40 astronomical units from the source. There the beam already has a diameter of 40 astronomical units. On theoretical grounds it is considered very likely that the jet is formed as close as several stellar radii from the source with a small diameter. Thereafter, as shown by the observations, the beam first widens sharply at ca. 60 degrees and then continues highly collimated for light-years.

The question whether the star itself produces the jet or whether it is given off by the circumstellar disc, still remains largely unanswered. Two studies carried out at MPIA in 1997 went some way towards solving this problem. A total of 38 T Tauri stars were examined spectroscopically, mainly with the 2.2-metre and 3.5-metre telescopes at Calar Alto: these stars exhibit forbidden lines, in particular [SII], [NII] and [OI]. This group of T Tauri stars is not associated with visible jets. However, the Doppler shifts of the emission lines show that a stellar wind exists in the stars' immediate neighbourhood. The interesting point is that two wind components can be discerned: a slow component with velocities between –5 and –20 km/s, and a fast component with velocities between –50 and –150 km/s.

The slow component reaches its highest brightness as close as ca. 0.2 arc-seconds from the star (corresponding to 30 astronomical units), whilst the fast component reaches its maximum only at a distance of ca. 0.6 arc-seconds (60 astronomical units). However, most probably these winds are generated considerably closer to the star. In addition, the spectra reveal that the slow wind is typically denser and at a lower level of excitation than the fast component.

The new observational data agree with a model in which the fast wind is created in a jet whose particle density drops with increasing distance from the star, whilst the excitation rises. The slow wind is apparently separated spatially from the other wind, and is possibly generated by the circumstellar disc.

Why some T Tauri stars generate a jet but others do not, is an unanswered question. It is conceivable that the two stellar groups investigated at MPIA represent stars at different stages in their evolution. Thus, the jet sources could be younger than the T Tauri stars with the observed fast and slow winds. This assumption is supported by the fact that the latter stars are not, in general, embedded as deeply in the surrounding dust, and therefore also appear optically brighter.

The influence of magnetic fields

It has long been suspected that magnetic fields play a significant part in the collimation of stellar winds and possibly also in particle acceleration. In 1997 it was possible to demonstrate for the first time a magnetic field in connection with outward flow from a young star. The object of this investigation was T Tauri, after which young stars of low mass are named. This star, with its surroundings having a very complex structure, has in recent years proved itself more and more clearly as a less than typical T Tauri star. T Tauri is a double star, of which only the northern component is visible in the optical spectrum (some astronomers even suspect a third stellar component in this system). The southern component is hidden behind so much dense dust that it can only be seen in the infrared. Images with a high spatial resolution, at a wavelength of 2.122 μm, were obtained at the Mauna Kea observatory on UKIRT, using MPIA's MAX camera and the tip-tilt mirror also provided by MPIA (Chapter I.1). They show the emission of molecular hydrogen at distances of up to 15 arc-seconds (900 astronomical units) from the star. These arc-like, apparently nested structures, could be the frontal waves of gas streaming out and excited into shock fronts (Figure IV.7).

These investigations confirm other studies in the near and intermediate infrared, according to which each of the two stars is surrounded by a circumstellar disc from which a jet-like streamer is given off, and the two streamers are almost perpendicular to each other. However, it is difficult to imagine how a double-star system can generate two orthogonal jets, if each jet axis is perpendicular to the disc's plane. The solution to this puzzle is probably that we are looking at the jets at a small angle of ca. 20 degrees. Two jets whose axes are not exactly identically aligned in space would then always be seen, when projected onto the sky, as almost perpendicular to each other.

Through international cooperation, astronomers from MPIA making radio observations with the MERLIN interferometer at Jodrell Bank (UK), detected circularly polarised radio emission from regions around both of T Tauri's components. The fields must be extended to several tens of astronomical units away from the stars, and have an intensity of a few Gauss in the outlying regi-

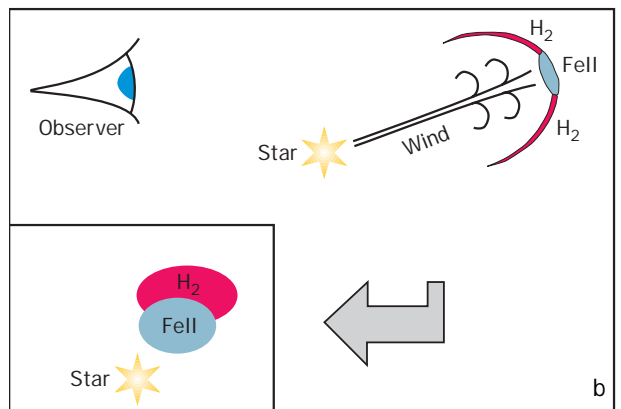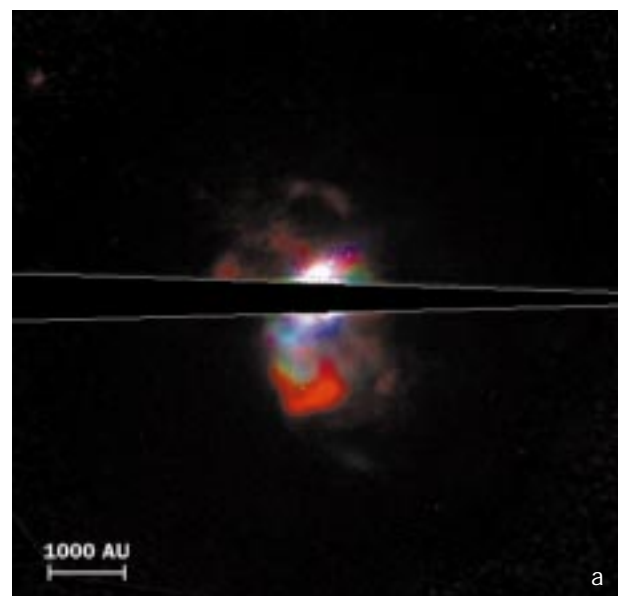Fig. IV.7: (a) The nebula around T Tauri. The false colours show the radiation emitted at different wavelengths: red is produced by hydrogen molecules (H_2 at 2.2 μm), green by ionised sulphur ([SII]) and blue by hydrogen (Hα). The arc-shaped structures are presumably shock-fronts in the outflowing gas. (b) represents a possible geometry of the system. The large illustration is a side-view, the small inset is the view from earth.
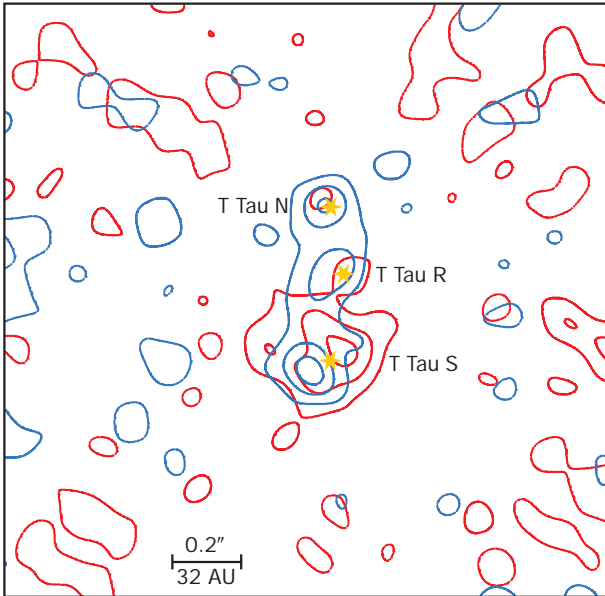
Fig. IV.8: Radio-chart of the region around T Tauri at a wavelength of 6 cm. Right- and left- circularly polarized radia- tion (red and black contours) points to extensive magnetic fields.

ons (Figure IV.8). This is the first demonstration of a magnetic field around a young star extending to such distances. The field discovered around T Tauri south is aligned roughly in the same direction as one of the two gas flows. It seems plausible that there is a causal link between the magnetic fields and the flow collimation, and that the fields may possibly be compressed into shock fronts. This would explain their comparatively high intensity.

Double and multiple systems in young stars

T Tauri stars

The sun is in a minority in being a single star. A study by the Swiss astronomers Antoine Duquennoy and Michel Mayor in the early 1990s showed that of 164 sun-like main-sequence stars (of spectral type G) up to a distance of 72 light-years, only around a third are single stars. All other objects are members of double or multi- ple systems. It remained unclear, however, whether this distribution was a direct consequence of star formation, or whether it could be explained through stellar evoluti- on up to the main-sequence phase. This question was to be answered by infrared observations in the star-forma- tion region of Taurus-Auriga, which an MPIA working group carried out in 1993. It searched for near compa- nions to 104 young T Tauri stars, using speckle inter- ferometry. With this technique the astronomers achieved a spatial resolution of 0.13 arc-seconds on the 3.5-metre

telescope at Calar Alto, so that they could recognise even very tight multiple systems as such.

The study showed that 42% of the examined young stars have a companion at a distance of between 18 and 1800 astronomical units. If a correction is made for the undetected tight and very wide systems, under the assumption that the same distance distribution applies as in main-sequence stars, then one reaches the surprising result that nearly all stars form in double and multiple systems.

The objects selected in this study included 46 so-cal- led classical T Tauri stars, which are distinguished by strong hydrogen (Hα) emission. However, according to a study using the ROSAT x-ray satellite, the overwhel- ming majority of young stars seem to exhibit only weak emission lines in the visible spectrum (»weak-lined« T Tauri stars), but more prominent x-ray lines. For this reason the investigation described above was repeated with stars from the ROSAT catalogue in the Taurus region.

The two-dimensional speckle interferometry was car- ried out on the 3.5-metre Calar Alto telescope; the 2.2- metre Calar Alto telescope and the one at La Silla were available for observing additional double stars and for photometry. The observations were complemented by direct photographs made on the 1.23-metre Calar Alto telescope. These studies used the MAGIC infrared camera at a wavelength of 2.2 μm, with which two stars with a separation of between 0.13 and 13 arc-seconds (corresponding to 18 up to 1800 astronomical units at the distance of the Taurus region) can be resolved.

Of 74 mainly weak-lined T Tauri stars from the ROSAT catalogue, 29 proved to be double, 6 triple and one as a quadruple system. However, these numbers must be corrected due to various effects.

Firstly, there exists the possibility that several of the wide systems are not genuine double stars, but merely two independent stars which when projected on the sky, are accidentally located close to each other. From an analysis of mean star density in the observed field, it is possible to calculate and take into account the probabili- ty of such constellations. Accordingly, 2.4 double and 1.7 triple systems are to be expected as such chance associations in the relevant data set.

In addition, a selection effect must be taken into con- sideration which affects the ROSAT data. Since ROSAT cannot resolve multiple systems, these appear brighter than the individual stars, as the x-ray emissions of their components add up. This means that several multiple systems are raised above the detection threshold and are recorded, whilst the individual components would be too weak on their own. Hence the proportion of multiple stars is artificially increased. This effect can also be esti- mated.

Finally, after taking into account all the effects, there remained 70 stars, of which 27 were double, two triple and one – a quadruple system. A comparison with the

study carried out in 1993 showed an almost identical result. Thus it was permissible to add up the numbers from both investigations in the interests of better statistics. This provided a total of 174 young stars.

In order to be able to compare the result with that of the study of main-series double stars, the measured projected separations had to be converted to periods of revolution. This was done using statistical arguments, with the mass of T Tauri stars assumed to be equal to one solar mass. The measured separations of between 0.13 and 13 arc-seconds then correspond to periods of between 86 and 86 000 years (Figure IV.9).

It turns out, firstly, that among the 174 T Tauri stars there are 85 companions in double, triple or quadruple systems, which is a ratio of 49%. This is nearly double the 25% calculated by Duquennoy and Mayor for G-type main-sequence stars. It is necessary to remember that tighter systems, with periods below 86 years, could not be discovered using the speckle method. The period distribution, with a maximum around 430 years, showed no significant differences between the classical and the weak-lined T Tauri stars.

An interesting finding was the analysis of luminosity ratios of the stellar components, as a function of their separation. Two groups were formed: 1) close systems with separations between 0.13 and 1.3 arc-seconds (corresponding to 18 to 180 astronomical units), and 2) wide systems with separations between 1.3 and 13 arcseconds (180 to 1800 astronomical units). This breakdown, which appears somewhat arbitrary, is based on the observed fact that the typical radius of protoplanetary discs seems to lie around 150 to 200 astronomical units.

It turned out that small luminosity ratios predominate in widely-separated pairs, i.e. T Tauri stars mainly possess low-mass companions. In tight systems the luminosity ratios are distributed almost uniformly, with a slight preference for large ratios, that is for pairs of comparable mass (Figure IV.10).

This interesting finding still needs to be statistically corroborated. However, it supports a prediction based on star-formation models constructed by our theory group (see below), according to which, in a tight pair, the lower-mass component takes up more matter from the surrounding dust disc than the higher-mass one, so that the masses of the two components even up. In a wide system, it is mainly the primary star which collects dust, which increases the difference in masses.

However, the essential result of the 1993 and 1997 studies is that apparently the frequency of double stars drops between the formation phase and the main series. The consequences of this new finding are discussed briefly below, in the next chapter.

Herbig Ae/Be double stars

T Tauri stars are sun-like stars with masses up to ca. two solar masses. Encouraged by the result described above, the Heidelberg group wanted to extend its study to young, more massive stars in the range between two and eight solar masses, so-called Herbig Ae and Be stars. It relied in part on older observations going back to the Eighties; the new data were obtained predominantly with the MAGIC infrared camera (Chapter I) at Calar Alto and in a few cases at ESO. Originally these observations served to detect circumstellar gas and dust envelopes, which is why Ae and Be stars with particularly intensive infrared radiation were selected.

Circumstellar and interstellar dust extinction makes determination of such quantities as the temperature, mass and luminosity of observed stars more difficult. However, since the MPIA study essentially concentrated on the question of double-star frequency, the astronomers could restrict themselves to a simple model when estimating these parameters. Here they assumed that the stars are surrounded by thermally radiating, geometrically thin discs (Figure IV.11). Thus, using the observational data, the temperature distribution of circumstellar matter as a function of distance from the star could be roughly modelled.

Observational data were available for 26 Ae and Be stars at various spectral bands in the near and middle infrared, relying also on observations made by other
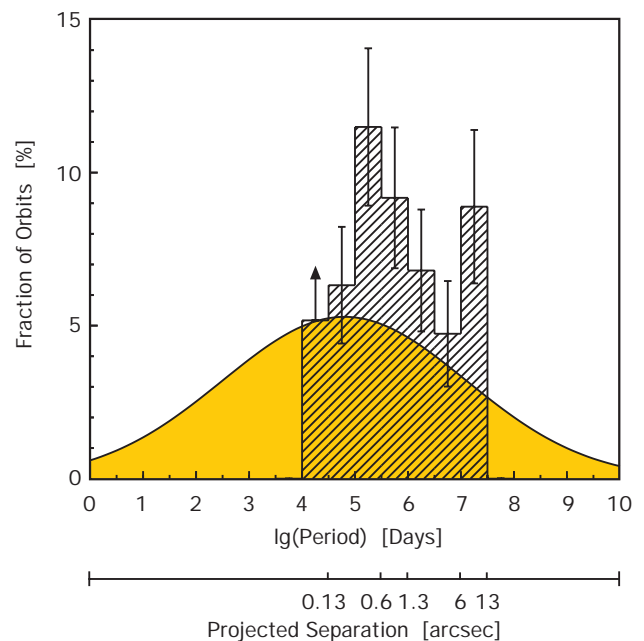

Fig. IV.9: Frequency of double systems as a function of the components' period and their projected separation. The histogram shows the distribution of T Tauri stars in the MPIA study, the grey curve – evolved main-series stars in the sun's neighbourhood.
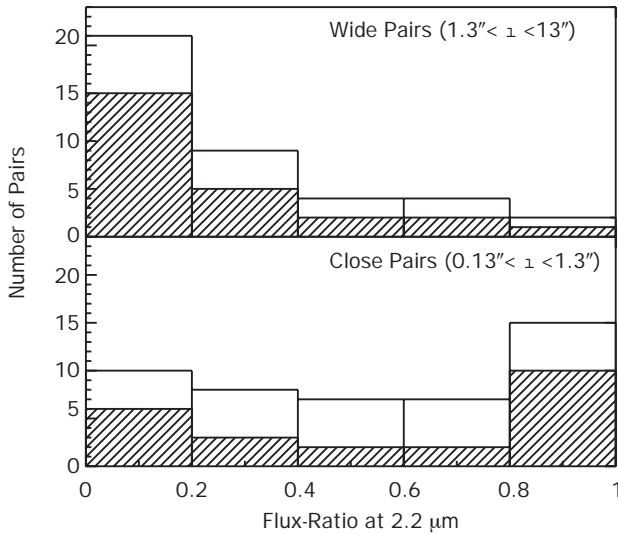
Fig. IV.10: The ratio between measured fluxes of radiation at 2.2 μm for wide and close pairs. The hatched histograms represent weak-lined T Tauri stars, the unhatched ones –- classic T Tauri stars. Apparently, T Tauri stars in wide pairs possess mainly low-luminosity, low-mass companions.

groups. Thus this set is neither particularly large or complete nor homogeneous. Nevertheless, it already allows some interesting conclusions to be reached.

Eleven of the 26 objects have a companion. Five of these are at a separation of less than one arc-second, corresponding to 160 astronomical units. Almost all of these were discovered by the Heidelberg group. Eight companions are at distances of between 50 and 1300 astronomical units from the primary star, the remaining three at as much as between 2000 and 3600 astronomical units. With these bodies one cannot rule out the possibility that they are only accidentally located relatively close to the relevant Ae or Be star in projection, without forming with it a gravitationally-bound pair.

From this small group one derives a double-star frequency of (31 ± 10) % or (42 ± 13) %, depending on whether one counts the three remote companions or not. To be able to compare this with the study of main-sequence double stars, the measured projected separations had to be statistically converted into periods of revolution, as with the T Tauri stars. The calculated figures are between 320 and 20000 years, plus 100000 years for the three hypothetical wide systems. In this range the Swiss astronomers found a proportion of 15% – or 18% – of G-type double stars. Hence the recent investigations at MPIA reach a comparable outcome as with the T Tauri stars previously: in the more massive Ae and Be stars too, a higher frequency – by a factor of two – is indicated, compared to main-sequence stars. Direct comparison with A- and B-type main-sequence stars was not possible, due to the absence of appropriate data. However, other investigations give rise to the suppositi-

on that the frequency of double stars does not vary significantly with spectral type.

The main effects which might distort the results are two-fold: for one thing, speckle interferometry cannot detect companions whose separation from the Ae star is less than 0.1 arc-seconds (or 16 astronomical units) and whose brightness is lower by a factor of more than 20. Secondly, as already mentioned, some of the widely-separated pairs might only be apparent associations which are only accidentally adjacent to each other in projection. Thus the two effects are counteractive, and might almost cancel each other out.

When comparing the pairs it was noticed that the brightness ratio from primary to secondary star increases sharply with low companion brightness (Table III.1). This was explained through the initial mass function of young stars, as proposed in 1979 by Miller and Scalo: according to this, 75% of all Ae stars with three solar masses should posses a companion with less than 0.5 solar masses.

Thus, the two double-star studies on T Tauri and Herbig Ae and Be stars lead to the discovery that the frequency of double-star systems drops between the formation phase and the main-sequence. This accords with the results of computer simulations, including those performed by the MPIA theory group (see below). They demonstrate that in a contracting gas cloud, fragmentation practically always leads to the formation of a multiple system. However, due to gravitational interaction between the systems and also because of trajectory instabilities, individual stars are often ejected from these systems.
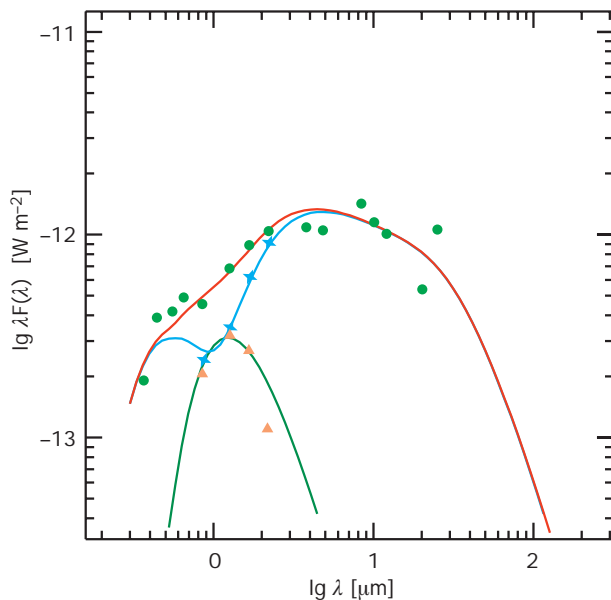

Fig. IV.11: Modelling of the measured spectral distribution (points) of an Ae/Be star, in this example HK Ori A and B. Component A (asterisks) predominates over component B (triangles).

Table. IV.1: Observed Ae/Be stars and their suspected companions.

Source	Luminosity of		Ref.	Typ
	system	companion		
LkHα 198	160 L$_\odot$	100 L$_\odot$	1, 2	Ae/Be
Elias 1	38 L$_\odot$	≈ 0.3 L$_\odot$	3, 4	WTTS[a]
HK Ori	41 L$_\odot$	≈ 5 L$_\odot$	5, 4	T Tau
T Ori	130 L$_\odot$	< 2 L$_\odot$	5, 6	T Tau?
V380 Ori	180 L$_\odot$	≈ 50 L$_\odot$	5, 4	Ae/Be?
LkHα 208	270 L$_\odot$	≈ 100 L$_\odot$	5, 4	Ae/Be?
Z CMa	≈ 3000 L$_\odot$	2100 L$_\odot$	7, 8	Ae/Be?
HR 5999	135 L$_\odot$	3.9 L$_\odot$	5, 9	T Tau
KK Oph	35 L$_\odot$	5–10 L$_\odot$	5, 4	T Tau?
LkHα 234	2300 L$_\odot$	?	5, 10	Ae/Be?
MWC 1080	6500 L$_\odot$	≈ 250 L$_\odot$	4	Ae/Be

a) »weak-lined« T Tauri-Stern
Ref.: (1) Charvarria 1985; (2) Lagage 1993; (3) Berilli 1992; (4) this paper; (5) Hillenbrand 1992; (6) Hillenbrand 1995; (7) Hartmann 1998; (8) Koresko 1991; (9) Stecklum 1995; (10) Cabrit 1995b.

Another possible explanation is that, as a the result of special conditions obtaining in the Taurus-Auriga complex, the number of multiple systems formed there is above average. This should agree with a theoretical study made in 1994, according to which more multiple systems are formed in cool clouds than in warmer ones. This hypothesis is supported by two investigations made in 1994 and 1995, which demonstrated a smaller proportion of multiple systems in the warmer star formation regions Ophiuchus and Scorpius-Centaurus, corresponding almost exactly to that of main-sequence stars. In order to test this hypothesis, many investigations are currently being conducted on multiple systems in various stellar formation regions.

Beyond that, the discovery that almost all young stars belong to multiple systems has repercussions on the determination of the ages of young stars. If one looked at young stars without knowing that they have a companion, their luminosity would be overestimated. Then they are assigned a position in the Hertzsprung-Russell diagram which is too far up, where according to the theoretically calculated evolutionary paths younger stars are located: the stars are thereby classified as too young. In lower-mass T Tauri stars, this effect can modify the calculated age by a factor of two to three. It is not quite so pronounced in Ae and Be stars, since here the luminosity ratio between the main and companion star is generally larger and thus the main star's luminosity dominates.

Luminous Blue Variables - Precursors of Type-II Supernovae?

When a star has almost used up its fuel supplies, processes are initiated deep inside which result in changes in its luminosity, colour, size and other observable properties. In the so-called Hertzsprung-Russell diagram, the star now moves away from the main-sequence where it had remained during its quiet combustion phase. The details of how the final stage proceeds depend almost entirely on the star's mass.

A sun-like star blows itself up, towards the end of its life, into a red giant. During this process it cools down, its colour becomes redder and its diameter increases a hundred-fold. In addition, it loses a considerable proportion of its outer layers to its surroundings in the form of a particle wind. This gas mantle shines later as a planetary nebula. The star ends as a white dwarf.

More massive stars end more spectacularly. They evolve into blue supergiants, which also give off a large proportion of their material as a wind. Finally they explode as type II supernovae, and leave behind a rapidly rotating neutron star or a black hole.

The course of the last evolutionary stage is not known precisely. It depends not only on the mass but also on the chemical composition of the stellar material. The decisive factor during this phase is how much material the star blows off into space before its explosion. Since little is known about this quantity, the final phase can only be understood theoretically with some uncertainty. And since evolution from main-sequence star to supernova proceeds relatively quickly, only a few stars are known of which one assumes that they are in this transitional stage. These objects include the luminous blue variables (LBVs).

In general, LBVs are distinguished by the following properties: they are blue supergiants with over 10^5 solar luminosities, their spectral type is O to A, they exhibit brightness variations of at least half a magnitude, and they generate a strong particle wind. Often they are surrounded by axially symmetric, bipolar nebulae. Among the best known LBVs one can name Eta Carinae in the Large Magellanic Cloud, a massive star surrounded by a carbon-rich nebula.

LBVs are also very bright in the infrared. Observations of their surrounding nebulae at wavelengths of 10 to 20 µm are particularly for three reasons: 1) The extinction of the circumstellar and interstellar dust is very low. 2) Matter in the nebula is of low optical density, which makes an estimate of mass possible. 3) Contamination through the star's light is lower than in the visual spectrum.

In 1997, a group at MPIA studied in detail an LBV with the designation HD 168625. It used the MAX infrared camera built at MPIA, on the 3.9-metre UKIRT in Hawaii (Chapter I) and obtained excellent images at wavelengths of 4.7 µm, 10.1 µm, 11.6 µm and 19.9 µm. Thanks to the tip-tilt mirror, also built at MPIA, the resolution of the images was diffraction-limited; these were the first high-resolution images of an LBV in the thermal infrared. They permitted the study of dust distribution in the star's neighbourhood, with a wealth of detail not previously achieved.

HD 168625 is one of the few LBVs in the northern sky. The star is currently in a quiet phase, but variations in the spectral index from B2 to B9.8 have been observed in the past. It is expelling a wind of high-speed particles, and is surrounded by an almost ring-shaped nebula with a diameter of 15 arc-seconds. Using observational data already available, the Heidelberg astronomers determined again the distance of HD 168625. Instead of 7000 light-years as assumed up to now, it is probably only 4000 light-years. This correction has repercussions on the physical stellar parameters derived from the distance (e.g. the luminosity), as well as on the star's presumed state of evolution. The following physical parameters can now be calculated: effective temperature: 14 000 Kelvin, radius: 70 solar radii, luminosity: 1.7×10^5 solar luminosities.

The image recorded at a wavelength of 11.6 µm shows an elliptical dust ring surrounding the star, whose dimensions are 12 arc-seconds × 16 arc-seconds (Figure IV.12). At the assumed distance 4000 light-years, this corresponds to 0.23 × 0.29 light-years). The ring is not uniformly bright, but rather has two arc-shaped bright parts roughly at the ends of the long semi-axis. It is sharply bounded at its outer edge, but weak diffuse emission can be discerned at the southern side below the bright arcs. In addition, the two arcs and the two weaker arc-sections of the nebula exhibit different radii of curvature and centres of curvature. This means that the nebula does not have a simple elliptical shape.

Precise analysis shows that this morphology cannot be explained either by a ring or a torus surrounding the star, or by a shell. A bipolar structure is best at reproducing the observation's findings: the astronomers suspect that a dust disc lies in the system's equatorial plane, and that a bipolar hourglass-shaped nebula surrounds the star, with the dust which radiates in the infrared being located in a thin shell. Since the bipolar nebula's long axis points towards us, it appears to us in the form of two bright arcs. Using a simple model which assumes dust particles ca. 1 micron in size, the astronomers estimate that the nebula contains a total of 2.8×10^{-3} solar masses in the form of dust, which radiates away power at wavelengths from 4 to 300 µm, at a rate of 5.7×10^4 that of the sun.

A new evolutionary scenario was derived for the star (Figure IV.13). According to this, the mass of HD 168625 on the main-sequence was 25 solar masses; from there the star evolved first into a red supergiant, and as such it produced a 10 km/s wind at a rate of 2×10^{-5} solar masses per year. After that it evolved into a blue supergiant and currently expels a 183 km/s wind into space, losing an estimated 3×10^{-6} solar masses per year. The nebula visible today is a remainder from the red supergiant phase.

If the nebula's morphology is really bipolar, then the previous red supergiant must also have given off a non-isotropic particle wind. How this came about is unclear. One possible explanation states that the slow particle wind is blown into the equatorial plane due to the star's rotation, and there it condenses into a disc. Another
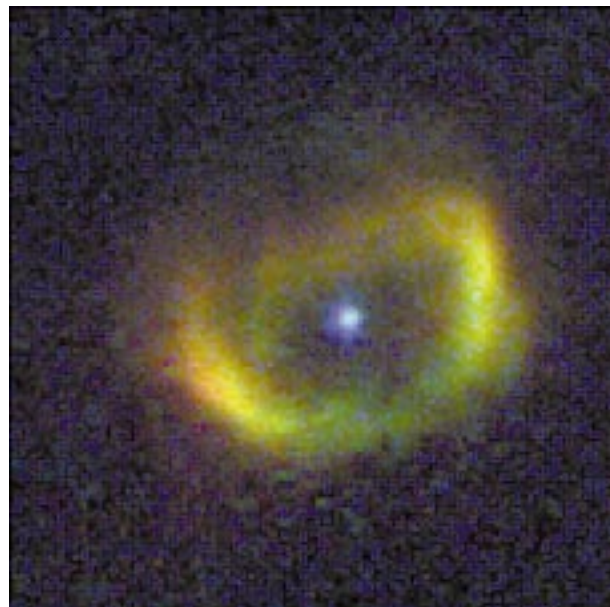

Fig. IV.12: The nebula of the luminous blue variable HD168625. The false colours show the infrared radiation emitted by the nebula at wavelengths of 4.7 µm (blue), 11.6 µm (green) and 19.9 µm (red).
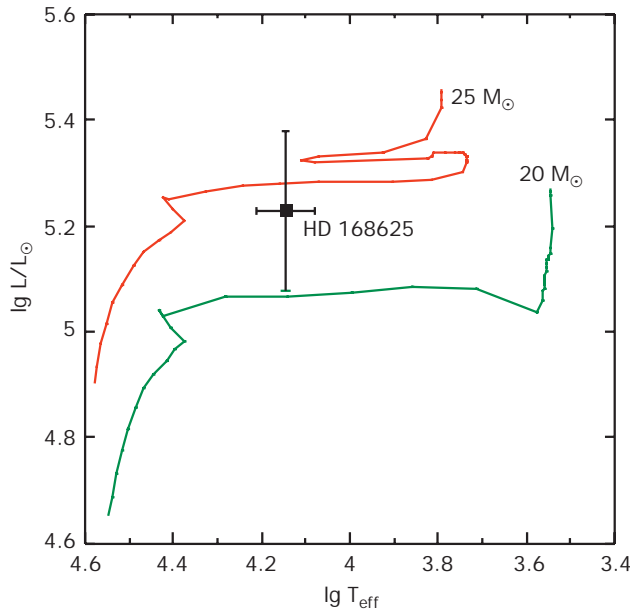
Fig. IV.13: The evolutionary status of the luminous blue varia-ble HD168625, according to the recently collected data. According to these, it is a blue supergiant of ca. 24 solar masses.

hypothesis bases the phenomenon on a near, invisible companion star. In this case the gas flows from the red giant across to the companion. and in this way forms the disc. The effect of this is that the later fast wind can only escape perpendicularly to the disc-shaped, dense dust cloud.

Theoretical Studies

The task of astronomy is to observe cosmic pheno-mena and interpret them in such a way that the numerous different snapshots fit together into an evolutionary timetable, thus making the history of celestial bodies comprehensible. However, due to the enormous time-scales, these processes are practically never directly observable. This is where theoreticians come to the observers' aid. They can make cosmic processes clearer through complex computer simulation, and attempt to interpret the observed phenomena. The group of theore-tical astrophysicists at MPIA supports their observing colleagues with their computations. Only when the models adequately reproduce the observed phenomena can one assume that one has understood the physical interconnections.

The Formation of Stars

Stars are created during the collapse of interstellar clouds, which may contain up to several million solar masses in the form of gas and dust. The interior of these clouds is protected against high-energy UV radiation, which is why very complex molecules can form there. Hence the dark clouds are also known as molecular clouds.

A molecular cloud can contract under its gravity when the gravitational force directed towards the cloud's cen-tre is stronger than the material's pressure directed out-wards. As early as the beginning of the 20th century, the British mathematician and astronomer Sir James Jeans discovered, on the basis of well-known physical laws, the minimum mass which a cloud of given density and temperature must contain in order to become unstable and contract under its own gravity. At a temperature of 20 Kelvin and a density of 3×10^{-24} g cm^{-3}, correspon-ding to 100 H$_2$ molecules per cm^3, this critical Jeans mass is around 400 solar masses. The Jeans mass is still considered today the decisive parameter for the initiati-on of star formation.

The reason why such massive gas and dust collections nevertheless give rise to stars with masses of around 0.1 to 100 solar masses, is that during their contraction phase the clouds break up into several fragments, which themselves are unstable. In general, a large cloud com-plex ends up forming very many stars. If, during a later stage, the remainder of the cloud evaporates, a cluster of stars becomes visible at this location. A familiar example is the Pleiades, an open star cluster with around 3000 members, whose age is estimated at ca. 50 million years.

Although the essential phases in star formation are known today, several important questions still remain unanswered: under which conditions will a single star or a multiple star system form, under which a planetary system? Which fraction of the gas cloud is used up in star formation? What is the effect of magnetic fields on the stability of clouds and on star formation? What is the frequency with which stars of different masses are for-med? Is this so-called initial mass function universal, and if so, can it be calculated theoretically? On what external conditions does it depend? It is already known from observations that the proportion of stars rises with reducing mass. However, up to which mass does this trend continue? Does this relationship level off at a par-ticular minimum mass? This question is particularly interesting since it relates to the frequency of brown dwarves. These objects are transitional between stars and planets, at masses supposedly around 0.08 solar masses. Their luminosity is extremely low, hence only detectable with great difficulty; therefore their share of the overall mass of the universe is unknown.

The Collapse of Molecular Clouds

From the total mass of molecular clouds in the Milky Way and the lifetime of the stars created in them, it is possible to estimate the mean lifetime of molecular clouds at several tens of millions of years. At the same time, the so-called mean free-fall time is calculated at merely a few millions of years. The free-fall time is the time within which matter collapses in free fall until it becomes optically thick. However, if the lifetime of clouds is around ten times longer than their free-fall period, an effective mechanism must be operating inside them which prevents their collapse at least for a period of time. This mechanism decisively influences the galaxy's star formation rate.

From radio observations it has been known for some time that the gas inside the clouds is strongly turbulent and is moving at supersonic speeds. Shock waves travel through the cloud and protect it against collapse. But computed models have so far shown that such turbulent motions dissipate their energy too quickly, namely roughly within the free-fall time, in the form of heat given off. That is, the shock fronts are damped and subside very rapidly. Hence they cannot prevent the cloud's collapse for long.

One has assumed that magnetic fields, which locally reach values of a few tens of microgauss, trigger so-called magnetohydrodynamic turbulences which dissipate their energy more slowly and thus stabilise the cloud against collapse within the free-fall time. It was only in the early Nineties that model calculations were possible which can take into account the interaction of the gas with an interstellar magnetic field.

In MPIA's theory group, using the most accurate computer simulations carried out so far, the three-dimensional behaviour of magnetohydrodynamic waves in a molecular cloud could be modelled (Figure IV.14). The physical basis for such models is the formation of so-called Alfvén waves. Let us imagine a homogenous magnetic field with parallel field lines in a partly ionised medium. In a moving gas, the field lines are dragged along by the (electrically charged) ions, and extended in various directions like rubber bands in dough. This generates magnetic forces, which on the one hand attempt to shorten the magnetic field lines again. The result is a wave in the field lines, which propagates along the lines as in a vibrating rubber band. At the same time, this magnetic wave reacts on the surrounding ions and imparts to them a momentum. This creates a matter-wave normal to the field lines, the Alfvén wave.

The temporal behaviour of Alfvén waves in gas clouds was simulated at MPIA with the lattice-based ZEUS-3D code on an SGI Origin 2000 computer. A further, so-called SPH Hydrodynamic program ran on a special computer used by the group, with so-called GRAPE (Gravity Pipe) processors. GRAPE is a special type of hardware which solves the relevant physical equations at a speed of 5 gigaflops per processor. The computations ran with a resolution of 2563 lattice points or 350 000 particles. Two cases were distinguished:

1) a strong magnetic field, in which the mean turbulent gas velocity in the cloud equals that of the Alfvén wave,
2) a weak field, in which the mean turbulent gas velocity in the cloud is ten times larger than the Alfvén speed.

It was shown that a weak field is better at reproducing the observations. In this case the cloud's interior contains numerous clump-like condensations and the magnetic field strength increases with particle density, whilst in the strong field it is almost constant throughout. Alfvén shock waves can even compress matter locally to such an extent that the Jeans mass is exceeded. That is where star formation can begin.

Furthermore, the simulations showed that apparently magnetic fields are unable to counteract decisively the dissipation of turbulences. In all the simulated cases, even with strong magnetic fields, the turbulent motions subsided long before the end of the observed lifetime of molecular clouds, i.e. several tens of millions of years. In none of the cases were the magnetic fields able significantly to inhibit the decay of the turbulence (Figure IV.15). Thus, in order to maintain the turbulence and effectively to counteract the cloud's collapse, kinetic energy must be supplied to the gas more or less continuously. This probably happens through stellar winds and jets (see above), high-energy radiation from young, hot stars and galactic shear movements. The latter are created through the differential rotation of the Milky Way system: regions nearer to the galactic centre have greater angular velocity than those further out.

Fig. IV.14: Three-dimensional computer simulation of a turbulent interstellar cloud. In this computation, the existence of an initially vertically-oriented, strong magnetic field was assumed, giving rise to Alfvén waves.
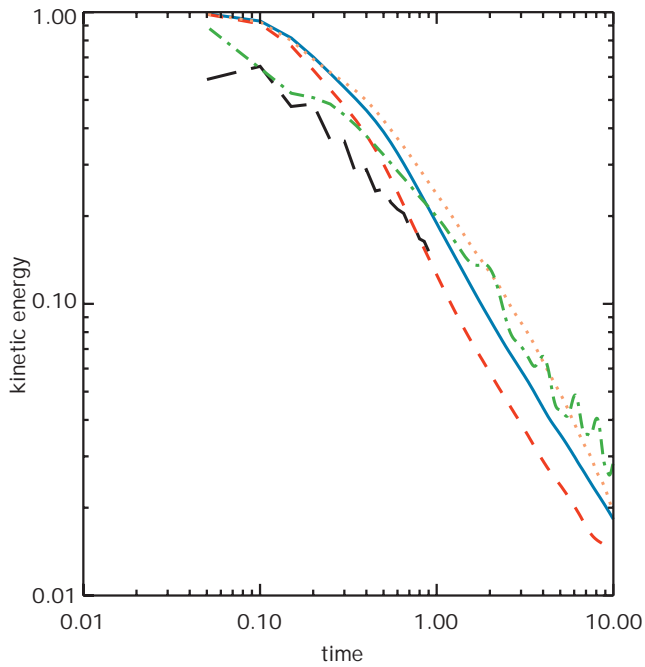
Fig. IV.15: Decay over time of the turbulent kinetic energy within a cloud, under various physical conditions: isothermal (continuous line), adiabatic (dotted), weakly magnetized (broken) and moderately magnetized (dots and lines). Time is given in units of L/c, where L is the characteristic length of the volume being considered and c is the speed of light.

Fragmentation of a Molecular Cloud

If a large region of a turbulent gas cloud exceeds the critical Jeans mass, gravitation predominates over gas pressure and the region collapses. The internal condensations which are already present begin to grow denser during the collapse, attract further material from the surrounding region and thus continue growing. These cloud fragments contract further and further, until a single star or a multiple system has formed out of them after a period which is of the order of a million years. However, today it is still not possible to simulate this overall process in a single computer model. Even from the cloud stage up to the formation of a protostar, which continues to evolve further by sweeping up more material and possibly fusing with other protostars, the gas density increases by 15 to 18 orders of magnitude. To be able to follow the entire evolution on a computer despite these difficulties, it is subdivided into individual phases which can be simulated separately.

The MPIA theory group has produced a program which simulates the formation of star clusters. The program considers a large region of cloud which becomes gravitationally unstable as a whole. Such a cloud, with 222 Jeans masses, is represented by 500 000 mass points. Translated to observed star formation regions, this means the following: in Taurus-Auriga, the simulated volume corresponds to a region whose edge is 17 light-years long and whose total mass equals 6300 solar masses. The time-scale is three million years. In a region containing many massive young stars, such as the star formation region in Orion, this volume would be reduced to a cube one light-year long, with 1000 solar masses and a time-scale of 95 000 years. Each run on a Sparc Ultra workstation in conjunction with GRAPE-3AF required two weeks of computer time.

During the phase of the cloud's collapse considered in this simulation, the material can be assumed to be isothermal; the behaviour of the gas results mainly from the interplay between gas pressure and gravitation. Since this investigation is not concerned with the later evolution of the generated protostar into a star or into a possible planetary system, but with the interaction of the cloud cores with their surroundings, the program simplifies such a core to a single spherical mass (a »sink particle«) when a specified density is exceeded. From then on the evolution of this protostar, which is not isothermal any more, is not followed further. However, the program does follow the further accretion of matter by the protostar from its surroundings and the interaction with other protostars.

The background to these simulations is the question of whether the initial mass function, i.e. the stars' frequency distribution as a function of their mass, can be derived theoretically.

In order to initiate the condensation of individual cloud fragments, fluctuations with a specified size-distribution were imposed on the density field. At first it was shown that thermal pressure very quickly »smears out« small condensations, whilst the spatially large-scale fluctuations continue to contract into elongated filaments and nodes (Figure IV.16). The first strongly condensed protostars form in the centres of the most massive clumps, whilst smaller condensations only develop later. This leads, finally, to a hierarchically structured star cluster with numerous mass-accreting and mutually-interacting protostars.

The further evolution of the investigated protocluster proves to be extremely complicated. The gas clumps continue to collect more gas, move around through the cloud whilst doing this as a result of the inhomogeneous gravitational field, and interact in manifold ways with each other. It can be shown that the rate at which surrounding gas falls onto the protostars depends very strongly on the dynamic interaction between them. Cloud cores which are very close to each other compete for the surrounding material. However, as an average it can be shown that the first protostellar cores form in the densest regions, and these also become the most massive (Figure IV.17). A close encounter between protostars can lead to an unstable multiple system, or change the trajectory of an object to such an extent that it moves from the central region of high-density gas to the outer regions which are poor in gas, or is even thrown out of the cloud (Figure IV.18).

During this simulation it became clear that the evolution of individual cloud cores is unpredictable, and can be best described using the methods of deterministic chaos theory. According to this, the mass distribution between the stars achieved at the end of this process is not unambiguously specified by the given density distribution. Nevertheless, it may be possible in the future to calculate it using statistical methods.

However, the result common to all simulation runs is a broad mass spectrum whose maximum lies around 0.2 solar masses (Figure IV.19). One needs to apply this result with care, since by the end of the simulation it is no longer possible to distinguish between individual stars and multiple systems: when two protostars join to form a double star, they are regarded by the program as a single sink particle. Hence, at the end of the day, the program provides the mass spectrum of multiple systems (mainly double stars). This reproduces well the observed mass function above 0.2 solar masses. The interesting region below this limit, which also contains the brown dwarves below ca. 0.08 solar masses, is not yet amenable to observation.

Nevertheless, further simulations already indicate that brown dwarves are only formed during a late phase in the cloud's gravitational collapse, a phase during which the interstellar gas had been largely used up. If this is the case, then brown dwarves do not contribute greatly to the total mass bound up in stars.

The Formation and Evolution of Protostars and Multiple Systems

Whilst the simulations described above follow the formation of a star cluster in a molecular cloud, MPIA's theory group also looked into the evolution of an individual cloud core into a single star or multiple system, using a series of further hydrodynamic n-bodies calculations.

Investigations of star-generating regions such as the Taurus-Auriga or the Orion complex have shown that nearly all young stars are part of a double or multiple system. In main-sequence stars, the incidence of single stars such as the sun seems to be somewhat higher. This implies that some double-star systems disassociate during their history (see above). In general one assumes

Fig. IV.16: Evolution over time of the fragmentation of an interstellar cloud of 222 solar masses. The time *t* is given in units of free-fall periods, the percentage denotes the proportion of the material used up in the formation of stars.

t = 0.0
M = 0 %

t = 0.5
M = 10 %

t = 0.9
M = 30 %

t = 1.5
M = 60 %
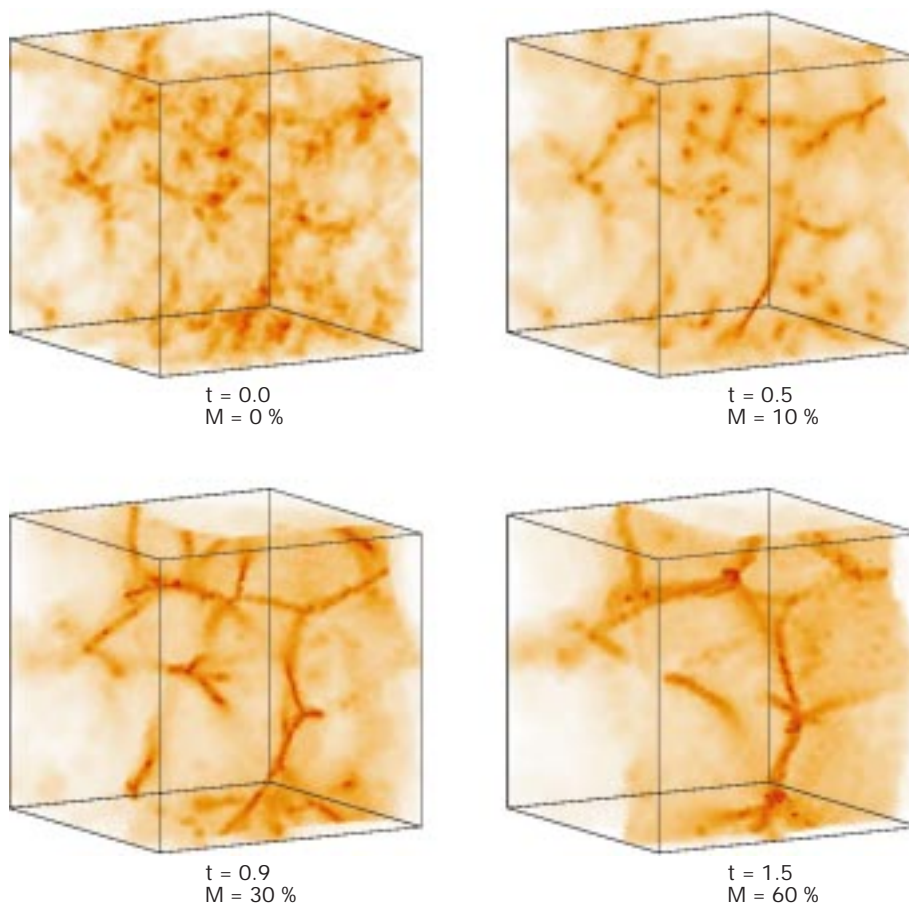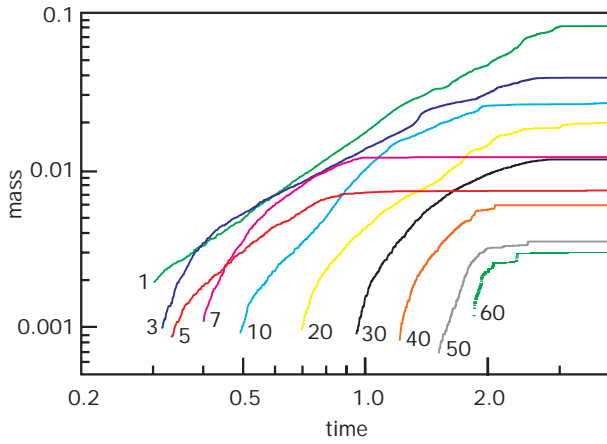
Fig. IV.17:Evolution over time of the increase of mass in proto-stellar cores. The numbers are the sequence of appearance of condensations. On average, the earlier a star begins to form, the more massive it becomes.
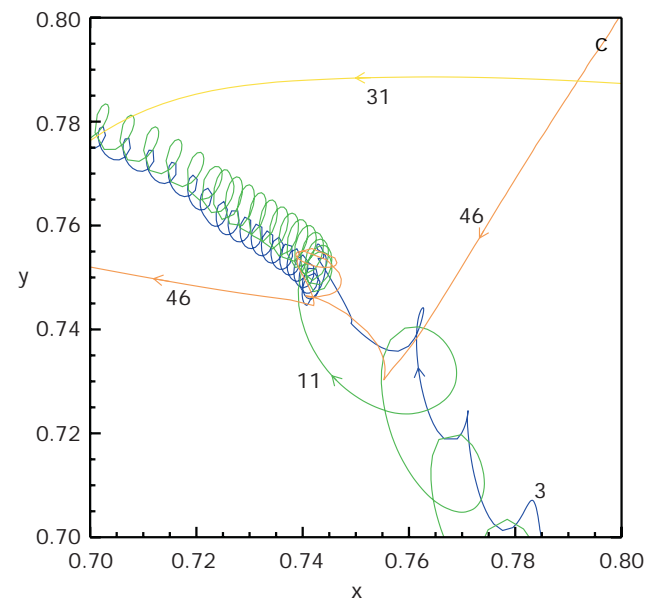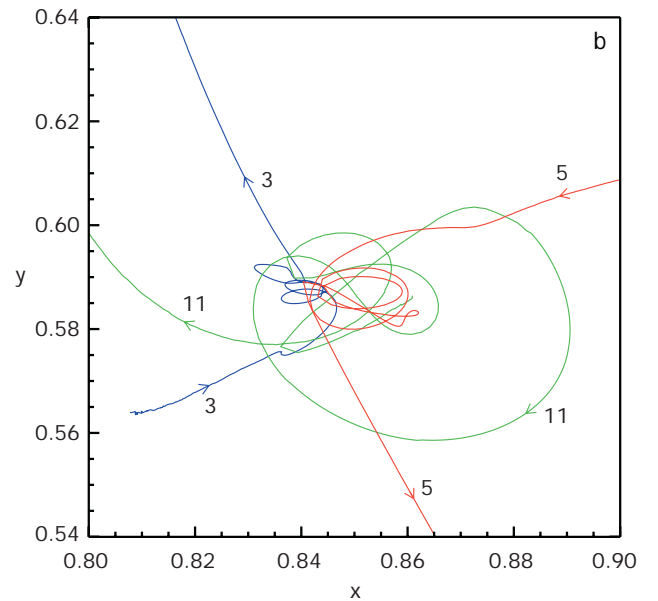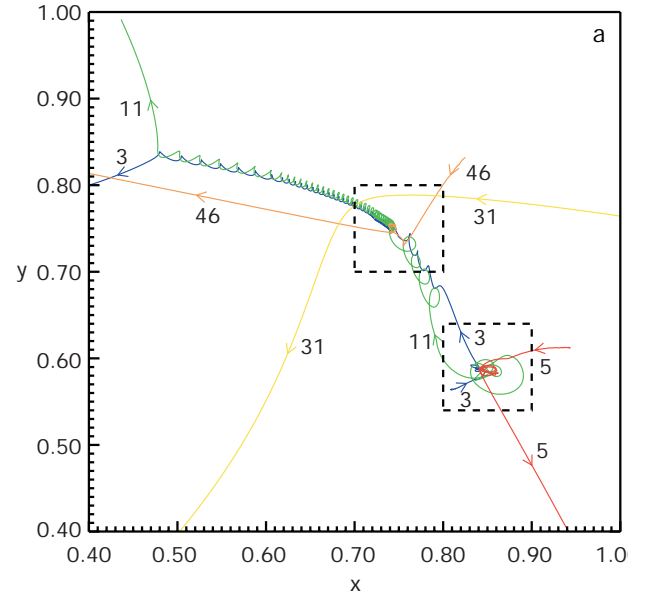
Fig. IV.18: Spatial motions of several selected protostellar cores within the cloud. (a) Core 5 forms shortly after its emergence a double system with core 11. Core 3 is added a short time later, so that the three cores form a triple system. However, this is unstable, and core 5 is ejected. (b) shows this region in detail. (c) also shows a very interesting interaction between several cores.
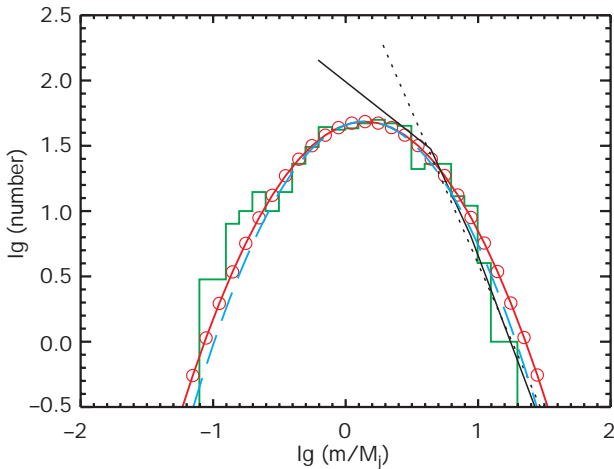
Fig. IV.19: Comparison of the calculated mass distribution in protostellar cores in units of the Jeans mass (broken curve) with a distribution calculated recently by other authors (continuous thin curve with circles). The thin continuous line reproduces a measured distribution, whilst the broken line corresponds to the »classical« Miller-Scalo distribution.

today that the overwhelming majority of multiple systems form as early as during the phase of collapsing to form a protostar.

In order to understand this process, the theory group simulated in three dimensions the contraction of a protostellar clump up to the protostar stage. At the start of this process the initially spherical cloud, equivalent to one solar mass, had a radius of 3300 astronomical units (one astronomical unit, AU, corresponds to the mean orbital radius of the earth, i.e. 150 million kilometres). A density distribution was assumed which drops exponentially from the centre outward, with the central density being 20 times higher than in the outer region. The free-fall time of such a cloud is 16000 years. The calculation covered 1.5 free-fall times. Isothermal conditions were assumed, which however are only valid up to a maximum density of ca. 10^{-10} g cm^{-3}, corresponding to 10^{14} hydrogen atoms per cm^3. Above this value the gas becomes optically dense, the radiation can no longer escape and the gas heats up. However, this state is only reached in the interior of the protostars, which is excluded from further simulation.

Two simulations with different degrees of resolution were carried out, with the lattice separation in both cases being chosen in accordance with the particular requirements. In the low-resolution calculations the lattice separation was 6 AU, in the high-resolution 1.6 AU.

Since the cloud rotates, the centrifugal forces pull it out initially, at right angles to the axis of rotation, into a disc (Figure IV.20). After roughly 1.3 free-fall times (20800 years), a central bar-shaped structure forms in the disc whose inner region rapidly breaks up into a new, smaller disc with a central thickening (Figure IV.21).

The formerly outer regions of the bar now form two spiral arms, in which gas continues to flow towards the central thickening. The outer disc remains intact. The noticeable thing about this configuration is that the inner disc (radius 20 AU) exhibits a substantially lower thickness than the outer one. Gas from the outermost regions falls onto the outer disc at supersonic speed, where it is braked in a shock front and continues to sink towards the centre point.

The result is that more and more material is fed to the inner disc, which above a critical mass fragments into two condensations after 1.42 free-fall times (22400 years); these revolve around the central thickening at a distance of 13 AU. The two new condensations initiate the formation of spiral arms pointing outwards, which eventually stretch into a circumstellar ring that in turn condenses into a further double system after 1,42 free-fall times (22700 years). At this point the system, with a total of five cloud cores, is still – as always – surrounded by a common disc. By the end of this phase the central condensation contains 0.015 solar masses, the two inner double condensations 0.01 solar masses each and the two outer cores 0.03 solar masses each.

The question now arises as to whether this quintuple system remains stable. The behaviour of the inner triplet was studied in a simulation with reduced spatial resolution. It was shown that the inner, triple system takes on a stable, hierarchical configuration, in which two of the objects form a tight pair around which the third body revolves in an orbit lying far out. Finally the latter fuses with one of the two outer fragments. Thus the system has evolved into an inner and an outer double star. Even this system is not stable in the final analysis. During a later phase the four protostars fuse into two, and another small star is formed which revolves around one of the other bodies. Later evolution could not be unambiguously worked out, due to limited computer time. It is possible that one of the bodies is ejected from the system as a result of gravitational interactions.

Hence these simulations show that the formation of double and multiple stars can be very simply explained
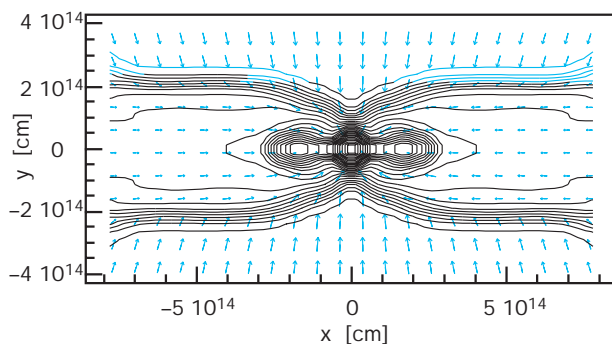

Fig. IV.20: Calculated density distribution in the circumstellar disc: side-view. One astronomical unit corresponds to 1.5 × 10^{13} cm.
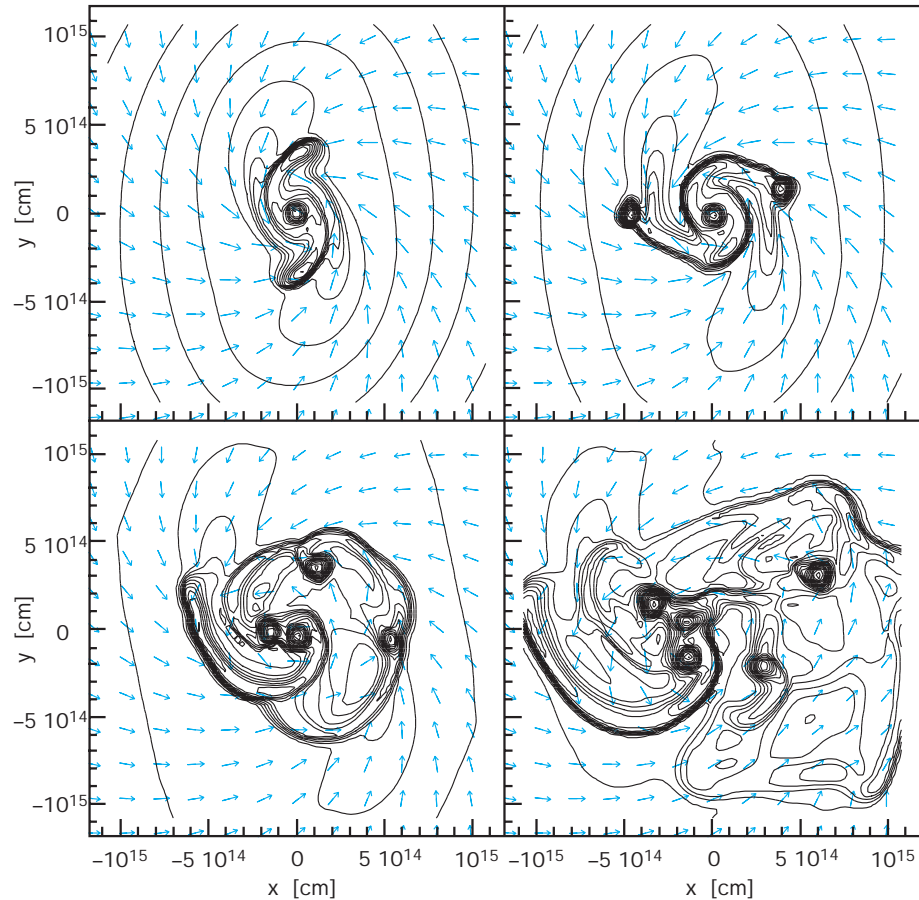
Fig. IV.21: The formation of protostellar cores in a disc of gas and dust.

as resulting from the fragmentation of an interstellar gas disc. This applies both to massive double stars in relatively widely-spaced orbits and to low-mass companions. Unfortunately, these calculations cannot be used to derive the observed distribution of the periods of revolution of double stars from simple initial conditions. The evolution of a multiple system depends on too many parameters to make this possible, such as the ratio between the rotational energy of the gas to the disc's potential energy, or the ratio between the kinetic and potential energy of the gas. Furthermore, the protostellar discs travel through the molecular cloud, which gives rise to gravitational interactions that can proceed up to the fusing of the discs.

One decisive initial condition in these calculations consisted of the assumption of an exponential density distribution of the gas, decaying from the centre outwards. However, observations in molecular clouds have shown that the density in these clouds tends rather to drop with increasing distance r from the centre according to a power law of the form $\varrho(r) \sim r^{-p}$ with $1.25 < p$

< 2.0. This means that in the above simulation the assumed density distribution was concentrated too much at the centre. However, earlier simulations which assumed a power law with $1 < p < 2$ did not exhibit the expected fragmentation of disc material. Thus they could not explain the formation of double and multiple systems.

Next, the evolution of a protostellar, initially spherical gas cloud was simulated at MPIA, whose density falls off inversely to the distance r from the centre ($p = 1$). In contrast to previous calculations, this simulation was carried out at substantially better resolution. As in the previous case, the disc's total mass was one solar mass and the original size was also 3300 AU. The simulations were carried out using two techniques: the first one with a lattice code in which the resolution (mesh size) was adjusted to the circumstances, the highest resolution being 1.6 AU. The second used Smoothed Particle Hydrodynamics (SPH) code with 200 000 particles. In SPH code, resolution increases automatically with increasing particle density. It was considerably accelerated in comparison with earlier versions, by selecting for each particle an individual time-step adapted to the situation. (Earlier versions defined a time-interval for all particles). In addition, computer time was reduced by a factor of 5 solely by using the special GRAPE hardware (see above).
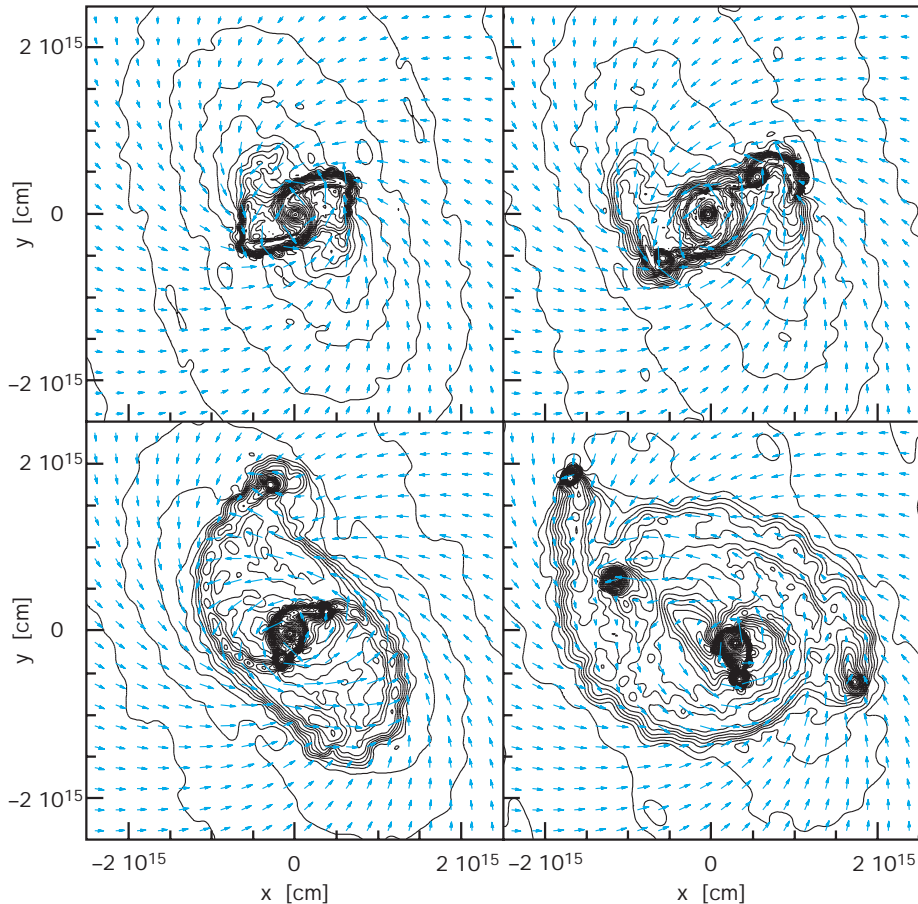
Fig. IV.22: An initially spherical, rotating cloud whose density drop is inversely proportional to the distance from the centre outward, forms over time a disc in which several protostellar cores emerge.

A relatively large value of 0.23 was assumed in the first simulation run for the ratio of rotational to potential energy. In this case, the density in the disc's inner region grew at first by six orders of magnitude, before it started fragmenting after 37 000 years. A spiral structure formed around the central condensation, with two condensations created in the former. Finally this system continued to evolve qualitatively in quite similar fashion to the one described above, with the initially exponential density distribution. Five protostars had formed after 38 000 years, whose later dynamic behaviour was not followed any further.

The cloud's rotational energy was reduced by half in the second run (Figure IV.22). In this case too the disc fragmented, but somewhat sooner than in the case of high rotational energy, and it also broke up into five condensations. However, compared with the first case, the distances between the protostars were now smaller by a factor of roughly four, and the masses somewhat lower.

This demonstrated for the first time that even protostellar cores with strong central condensations can fragment. In the earlier calculations, low spatial resolution caused an essential effect to be overlooked: even during the initial stage, gas pressure increases in the central region more than gravitational pressure. Hence the central region expands, leading to a density profile whose drop is flatter. However, a disc with a small density gradient fragments more easily than one with a steep profile, i.e. with a sharper central condensation. Moreover, it was reassuring to find that both simulation techniques, lattice code and SPH, produce almost identical results.

According to this, the formation of double and multiple systems appears to be the rule, which is why today the origin of single stars is the one which seems to be problematic. One possibility is that a system which to begin with was a triple one, becomes unstable and one of its members is ejected.

What is the relationship between these theoretical results and reality? An investigation carried out in 1991 by the Swiss astronomers Antoine Duquennoy and Michel Mayor into 164 G-type stars on the main-sequence up to a distance of 72 light-years, showed that only one third of the objects were single stars. Their investigation exhibited several general properties of the observed double stars:

- the distance between the components can be several stellar radii up to 10 000 AUs;
- the distance distribution exhibits a maximum around 30 AU, corresponding to a period of revolution of ca. 180 years;
- orbital eccentricity increases with orbital radius. The components travel along circular paths only in tight systems, which can be explained by the effect of strong tidal friction;
- the mass distribution of the two components appears to have a wide maximum around 0.2 solar masses.

How can these observed properties be understood as arising from the processes of star formation? To this end, the MPIA theory group considered the evolution of an existing double star system, which continues to accrete material from its surroundings. This process has various consequences: for one thing, the stars' mass continues to increase, which adds to their gravitational attraction and therefore reduces their distance from each other. At the same time, the material falling in from the surrounding disc has an angular momentum which it transfers to the stars, hence the distances increase (the angular momentum is calculated from the product of mass times the discs angular velocity). On the other hand, the two components can lose angular momentum through friction with the gas remaining in the surrounding disc, thus in turn reducing the distance between them yet again.

In order to reproduce these processes, further simulations were carried out using an SPH code and sink particles. This means that when particles from the disc were captured by a star, they disappeared inside it and were not taken into consideration any further. At the same time, the disc was continually fed with particles from outside having constant angular momentum, so that the reservoir could not become exhausted. The gas was assumed to be hydrodynamic, i.e. was assigned pressure and viscosity. Particle density was so low that the disc could not fragment into another protostar. The disc always contained 3000 particles, each with a mass of 5 $\times$ 10^{-7} of the total mass of both stars together (i.e. with an overall mass of both stars together equalling two solar masses, each »particle« would have about half the mass of the planet Mars). The simulations were terminated when ca. 20 000 particles had been added to the disc.

The simulations showed that the evolution of a material-accreting double star system depends critically on the disc's angular momentum, i.e. substantially on its angular velocity (Figure IV.23). Such a system exhibits three different regimes. Below a certain angular momentum, a disc is formed around the primary star; above this value, a disc forms around each of the two stars. If the angular momentum becomes even greater and exceeds a second critical value, then a common, circumbinary disc forms around both stars. This range of behaviours is also exhibited as different stages of evolution of the double stars.

Gas from a disc with low angular momentum (disc around a primary star) falls mainly on the primary star and increases its mass. This reduces the mass ratio between the secondary and the primary star, and the distance between them drops. This is true of all double systems, regardless of the initial mass ratio. With increasing angular momentum in the disc (each star surrounded by a separate disc), the secondary star collects more matter, so that the mass ratio becomes closer to 1. In this case the transfer of momentum to the stars is so great that their separation increases. If the angular momentum continues to increase, the circumbinary disc slowly grows. In this case too, the secondary star accretes more mass than the primary star, and the separation increases.

Hence this simulation shows: with low angular momentum, the mass ratio of the stars drops and so does the distance; with higher angular momentum, the mass ratio increases and so does the distance.

If the accretion of material from a disc strongly affects the physical parameters of double star systems, then one would expect a low mass ratio in double stars with intermediate to long periods, with fairly equally massive components in close double stars. The reason is that in close systems the specific angular momentum of the accreting material tends to be higher than that in the double stars, and smaller in widely-separated systems. Observations made during two studies indicate that this situation does obtain.

The predictive power of these calculations is limited by the fact that in reality the disc can fragment, so that a further protostar is formed in it. In addition, the protosystem travels as a whole through the molecular cloud and thus interacts gravitationally with other systems, or fuses with them.
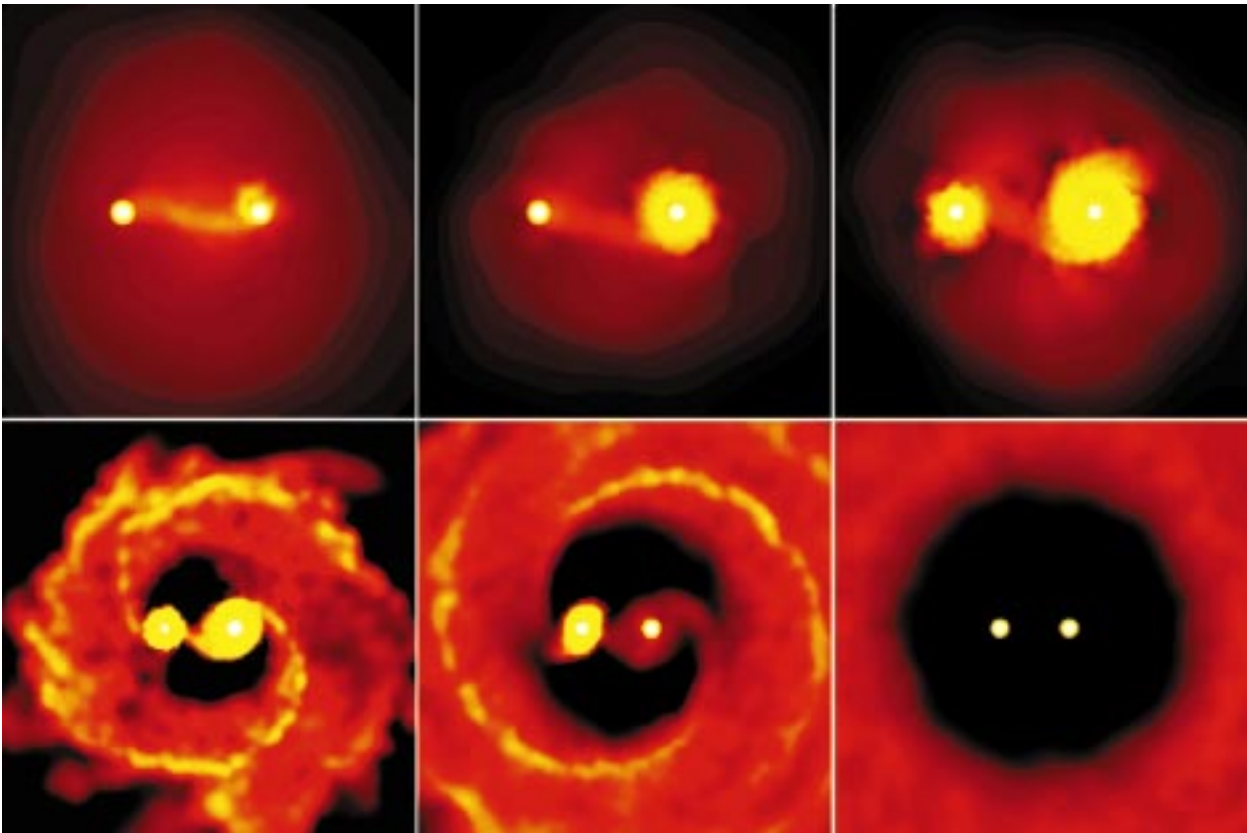
Fig. IV.23: Material falls from a disc of gas and dust onto a rotating double system of protostellar cores with different angular momentums. The angular momentum increases from top left to bottom right. A disc which at first surrounds both cores becomes two discs, which later evolve into a circumbinary disc surrounding both cores.

IV.2   Extragalactic Astronomy

Jets from Galaxies and Quasars

Since the 1980's, astronomers at the MPIA have made repeated contributions towards decoding an extraordinary phenomenon: the extragalactic jets. Research into these jets had already begun more than half a century ago.

In the year 1946, a strong radio source was discovered in the sky and it was given the designation Cygnus A. But it was not until the 1950's that radio telescopes attained sufficient spatial resolution to enable them to identify Cygnus A with a celestial body in the visible range. A galaxy of the 18th magnitude was found at this point, but it was only emitting a small part of the radio radiation which had been observed. The overwhelming majority of it originated from two extended radiation sources located a long way out, almost symmetrically in relation to the galaxy. The distance between these two »radio lobes« was 650 000 light years. In 1984, a jet of particles was finally discovered linking the core of the galaxy with one of the two radio lobes.

This basic structure (central galaxy – jets – radio bubbles) is now known to exist in the case of many extragalactic radio sources (Figure IV.24). More than a hundred jets have already been observed, and the number of double radio sources is far larger than this. The extent of these objects, that is to say, the distance between the two radio lobes, can amount to more than a million light years. This makes them the largest known coherent formations in the universe.

Jets and radio bubbles emit synchrotron radiation. This is created when electrically charged particles move at virtually the speed of light in strong magnetic fields. For the most part, there are probably electrons flowing in the jets, and possibly positrons (their anti-particles) as well. Since synchrotron radiation is a pure continuum without absorption or emission lines, it is impossible to measure the flow speed of the gas by spectroscopic means. On the basis of numerous findings, however, it is now thought to be certain that the nodes in the interior of the jets are moving at approximately the speed of light, and are supplying the radio bubbles with energy.

The central objects are radio galaxies or quasars. Their core regions, in which the jets are generated, cannot be resolved with present-day telescopes. According to current ideas, it is suspected that Black Holes are present there with several hundred million times the mass of the sun; these are surrounded by gas disks from which matter crashes down on to the black holes, releasing large quantities of energy as it does so. The jets emerge perpendicularly to this disk, and magnetic fields play a decisive part in accelerating the particles and collimating the jets.

Fig. IV.24: A typical double radio source: at the centre is the quasar 3C 334, from which a jet leads to one of the nearly symmetrical radio-lobes. (NRAO/VLA).
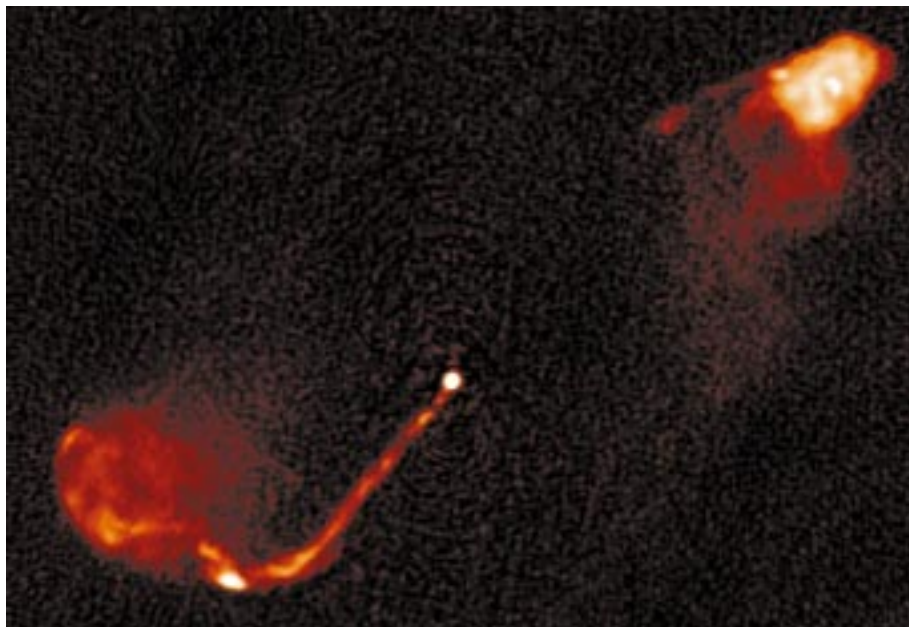
The Jets

There are more than one hundred known jets, and they can almost exclusively be detected in the radio range. Only four relatively bright jets have so far been observed in the optical range, and only one of these emanates from a quasar: 3C 273. This jet has also been the subject of intensive investigation at the MPIA since as long ago as the 1980's. The jet of particles can be detected in the optical range at a distance of between 11 and 20 seconds of arc from the quasar, corresponding to a projected length of 38 000 pc (123 000 light years), measured from the core of the galaxy. The knotty structure which can also be observed on the jet of 3C 273 is typical of these jets of matter.

Although detailed investigations of the jet have been carried out from earth in the optical range, there have so far been no observations in the infrared range. IR data close the gap between the optical range and the radio range, making them very important for a precise determination of the progression of spectral intensity of the synchrotron radiation. Using the MAGIC camera on the 3.5 metre telescope, a deep image at the wavelength of 2.1 mm was obtained for the first time in 1997 (Figure IV.25). This image has an excellent resolution of 0.7 seconds of arc. The jet can be traced from the first knot. A as far as a distance of 23 seconds of arc from the quasar.

The spectral distribution of the synchrotron radiation, that is to say the intensity of the emission in relation to its frequency, contains essential information about the physical state of the electrons in the jet. For the first time, the new measurements made it possible to determine the spectral progression for the whole range from blue, through near infrared, and as far as the radio range.

In general, the intensity of synchrotron radiation declines as the frequency increases. However, for the purposes of physical interpretation, it has proven useful to plot the radiated power per frequency interval in relation to the frequency (Figure IV.26). This procedure clarifies the frequency range in which the particles radiate most energy. It can be seen that this power rises constantly up to a certain frequency, beyond which it falls sharply. The turnaround point drops consistently as the distance from the quasar increases (in the area of the main knots B to D), from about 10^{14} Hz to 10^{13}. This means that it shifts from the near to the medium infrared range. This behaviour underlines the special importance of infrared observations. Only in the first knot, A, was it impossible to observe a break-off point in the spectrum: it must therefore lie beyond 10^{15} Hz.

This turnaround point directly reflects the energy distribution of the radiating electrons: from this value onwards, the number of particles decreases rapidly as the energy increases. If the critical frequency in the jet moves »downstream« towards lower values, this means that the average energy of the electrons decreases as the distance from the galaxy increases.
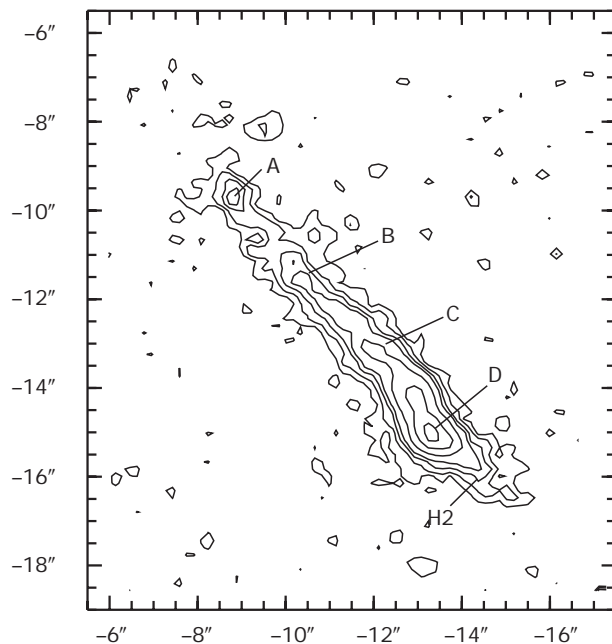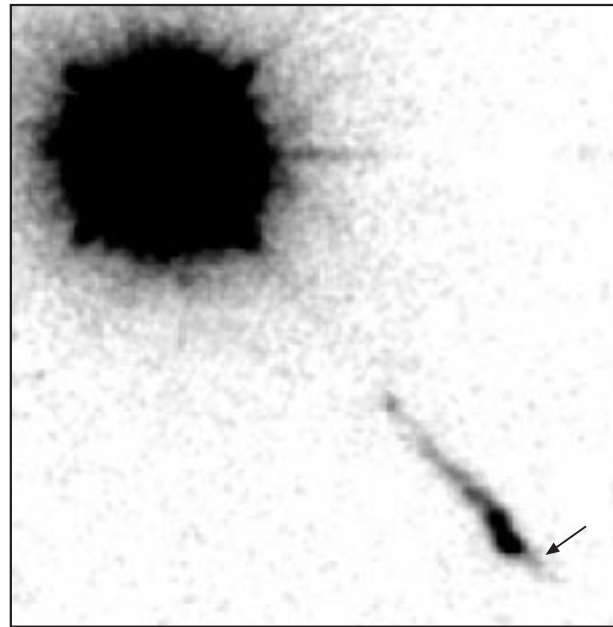
Fig. IV.25: The jet of quasar 3C 273. Top: the first image in the near infrared (exposure: 90 minutes). Bottom: intensity contours. A to D denote the bright knots in the jet, H2 - the hot spot. The coordinates designate the distance form the quasar in seconds of arc.

Astonishingly, a large part of the infrared emission originates from the regions between the knots. The spectral progressions inside and outside the nodes do not vary substantially from one another. This highlights an unsolved problem which has already been known for a long time: it can be calculated that an electron which emits optical or infrared synchrotron radiation can only move a few hundred light years from the place of acce-

leration, since it loses energy due to the emitted radiation, and quickly decelerates. At the remoteness of 3C 273, the bridgeable distance only corresponds to about one tenth of a second of arc. The electrons which originated from the central source therefore have to be constantly re-accelerated, and this must happen at the point from which we receive their synchrotron radiation. From the IR data, it has to be concluded that the particles are accelerated not only in the interior of the knots (as has long been suspected) but also in the regions between the knots. How this functions is not clear.

The Hot Spots

In the outer areas of some radio lobes, compact regions with particularly intense emission are often found in the radio range. It is now suspected that these so-called hot spots mark those points at which the jets are decelerated. As might happen in a gigantic power station, the kinetic energy of the jet flow is converted here into the acceleration of highly energised electrons. These electrons then flow into the radio bubbles and generate the radio radiation which is observed. The fact that different physical processes are taking place in these hot spots than in the jet nodes is proven by the synchrotron spectrum of 3C 273 (knot H2 in Figure IV.26), whose shape is markedly different from the shapes measured in the jet. It already bends sharply downwards at a frequency of 10^{10} Hz.
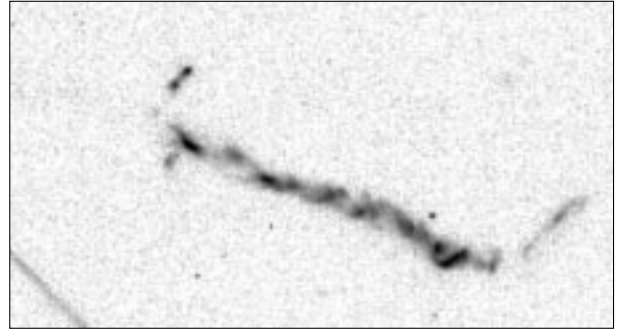
Fig. IV.27: Picture of the jets of 3C 273 taken with the Hubble Space Telescope. (NASA)

In the middle of the 1980's, astronomers at the MPIA were able to prove for the first time that some of the hot spots in the radio range also emit synchrotron radiation in the visible range. The electrons required for this purpose are at least one thousand times more rich in energy than those which emit the radio radiation.

The radiation emanating from the hot spots can be explained astonishingly well with the help of a model which was created at the MPIA in collaboration with colleagues from the University of Edinburgh. This is a slightly modified version of the so-called first order Fermi acceleration. According to the model, the hot spot represents an impact front perpendicular to the direction of flow, in which a relatively strong magnetic field is present. Within this, the incoming electrons are accelerated to and fro like ping-pong balls by the magnetic field, which is positioned more or less perpendicularly to the direction of flow, and the momentum increase in the original direction of movement (away from the quasar) is greater than the increase in the reverse direction. The sum result is that the particles are accelerated in the forward direction, emitting intensive synchrotron radiation. The radiation losses cause a subsequent deceleration of the particles, which now either swirl round in the radio bubbles or flow back in the direction of the source, outside of the jet channel.

Since these processes take place on very small scales of about one tenth of a second of arc, extremely high-resolution images were required in order to test the Fermi acceleration model. This became possible with images of the jet of 3C 273 taken by the Hubble Space Telescope (Figure IV.27). For the first time, they allowed a detailed comparison of the jet structure in the optical and radio ranges, with a resolution in the range of 0.1 seconds of arc. Superimposing the two maps (Figure IV.28) shows that the maxima of the optical and radio radiations from the hot spot diverge significantly from one another. The radio emission has its maximum in a region about 0.15 seconds of arc »downstream« from the optical radiation.
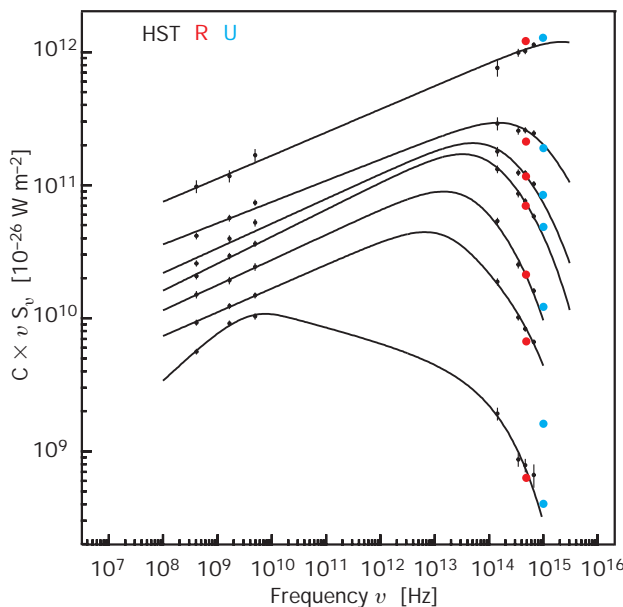

Fig. IV.26: Radiated power as a function of frequency. It is possible to identify the turn-around point, whose position is displaced along the jet with increasing distance from the quasar (A12 to DH3), towards lower frequencies from the near to the intermediate infrared. In the hot spot (H2), the turn-around point is located at a considerably lower frequency.
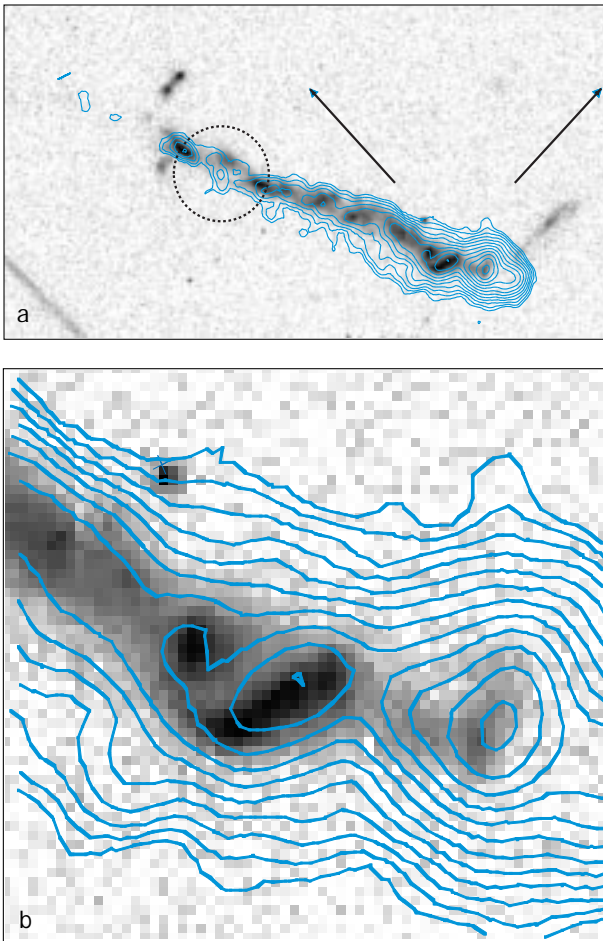
Fig. IV.28: (a) Overlapping the optical HST image with the contours of a radio image. (b) In the hot spot it is possible to see that the radio emission appears to be displaced by about 1.5 arc-seconds behind the optical emission (downstream). The x-ray emission originates in the region marked by a dotted circle.

This provided outstanding confirmation for a prediction from the model, according to which the electrons behind the hot spot lose energy as a result of synchrotron emission. As this happens, the radiation maximum moves downstream from the optical range (higher energy) to the radio range (lower energy) – that is to say, towards lower frequencies.

Another possibility for investigating the theory of electron acceleration in the hot spots was created on the basis of IR images which were obtained by the MPIA group on the UKIRT. For the first time, a total of four hot spots in the radio lobes of bright radio galaxies (which are visible in the optical range too) could also be detected by the astronomers in the near infrared range, at a wavelength of about 2.1 mm. These objects were 3C 20 (West), 3C 33 (South), 3C 111 and 3C 303. The additional IR measurements made it possible to determine the intensity distribution of the entire spectrum more precisely than before, and to use it as the basis for a synchrotron radiation model into which various physical variables are entered.

The Fermi acceleration model was able to provide very good explanations for the observation data in some of the hot spots which were investigated. Accordingly, the diameter of the hot spots is typically 2000 pc (6500 light years), and the elongation along the direction of flow varies between 100 pc (320 light years) and 2000 pc. The magnetic field strengths lie in a narrow range from 30 to 50 nT, and the particles flowing within the jet enter the hot spot at 30 to 50% of the speed of light. In connection with this model, these data allow the conclusion that the time scale for the acceleration of the electrons is between 300 and 20 000 years. This indicates the period within which the electrons double their energy.

It seems as if the particles had to be accelerated very quickly (within about 500 years) to enable them to attain adequately high energy for the emission of optical synchrotron radiation. The conditions required for this purpose are not clear. A part in this is evidently played by special conditions in the plasma, such as turbulence or shear flows which can generate strong magnetic fields. Moreover, it has emerged that Fermi acceleration is not adequate as an explanation in every case. Examples of this are the hot spots in radio sources 3C 33, 3C 303 W and Pictor A.

X-Ray Imaging of the Jet

The fact that there is no break-off point in the synchrotron spectrum in the first knot, A, as far as the ultraviolet range (1015 Hz) (Figure IV.26), gave rise to the suspicion that this emission region might even be detectable in the X-ray range. During the 1980's, vague indications of X-ray radiation from this region had been obtained from the Einstein observatory. On a first image taken with the ROSAT X-ray telescope in 1992, the jet already was clearly recognizable with an exposure time of almost five hours. A second image with 19 hours of exposure time was obtained three years later.

On the resultant X-ray image, an X-ray spot is apparent in the area of the optically visible jet, just on 15 seconds of arc away from the quasar. However, this knot does not coincide with knot A, as was expected. Rather, the X-ray emission appears to originate in an area close to node B. At that point, there is a small but significant spatial divergence between the radiation distributions in the optical range and those in the radio range – which, as has been shown above, match one another very well in the remainder of the jet. However, the measured X-ray luminosity is so high that it cannot be explained as synchrotron radiation. So far, its nature remains totally unclear. At present, we cannot rule out the possibility that it does not come from the jet itself at all, but from

another object which merely happens to lie on the line of sight to the jet.

Despite further progress in understanding the radio galaxies and their jets, a large number of questions still remain open. In particular, these include the question of particle acceleration. The MPIA group has already undertaken further high-resolution observations in order to look as far into the acceleration zones as possible.

Galaxies in the Environment of Quasars and the Gravitational Lens Effect

Quasars are the most luminous objects in the universe. In a region which is probably not substantially larger than our planetary system, these celestial bodies generate up to 10^{15} solar luminosities, making them several tens of thousands of times brighter than whole galaxies, assuming isotropic radiation. This means that they can even be detected at great distances. The highest red shift known so far was measured for a quasar, and it amounts to $z = 4.92$. Although quasars always appear on images in point form, it has been possible to detect galaxies around some of them. This means that quasars are extremely compact and luminous central regions of galaxies.

The investigation of the quasar galaxies has been among the focal points of research at the MPIA since as long ago as the start of the 1980's. But in 1997, prominence was given to another question which has been the subject of controversial discussion for more than ten years: is there a significant over-frequency of galaxies in the vicinity of quasars?

Ten years ago, for example, American astronomers believed that they had proven the existence of an accumulation of galaxies which were apparently brighter than 21 mag within a specified radius around certain quasars. They interpreted this as meaning that galaxies in the vicinity of quasars develop greater luminosity. A subsequent study was unable to confirm these findings, but it did indicate that there was allegedly an accumulation of weaker galaxies in the more immediate vicinity

of the quasars. Doubts were later cast on this result as well, and it was considered not to be statistically significant.

Investigations have so far been limited to very close quasars up to about $z = 0.3$. A study undertaken at the Calar Alto Observatory using very deep images was intended to go to include weaker objects, and therefore larger red shifts. So that weak galaxies of up to magnitude 26 could still be registered, long exposure times ranging from about four to seven hours were required in the primary focus of the 3.5-metre telescope. A celestial body of the 26th magnitude appears about as bright as a candle burning on the moon! Three fields were selected: each of them had a quasar located at its centre with a red shift of about $z = 1$ (Figure IV.29). At this distance, galaxies could still be recognised on the images at up to 2.5 magnitudes (or a factor of 10) more faint than the Milky Way system. This meant that the study went three magnitudes deeper than all previous ones.

Since no spectra were obtained from the galaxies, only statistical statements were possible with regard to the distances, on the basis of the apparent brightnesses of the stellar systems. According to this information, foreground galaxies should appear in the brightness range between 18 and 23 mag, while galaxies at about the distance of the quasars should appear at between 23 and 26 mag. The galaxy density for these two sub-groups was determined in areas at three different distances around the quasars. The result was unambiguous: neither the group of bright suspected foreground galaxies, nor the group of weaker galaxies probably associated with the quasar, showed a significantly increased surface density in the close vicinity of the quasars. Accordingly, this investigation – so far the deepest ever undertaken – clearly contradicts earlier suspicions that galaxies might

Fig. IV.29: Sections of the three fields surrounding the quasars OT 566, PKS 2216-038 and PKS 2356+196.
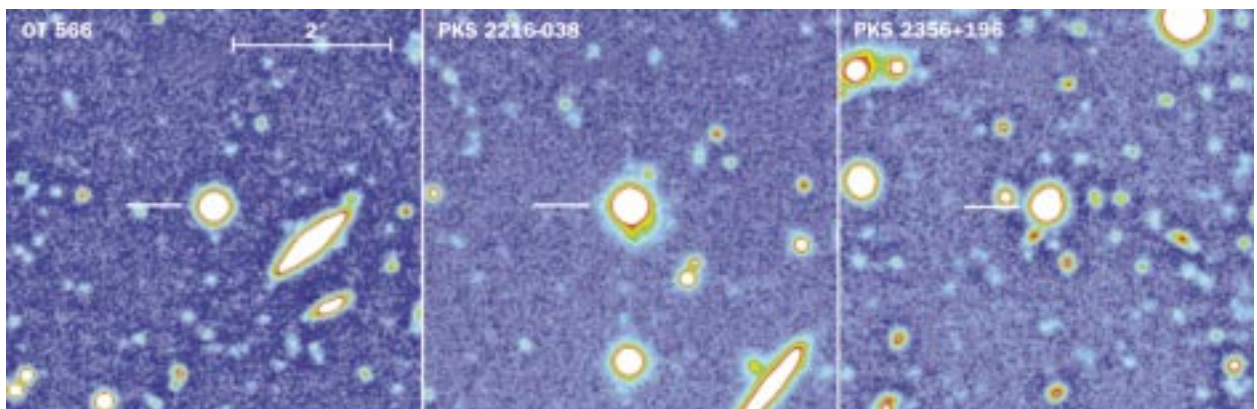
Fig. IV.30: The principle of the gravitational lens effect. The gravity field of a cluster of galaxies deflects the light of a remote quasar. As a consequence, two images A and B of the one quasar are visible in the sky. One of the two images is intensified compared with the undisturbed image.
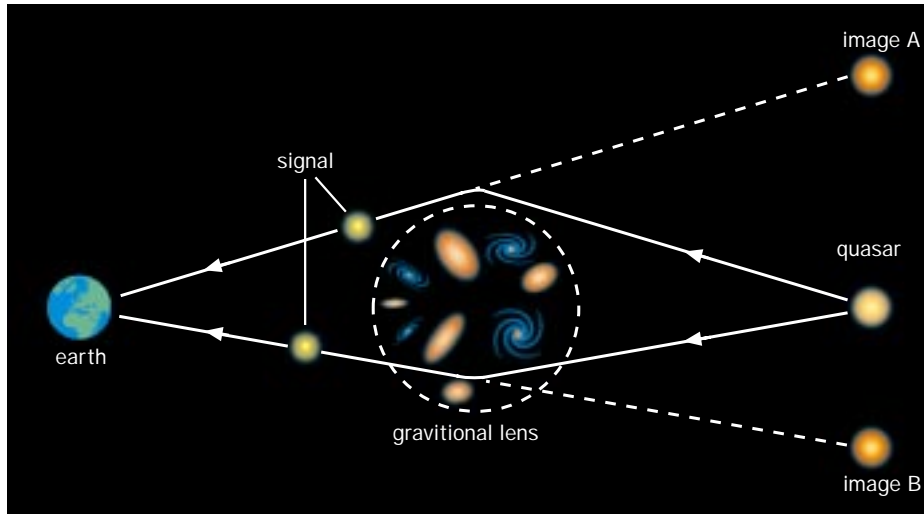
accumulate around quasars, or might be made brighter by interaction with quasars.

As well as this important result, the quasar study has also led to another major conclusion: virtually all galaxies with red shifts of $z > 1$ are probably influenced by the gravitational lens effect, and their brightness is statistically increased by factors of 1.2 to 2.

The gravitational lens effect is based on the fact described by the General Theory of Relativity, that matter bends the space-time which surrounds it (Figure IV.30). Light from a distant object which passes through such a curvature of space-time en route to the earth will deviate from the straight line of its direction of propagation. The angle of deflection is proportional to the acting mass, and is inversely proportional to the smallest distance of the beam of light from the mass center. Areas of space-time which are bent by gravitation in this way act like optical lenses. Depending on the geometry, the rear »lensed« object appears (when viewed from the earth) either as a multiple image or as a ring because of this effect. It appears as a ring when the background object and the »lensing« mass in front of it lie on precisely the same line of sight for the observer.

Above and beyond this, the gravitational lens effect increases the intensity of one of the images that are generated. A »lensed« object appears to be brighter than it would do without this effect.

In the case of two out of the three quasars observed in the MPIA study, there were faint galaxies (probably in front of the quasars) located virtually on the line of sight.

It is therefore suspected that the quasar images are intensified by the gravitational lens effect.

Since neither the distance nor the mass of the foreground galaxies were known, the effect had to be estimated according to its brightness, on the basis of statistical arguments. In this instance, it emerged that the apparent brightness of the quasars is increased by a factor of 1.2 to 2.

The three images went very deep, allowing a high density of galaxies to be discerned on them. Up to the limit value of 26 mag, the surface density is approximately 2×10^5 galaxies per square degree. This means that every two neighbouring galaxies are only an average distance of 8.2 seconds of arc from one another. The question therefore arises as to whether this high density of galaxies means that we generally see remote objects subject to the influence of the gravitational lens effect.

It has been possible to assess this question statistically. For this purpose, it was assumed that the galaxies are randomly distributed in a red shift range of between 0 and 1. It emerged that at a red shift of $z = 1.2$, any given source is highly likely to be »lensed« and that its apparent brightness is increased by 1.1 to 1.5 times. This means that we can never observe the remote universe with no interference whatsoever. The gravitational lens effect changes the apparent brightnesses, and in some cases the appearance of the objects as well.

The question of the so-called micro-gravitational lens effect is also an interesting one in this context. This effect is not caused by the entire gravitational field of a galaxy, but by the field of gravity of the individual stars located within the galaxy. Due to the movement of the individual stars relative to the background object, the micro-gravitational lens effect causes brief fluctuations in the apparent brightness. For some considerable time already, this has given rise to the suspicion that observed fluctuations of intensity in quasars over periods from hours to days are not attributable to intrinsic variations

of brightness in the quasars themselves, but rather that they are merely illusions created by the micro-gravitational lens effect. This would have some important consequences, since the rapid variation of the brightness is taken as the basis to draw conclusions about the spatial extent of the quasar which emits the light.

However, the surface density of the galaxies detected in the new study indicates that the micro-gravitational lens effect doe not have any significant influence. Even so, this only applies up to the observed limit of 26 mag. But should there be a continuing rise in the frequency of galaxies with brightness reducing to a magnitudes of (say) 30, as is suspected by certain astronomers, then the micro-gravitational lens effect would in fact affect virtually every remote quasar. In this case, it would also be true that quasars with red shifts of $z > 1$ cannot be observed without interference.

Optical Identification of a Gamma Ray Burster

For almost 30 years, astronomers have been recording a cosmic phenomenon whose nature remained unclear until just recently: somewhere in the sky, a source of radiation in the gamma range suddenly lights up for a few seconds or minutes, and then it disappears again. In this short interval of time, these so-called Gamma Ray Bursters are the brightest gamma sources in the entire sky. Since gamma telescopes are only able to locate the positions of these outbreaks very inaccurately, it remained impossible to identify these sources with optical telescopes for a long time. Thanks to NASA's Compton Gamma Ray Observatory (launched in 1991) in which physicists from the MPI für extraterrestrische Physik / MPI of Extra-Terrestrial Physics in Garching are also participating, it has now been possible for the first time to observe this phenomenon continuously over several years.

The Compton satellite was able to show that a Gamma Burst can be observed approximately once per day, and that the distribution of these ominous sources over the sky is completely uniform. They must therefore be located either in a relatively close spherical region around the solar system or the Milky Way system, or else in other remote galaxies. More than a hundred theories have been drafted to explain the nature of the bursts.

The turning point came in 1997 with the BeppoSAX satellite built by Italy and the Netherlands, which is capable of registering the Gamma Bursts and of locating them within a short period thanks to an X-ray telescope which is also carried on board. On 28.2.1997 and 8.5.1997, it was therefore possible to determine the positions of two bursts accurately. When first follow-up observations were made with optical telescopes such as the Hubble Space Telescope and the Keck Telescope, light sources which were slowly becoming fainter were to be found at the points in question: these were very probably the optical counterparts to the Gamma Bursts. There were even spectroscopic observations in one case, leaving virtually no doubt that the outbreaks take place in remote galaxies.

In the third case, on 14.12.1997, the 3.5-metre telescope on Calar Alto was also able to make an important contribution to this highly topical area of research. The Gamma Burst with the designation GRB 971214 took place at about 23.34 hours universal time, and lasted for 25 seconds. Alberto Castro-Tirado of the Madrid Astrophysical Institute telephoned Calar Alto and requested the MPIA's astronomers observing there to obtain images of the corresponding area of the sky in the infrared range. This resulted in two exposures with the OMEGA infrared camera at a wavelength of 2.2 μm, taken 3.5 and 5 hours after the burst. In actual fact, these

Fig. IV.31: (a) An infrared image of the gamma-ray burst GRB 971214, obtained with the 3.5-metre telescope. It is the sum of two exposures, 3.5 and 5 hours after the gamma-ray burst appeared. (b) Image of a smaller region around the gamma ray burst with the Keck telescope, two days after the gamma burst, and (c) with the Hubble Space Telescope, four months after the burst. (Pictures: (b) Keck telescope, (c) NASA).
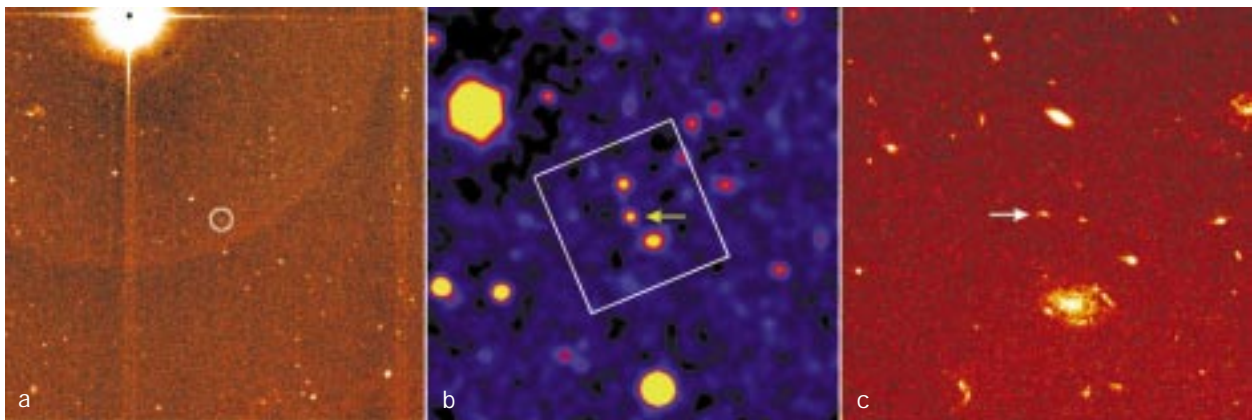
images showed a faint object of the 18th magnitude (Figure IV.31a), which could be unambiguously identified as the »after-glow« of the Gamma Burst, by comparison with later observations from other optical telescopes (Figure IV.31b, c).

Observations at other observatories, together with those at Calar Alto, showed that the spectral energy distribution of the source extends over a wide wavelength range up to 2.2 mm, and this serves as a basis for theoretical models. Unfortunately, poor weather conditions during the following night meant that no further observation was possible, and the development of the IR brithtness with time could not be tracked any further. Nevertheless, the data indicate that the Gamma Burst attained its maximum brightness in the infrared range approximately ten hours after the burst in the gamma range.

Many astrophysicists consider that the probable explanation for the bursts is the fusion of two neutron stars. Neutron stars are extremely dense celestial bodies with a diameter of only twenty kilometres, but with a mass of about one solar mass. If two neutron stars are orbiting one another in a close double star system, they radiate gravitational waves. As a result of this, they lose energy and slowly approach one another. Finally, their surfaces touch and the two bodies fuse in fractions of a second. This triggers an explosion in which the matter heats up to several hundred billions of degrees and explodes at almost the speed of light. Intensive gamma radiation is also generated in this fireball, and it escapes as a flash.

In a process of this sort, energy of up to 1051 erg should be liberated. While this hypothesis could explain the first two bursts, GRB 971214 revealed itself to be an unusual case. Spectroscopic investigations showed that this outbreak had taken place in a galaxy with a very large red shift of $z = 3.42$, which means a very large distance and luminosity: if GRB 971214 has emitted its radiation isotropically, then energy of more than 1053 erg will have been released in the gamma range alone. This is approximately one hundred times more than a supernova radiates over the entire wavelength range.

The phenomenon therefore continues to be a puzzle. In order to track it down, the decisive objective will be to investigate considerably more Gamma Bursts, particularly those in close galaxies.

Theoretical Work

The Shining Arms of Spiral Galaxies

Spiral galaxies are among the most aesthetically attractive objects in the universe. Our Milky Way system is also a galaxy of this type, although its characteristic feature – the spiral structure – still conceals much that is unclear. This phenomenon is explained by means of the so-called density wave theory. For several years, the theory group at the MPIA has been dealing with the question of how certain physical parameters of this theory can be derived from the observed form of the galaxies.

It has been known for a long time that spiral galaxies rotate differentially. This means that at different distances from the centre, stars and gas clouds are moving at different angular speeds. In general, a star orbiting at a long distance from the centre will need longer to make one orbit than a star which is orbiting further in. If the spiral arms always consisted of the same stars, these arms would be winded up within a few rotation periods. But in nature, almost all the spiral galaxies that are observed have open spirals. It follows from this that (unlike the stars) the spiral arms rotate at a constant angular speed, like the spokes of a wheel. However, what is involved here is not the movement of matter, but a wave in the gravitational field of the disk.

As long ago as the 1920's, the Swedish astronomer Bertil Lindblad expressed some first thoughts on a density wave theory. In 1964, Chia C. Lin and Frank Shu developed the first mathematically formulated theory. Since then, the spiral galaxies with large arms, or Grand Design Galaxies as they are known, have been described with the help of this density wave theory.

The density wave theory is based on the following concepts. All stars, and the interstellar gas, create a gravitational potential. In the ideal case, this potential would be symmetrical to the centre. In the density wave theory, it is assumed that this potential is overlaid with a spiral-shaped disturbance which covers the entire matter of the disk (the gas and the stars), and is moving relative to these objects. It rotates around the centre at a fixed angular speed. The visible spiral arms identify the local maxima of this wave.

The matter is decelerated slightly in the area of influence of the wave. As a result of this, the interstellar gas is locally compressed, and it can condense further to form new stars. The young hot stars and shining gas nebulae are then positioned along the spiral shape of the density wave, and they mark its progression, rather like the lamps which make a city's network of streets visible at night.

However, many questions still remain unclear today: by what are the potential disturbances triggered? Which dynamic behaviour stabilises the waves, and over what period of time? How quickly do the waves move through the disk matter?

According to the most important density wave theory, so-called resonances play a major role in answering these questions. These may be understood as follows: the stars are moving in epicyclic paths around the centre (Figure IV.32). A path of this sort may be illustrated by two path components: one large circular component around the centre, and a second, smaller, elliptical path whose centre point migrates along the large circle. This is an epicyclic path. Now, resonances may occur bet-
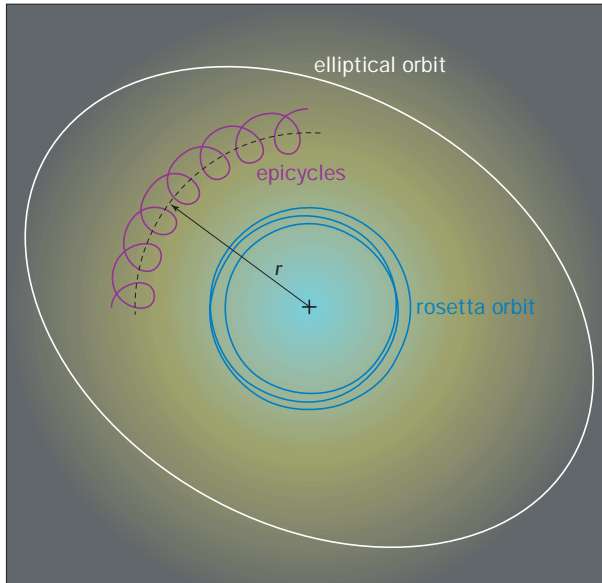
Fig. IV.32: Visualization of the epicyclical orbits of stars in spiral galaxies.

ween the frequencies of the path components: in this instance, a resonance is defined by an integral ratio between the respective frequencies. In the case of the stars, a distinction is drawn between the epicycle frequency k and the rotation frequency Ω, and the frequency of the density wave Ω_S. Three resonances are singled out for particular mention in the work: the inner 4/1 resonance ($\Omega - \Omega_S = k/4$), the inner and outer Lindblad resonance ($\Omega - \Omega_S = \pm k/2$) and the co-rotation ($\Omega = \Omega_S$). In the last case, therefore, the density wave and the stars are moving around the centre at the same speed on the large circular path.

Many theoreticians now agree that the large, open spiral arms in Grand Design Galaxies end at one of these resonances – but it is not clear at which one. The answer to this question is very significant for the understanding of the dynamic evolution and stability of the spiral struc-

ture. Initially, the outer Lindblad resonance and the co-rotation resonance were preferred as the limitation of the spiral arms, but in the 1990's, an increasing number of arguments spoke in favour of the spiral arms ending at the 4/1 resonance in galaxies with very distinctly formed open arms (»angle of incidence« greater than 20 degrees). A 4/1 density wave would be the slowest of the three possibilities mentioned.

At the MPIA, the theory group has already been working on the dynamics of the spiral structure for several years. In the reporting year, there has been progress in the question of the movement of waves in the disk. Computer simulations portrayed galaxy disks by using 20000 particles with an initially uniform distribution. Then, a density wave was superimposed on this ensemble, in the form of a logarithmic spiral, and the way the gas reacted to this was observed. Calculations were carried out with the Smoothed Particle Hydrodynamic Code (SPH), into which various values were entered for several physical variables, such as the sonic speed, viscosity of the gas and amplitude of the density wave. A comparison with the observed spiral pattern was taken as the test for the models. An essential point here is that the rotation curve (the speeds of the stars in relation to their distance from the centre) can be measured, whereas neither the position of the resonances nor the rotation speed of the density wave can be derived from observations. These two values can only be obtained from the model.

In the first instance, three simulation runs were carried out in which the spiral arms ended respectively at the 4/1 resonance, at co-rotation or at the outer Lindblad resonance (Figure IV.33). After ten orbits, for example, the spiral patterns that had been generated were compared with that of galaxy NGC 5247, an Sc galaxy. The co-rotation model did not provide an adequate reproduction

Fig. IV.33: Computer simulation of spiral patterns at different assumed resonances. (a) 4/1 resonance, (b) co-rotation, (c) outer Lindblad resonance. The 4/1 resonance model is best at reproducing the observed structures.
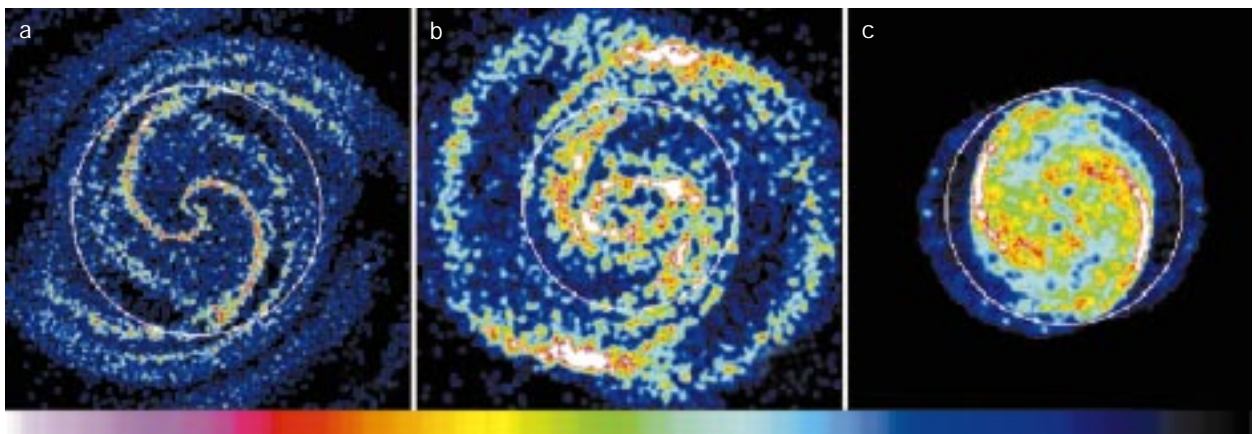
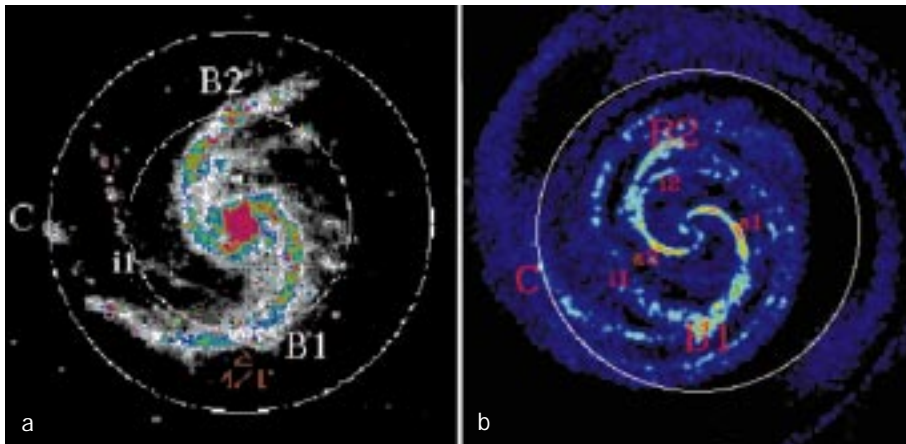Fig. IV.34: Comparison of the observed spiral pattern in the galaxy NGC 5247 (a) with the simulated 4/1 model (b). This explains not only the large-scale structure, but also details such as gaps in the arms (i1 and i2).

of reality in various respects. In the inner area, for example, a lozenge-shaped structure developed which is not observed in nature. Further out, a ring was created: this is not observed either. Nor did the case in which the spiral ended at the outer Lindblad resonance correspond to the observations. A fundamental problem in the morphology of this model is that its inner spiral structure is far too weakly defined, and the arms are also wound more tightly than is the case in real galaxies.

Since the 4/1 model provides the best description of the real conditions, it was examined in greater detail. First of all, a symmetrical, two-armed density wave was imposed on the ensemble of particles. After a few revolutions, this resulted not only in the formation of the two main spiral arms, but also in a split in the two arms. This phenomenon certainly does not take place by chance: rather, it is a typical feature of the 4/1 resonance models, and it had already been explained theoretically during the 1980's. Splits of this sort are also observed very frequently in spiral galaxies.

Improved coincidence of the 4/1 models with reality was achieved when a single-armed disturbance was incorporated in addition to the two-armed density wave – the disturbance rotates at the same angular speed as the spiral structure. Asymmetries then occur in the spiral arm pattern too, like those which can be observed in NGC 5247 (Figure IV.34). For example, the split in one arm occurs closer to the centre than on the opposite one (shown in the Figure by i1 and i2). Other details observed in galaxies also occurred in the simulations, such as gas bridges between two arms or faint branches of the main arms in the area of the outer Lindblad resonance.

In two further simulation runs, one density wave was entered with constant amplitude, and another with a slowly increasing amplitude. There was no major difference in the resultant spiral patterns. A higher viscosity led to more concise spiral arms.

The impressive coincidence of the depicted models with the morphology of five observed spiral galaxies provides further powerful arguments in favour of the assumption that the end of the symmetrical part of the spiral structure occurs at the 4/1 resonance in Grand Design spiral galaxies with open arms.

Dark Matter in Spiral Galaxies

The shining arms dominate the visual image of a spiral galaxy. But since the middle of the 1970's, observations have suggested that these stellar systems are surrounded by matter which does not shine, but which does control the dynamic behaviour of the galaxies over large areas. Investigations indicate that this Dark Matter could contain up to ten times as much mass as all the shining matter (that is to say, stars and clouds of interstellar matter) taken together. With the help of computer simulations, the theory group at the MPIA is attempting to gain some hints as to the nature of the Dark Matter.

The total mass of the shining matter in a galaxy – that is, the stars and gas clouds – can be determined by measuring the brightness and the distance, and then by calculating the luminosity on this basis. The total mass of the shining matter is obtained if we assume a typical ratio of mass to luminosity for spiral galaxies. This figure is between two and three solar masses per solar luminosity.

Another method is used to determine the mass of all the matter which acts gravitationally in the galaxy. For this purpose, the rotation speed of the stars and gas is measured at different distances from the centre. Newton's law of Gravity enables the mass which lies within the orbit of objects to be calculated solely from
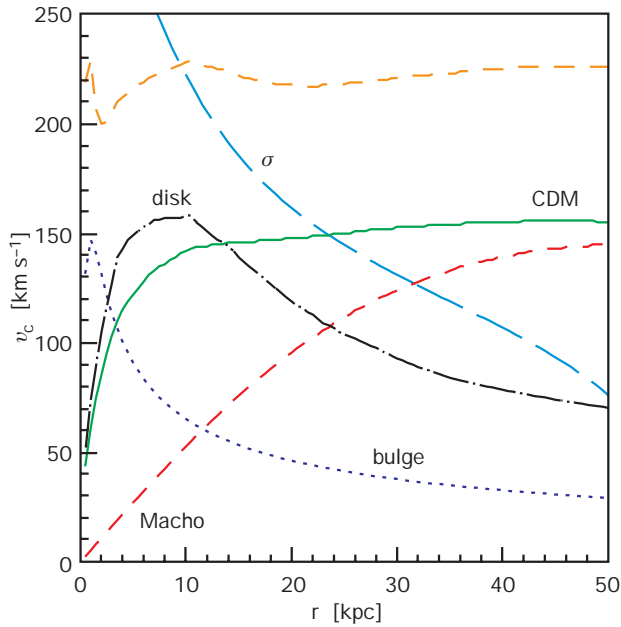
Fig. IV.35: : The measured rotational speed of the galaxy DDO 154 as a function of distance r from the centre (upper wide dashed curve), can be explained by the gravitational effect of several components. CDM = cold dark matter, disk = stars and gas in the galactic disk, bulge = stars and gas in the galaxy's central region and MACHO = dark objects in the galaxy's halo.

the orbiting speed of those objects. This means that the greater the distance of the observable objects from the centre, the better the total matter of a spiral galaxy can be determined.

Measurements of rotation curves have now shown that all spiral galaxies must contain substantially more gravitationally effective matter than had been concluded on the basis of the luminosity determination. To express it differently: if only the visible stars and the gas were present, the centrifugal forces caused by the observed speed of rotation would tear the spiral galaxies apart. There must therefore be large quantities of Dark Matter holding the stellar systems together.

For a variety of reasons, the theoreticians assume that the Dark Matter is not concentrated in the disks of the spiral galaxies, but is distributed in a halo which surrounds the galaxies in a spherical shape. One of the most exciting questions of modern astrophysics now concerns the nature of this matter. Two possibilities basically enter into consideration:

- faint objects consisting of »normal« material, such as low-mass stars, Brown Dwarves, neutron stars or Black Holes. These are referred to as Massive Compact Halo Objects, or MACHO's for short.
- a finely distributed mixture of unknown, so-called non-baryonic elementary particles. These are known

as Weakly Interacting Massive Particles, or WIMP's. Again, a distinction is drawn here between Hot Dark Matter (HDM) and Cold Dark Matter (CDM).

Our Milky Way System must also be surrounded by a Dark Halo of this sort. In 1993, a group of American astronomers succeeded in gaining indirect evidence of invisible celestial objects, the MACHO's. A statistical analysis based on only six proven objects led to the result that the MACHO's are low-mass objects in the range of 0.5 ± 0.25 solar masses. It should therefore be possible to prove the presence of a population of this sort in the infrared range in other spiral galaxies, if they are stars. However, a model assumption concerning the spatial distribution of the MACHO's is a decisive element in this analysis, and this is not known.

In order to test this model assumption, the theory group at the MPIA turned its attention to the dwarf spiral galaxy DDO 154. Of all the galaxies, this one probably has the most precisely measured rotation curve to date. This suggests that there is approximately 15 times as much Dark Matter in the halo as there is shining matter in the disk. However, the rotation curve (which has been measured as far as a distance of 30 000 light years from the centre) has not yet been able to explain this. Cosmological models with Cold Dark Matter (CDM) gave a good reproduction of the inner part of the rotation curve, but they supplied far too much Dark Matter in outer areas – whereas those models which describe the outer rotation curves contained too much Dark Matter in the central area.

Adopting a new approach, the group at the MPIA assumed that there were MACHO's as well as CDM particles in the halo of DDO 154. The rotation curve could be excellently described in all areas with a model in which the MACHO's are located in a spherical area with a radius of about 16 000 light years (Figure IV.35). The density distribution of the objects then corresponds to an isothermic sphere. On the other hand, the CDM cloud extends up to a radius of at least 30 000 light years. The following mass proportions are obtained from this model for DDO 154: 74% CDM, 22% MACHO's and 4% shining matter.

This two-component model for the dark halo was now able to be transferred surprisingly well to the Milky Way System as well, scaling all dimensions up by a factor of ten. The measured rotation curve could best be described with the following values: shining material in the central bulge: 10^{10} solar masses; shining matter in the disk: 5.6×10^{10} solar masses; MACHO's in the halo: 3.4×10^{11} solar masses; CDM in the halo: 6.5×10^{11} solar masses. This means that the Dark Matter in the halo accounts for 97% of the total mass of the Milky Way system. About one third of this would consist of MACHO's.

This model has a different density distribution for the MACHO's in the halo than has been hitherto assumed, and this fact has an effect on the statistical determinati-

on of mass mentioned above for the six observed MACHO events. With the new model, the mass of the dark bodies is now in the range of 0.06 ± 0.03 solar masses. Consequently, at least a major proportion of this could consist of Brown Dwarves. These are very faint objects with masses between those of the stars and the

planets. Depending on their chemical composition, the upper limit for their mass is approximately 0.08 to 0.1 solar masses. The search for Brown Dwarves will also play a major part at the MPIA in the future. It should be possible to prove their presence in the infrared range.

IV.3   Solar System

Striae in the Tail of Comet Hale-Bopp

The years 1996 and 1997 rewarded comet researchers with a rich harvest: comet Hyakutake appeared in the sky in spring 1996. It became very bright, but within a year it was to be surpassed by Hale-Bopp. C/1995 O1 – to give comet Hale-Bopp its full designation – reached a maximum brightness of -0.5 magnitudes in spring 1997, and remained below a magnitude of 0 for a full seven weeks. This brightness was only exceeded this century by comets Ikeya-Seki (1965) and West (1976). For many people, Hale-Bopp was the first bright comet they had ever seen.

At the Calar Alto observatory, the bright Schmidt reflector with its large field of view is ideally suited for investigating the manifold and partly still little understood phenomena which take place in the coma and in the tail. This includes the so-called striae.

Striae are bright, elongated »stripes« in a comet's dust tail. They do not converge to a definite point, but run nearly parallel to each other from the dust tail in a direction inbetween that of the gas and the dust tails. Thus, they are not formed directly in the comet's core.

Striae are visible over several days. So far they have only been observed in the tails of bright comets, such as Donati (1858) and most recently West (1976). They always evolved only after the comet had passed perihelion, at distances of less than one astronomical unit from the sun, but have not occurred in all bright comets; for instance, they did not occur in Halley's comet.

In the case of Hale-Bopp, Calar Alto was the first to announce the sighting of striae (Figure IV.36). On 17. and 18.3.1997 they were clearly visible on exposures made on Calar Alto's Schmidt telescope as part of the dust tail. After contrast enhancement it was possible to

see 21 striae in one case and 16 in another. The discovery was immediately notified by IAU circular. Later it turned out that a Japanese astronomer at the Kiso observatory observed these stripes in the dust tail as early as 5.3.97, but did not announce the sighting. The surprising thing was that the striae appeared even before perihelion. In conjunction with images made by other astronomers, they could be demonstrated during the period from 2 March till 8 April.

The photographic plates from MPIA's Schmidt camera were measured, and the first attempt to interpret the data used a model by Zdenek Sekanina. According to this model, the striae are created as follows: large chunks and also loose dust clouds detach themselves from the comet's core, and move at first within the tail away from the core, being driven by the radiation pressure of the solar light. After some time these chunks or dense clouds break up into innumerable dust particles, which depending on their size are differentially accelerated by sunlight. Finally this swarm of particles spreads out into elongated stripes - the striae.

This model possesses three free parameters: 1) The time when the chunk or the particle cloud is ejected from the core, 2) acceleration by radiation pressure, and 3) the time to break-up. First analysis of the images indicates that ejection takes place at time-intervals of 11 to 12 hours. This agrees well with the observed rotation period of the comet's core of 11 hours 21 minutes. It therefore appears plausible, though by no means certain, that the cause of the striae can be traced back to a single active region on the core's surface. Such active centres are known to generate bright gas streamers known as jets, as was also observed in Hale-Bopp. The time-interval between the material leaving the core and its break-up to form the striae is up to a maximum of 15 days.

The model accordingly explains the observed striae in satisfactory fashion. Further evaluation of the observational data may perhaps provide information as to whether the jets are really linked causally to the striae, and thus eventually also about the structure of the comet's core.

Fig. IV.36: Image of the comet Hale-Bopp in spring 1997 with the Schmidt telescope at Calar Alto. It shows the rare phenomenon of elongated, stripe-like structures in the dust tail, so-called striae.

Staff

In Heidelberg

Directors: Beckwith (Acting Director), Elsässer (until 31.3.)

Scientists: Abraham (since 1.2.), Beetz, Bogun, Braun (since 1.1.–31.12.), Burkert, DiNella (until 16.6.), Finocchi (1.9.–31.12.), Fried, Glindemann (until 30.9.), Graser, Haas, Hamilton (until 31.12.), Herbst, Herbstmeier, Hippelein, Huang (since 1.9.), Huth, Kalas, Kinkel (15.8.), Klaas, Kunkel, Leinert, Lemke, Lenzen, Mac Low, Marien, Meisenheimer, Meyer (until 31.8.), Th. Müller (since 1.8.), Mundt, Neckel, Neeser (1.2.–30.9.) Pitz, Porro (since 15.10.), Röser, Schubert (until 31.1.), Staude, Stickel, Thommes (until 16.11.), Thompson, Tusche, R. Wolf.

Ph.D. Students: Baumann, Berkefeld, Eckardt, Fokkenbrock, Kasper (since 15.8.), Kessel, Klessen, Petr, Seidel, v. Kuhlmann (since 1.11.) Woitas, Wolf, Chr.

Diploma Students: Kranz (since 1.9.), Martin (until 31.3.), Nasince (since 1.2.), Phleps (since 1.9.). Von der FH Mannheim: Cordoba (10.3.–9.5.), Hipp (since 1.9.), Lehmitz (since 1.9.), Marx, Röttker (until 28.2.), Schwenker (1.3.–31.8.), Sebb (until 28.2.), Spar (1.3.–31.8.).

Scientific Services: Birk (until 30.6.), Bizenberger, Hille, Hiller, Ortlieb, Quetz, Rohloff.

Computers, Data Processing: Brüge, Engelhardt, Hippler, Kallidis (1.2.–30.11.), Rauh, Storz, Tremmel, Zimmermann.

Elektronics: Becker, Ehret, Grimm, Grözinger, Klein, Ridinger, Salm, Schnürer (until 31.3.), Schütz (until 31.1.), Unser, Wagner, Werner, Westermann, Wrhel.

Fine Mechanics: Bellemann, Benesch, Böhm, U. Dorn, Ebert (since 1.2.), Franke, Heitz, Meister (since 1.8.), Meixner, Morr, Münch, J. Pihale, Plottke (until 30.9.), Sauer.

Photo shop: Anders–Özáan, Meißner–Dorn, Neumann, Weckauf.

Administration, Secretariate: Behme, Cronin (until 31.12.), Fink, Flock, Gieser, Hartmann, Janssen-Bennynck, Kellermann, Klenk, Papousado, Rushworth, Schleich, Schnell, Schürmann, Thüringer (until 31.12.), Zähringer.

Technical Services: Gatz, O. Götz, Klingmann, Lang, Nauss (since 1.10.), Reutner (until 6.5.), B. Witzel, F. Witzel, Zergiebel.

Trainees: (Feinmechanik) Fsinceianatz (since 1.9.), Ebert (until 31.1.), Engel (until 31.3.), Greiner (since 1.9.), Geuer, Jung (since 1.9.).

Free Collaborators: Dr. Hirth, Dr. Preiss.

Scholarship Holders: Sinceraham (until 31.1.), Andersen (since 1.9.), Bate, Eislöffel (until 31.7.), Fernandez (until 31.12.), Heraudeau (since 1.3.), Kania (since 1.6.), Köhler (since 1.6.), O'Dell (until 15.8.), Patsis, Popescu (until 28.2.), Robberto, Surace, Toth (since 1.2.),

Probationers: Bugert, Grözinger, Krause, Stracker.

Calar Alto/Almeria

Local Directors: Birkle, Vives.

Astronomy, Night Assistents: Aguirre, Alises, Frahm, Hoyo, Quesada, Thiele.

Telescope Techniques: Capel, de Guindos, Garcia, Helmling, Henschke, L. Hernández, Lingenfelder, Raúl López, Morante, W. Müller, Nuñez, Parejo, Schachtebeck, Usero, Valverde, Wilhelmi.

Technical Services: A. Aguila, M. Aguila, Ariza, Barón, J. Braun, Carreño, Dominguez, Gómez, Góngora, Manuel Hernandez, Klee, Rosario López, Marquez, Martinez, Puertas, F. Restoy, Romero, Sáez, Sanchez, Schulz, Tapias.

Administration, Secretariate: Magdalena Hernández, M.J. Hernández, M.I. López, C. Restoy.

Guests

Dr. Bodenheimer, Santa Cruz (Sept.); Prof. K.-H. Böhm, Seattle (August); Dr. Cao, Peking (Nov.–Dec.); Dr. Faucherre, Montpellier (July); Dr. Hozumi, Shiga (June); Dr. Kaufmann, Maryland (Nov.–Dec.); Dr. Manucci, Florenz (Sept.); Dr. Perley, Socorro (Jan.); Dr. Ratnam, Bangalore (Sept.); Dr. A. Sargent, Pasadena (July); Dr. W. Sargent, Pasadena (July); Dr. Sun, Peking (Nov.–Dec.); Dr. Tsuchiya, Nagoya (June–July); Dr. Walker, Chilton (June–Aug.).

Due to the regular meetings of the ISOPHOT Co-investigators associated to other Research Institutes and industrial Firms in Germany and from abroad, numerous guests were at the MPIA for short times, who are not mentioned here individually.

Working Groups and Scientific Collaborations

Instrumentation Projects

ALFA
A. Glindemann, P. Kalas, S. Hippler, M. Kasper, R.-R. Rohloff, K.Wagner with all Departments of MPIA and Calar Alto Observatory
in collaboration with:
MPI für extraterrestrische Physik, Garching
University of Massachusetts, Amherst, USA

CAFOS 2.2
K. Meisenheimer, L. Brüge, C. Storz

CONICA
R. Lenzen, H. Bellemann, Benesch, Franke, B. Grimm, Münch, Ortlieb, Storz, Salm, Tusche, K. Wagner
in collaboration with:
MPI für extraterrestrische Physik, Garching

MAX
T. Herbst, S.V.W. Beckwith, M. Robberto, P. Bizenberger, C. Birk

MIDI
Ch. Leinert, U. Graser, B. Grimm, T. Herbst, St. Hippler, R. Mundt, R. Lenzen, E. Pitz, I. Porro, M. Robberto, R.-R. Rohloff, N. Salm
in collaboration with:
Universität Amsterdam,
Sterrewacht Leiden,
Observatoire Meudon, Meudon,
Observatoire Nice, Nizza,
Kiepenheuer-Institut,
Thüringische Landessternwarte Tautenburg

MOSCA
J. Fried, H. Bellemann, Benesch, Franke, Münch, N. Salm, Grün, K. Marien, Zimmermann, Brüge, v. Kuhlmann

OMEGA-Cass
R. Lenzen, T. Herbst, H. Bellemann, P. Bizenberger, P. Frank, N. Salm, C. Storz

OMEGA Prime
M. Mc Caughrean, D. Thompson, R. Lenzen, H. Bellemann, C. Birk, P. Bizenberger, Franke, B. Grimm

PACS for FIRST
D. Lemke, S. Eckardt, U. Grözinger, U. Klaas
unter Federführung des MPI für extraterrestrische Physik, Garching, in collaboration with:
DLR, Berlin

Observational Projects

Jets from Young Stars and T Tauri
R. Mundt, G.A. Hirth, T.M. Herbst, M. Robberto, S.V.W. Beckwith in collaboration with:
Institute for Advanced Studies, Dublin,
Univiversity of Hawaii, Honolulu,
NRAL Jodrell Bank,
STScI, Baltimore,
University of Colorado, Boulder,
Leeds University,
Thüringer Landessternwarte, Tautenburg,
MPI für extraterrestrische Physik, Garching

Molecular Flows Near Young Stars
T.M. Herbst, S.V.W. Beckwith, M. Robberto, M. McCaughrean, M.-M. Mac Low

Bipolar Nebulae
Th. Neckel, J. Staude,U. Kania
in collaboration with:
Osservatorio Astrofisico di Arcetri, Florenz,

Ae/Be and T Tauri Double Stars
Ch. Leinert, M. Haas, R. Köhler, T. Herbst
in collaboration with:
Osservatorio Astrofisico di Arcetri, Florenz,
State University of New York, Stony Brook

Structure of L 1521B
D. Lemke in collaboration with
Universitätssternwarte Helsinki

Near-infrared Halo of Elias 1
M. Haas, Ch. Leinert in collaboration with:
Osservatorio Astronomico di Arcetri, Florenz

Circumstellar Disks around Evolved Stars
P. Kalas

Luminous Blue Variables
M. Robberto, T.M. Herbst

Cool M Dwarfs
C. Wolf, R. Mundt, D. Thompson, S.V.W. Beckwith, R. Fockenbrock, H. Hippelein, J.-S. Huang, B.V. Kuhlmann, Ch. Leinert, K. Meisenheimer, S. Phleps, H.-J. Röser in collaboration with
W.M. Keck Observatory, Kamuela, Hawai,
Royal Observatory, Edinburgh

A Wolf-Rayet Ring Nebula
M.-M. Mac Low in collaboration with:
University of Colorado, Boulder,
Goddard Space Flight Center, NASA,
University of Illinois, Urbana,
California Institute of Technology

CADIS
K. Meisenheimer, H.J. Röser, H. Hippelein, S.V.W. Beckwith, J. Fried, R. Fockenbrock, C. Leinert, E. Thommes, Ch. Wolf

Jets from Galaxies and Quasars
K. Meisenheimer, H.-J. Röser, M. Neumann, M.G. Yates
in collaboration with:
Oxford University,
Jodrell Bank, (GB),
NRAO, Socorro, (USA)

Emission of the Radio Galaxy 3C34
M.J. Neeser, K. Meisenheimer, H. Hippelein

Quasars
J. Fried

Gamma Ray Burst
H. Hippelein
in collaboration with:
Palomar Observatory, Pasadena,
Lsinceoratorio de Astrofisica Espacial y Fisica Fundamental, Madrid,
Instituto de Astrofisica de Andalucia, Granada,
Oxford University,
Astrophysikalisches Institut Potsdam,
Astronomisches Observatorium, Nikolaew, Ukraine,
Istituto die Astrofisica Spaziale, Frascati, Italien
Universita di Ferrara, Ferrara, Italien
Istituto Astrofisica Spaziale, Rom, Italien
Istituto Tecnologie e Studio Radiazioni Extraterrestri, Bologna

Infrared Emission Line Galaxies
S.V.W. Beckwith, D. Thompson
in collaboration with:
C.A.I.S.M.I. – C.N.R., Florenz,
Goddard Space Flight Center, NASA

Clustering of Galaxies in Corona Borealis
H. Hippelein in collaboration with:
University of Wales, Cardiff

A Supercluster of Galaxies in Corona Borealis
D. Hamilton in collaboration with
Palomar Observatory (California Institute of Technology, Pasadena)

Stellar Populations in M 3
D. Hamilton in collaboration with:
Osservatorio Astronomico di Bologna,
Osservatorio Astronomico di Roma,
Dipartimento di Astronomia, Bologna

The possible »Superwind Galaxy« NGC 4666
M.G. Petr in collaboration with:
Space Telescope Science Institute, Baltimore
Observatorium Leiden,
Lawrence Livermore National Lsinceoratory,
Johns Hopkins University,
ATNF/CSIRO, Australien

Galaxies in Voids
B. Kuhn, H. Elsässer, C.C. Popescu
in collaboration with: Universitätssternwarte München

A Multiwavelenght Study of the BL-Lacertae Object PKS 2155-304
B. Kunkel in collaboration with:
25 international Institutes

First Supernova in a Blue Compact Dwarf Galaxy
C.C. Popescu, K. Birkle, H. Elsässer
in collaboration with:
Universitätssternwarte München,
Universität Padua,
ESO, Chile,
Astronomisches Institut Bukarest

Seyfert Galaxies
K. Birkle, U. Thiele in collaboration with:
Universität Padua,
Astrophysikalisches Institut Potsdam

Comet Hale-Bopp
K. Birkle in collaboration with:
Jet Propulsion Laboratory, Pasadena,
ESO, Garching und Chile,
Hamburger Sternwarte, Hamburg-Bergedorf,
Universitätssternwarte München,
MPI für Aeronomie, Katlenburg-Lindau,
MPI für Kernphysik, Heidelberg,
DLR, Berlin,
ESA, Noordwijk,
Osservatorio Astrofisico di Arcetri, Florenz

ISO Data Centre
D. Lemke, ISOPHOT-PI and the ISO-Team at the MPIA: P. Ábrahám, M. Haas, P. Heraudeau, S. Hotzel, U. Klaas, T. Kranz, M. Kunkel, T. Müller, M. Radovich, L. Schmidtobreick, M. Stickel, C. Surace, L.V. Toth

Projects with ISOPHOT:

Dust in the Coma Cluster
M. Stickel, D. Lemke, M. Haas
in collaboration with: Universität Helsinki

Starburst Galaxy NGC 6090
J.A. Acosta-Pulido, U. Klaas, R.J. Laureijs, U. Kinkel, P. Sinceraham, H.O. Castaneda, U. Herbstmeier, H. Krüger, G. Pelz in collaboration with:
ISO Science Operations Center, Madrid,
Rutherford Appleton Lsinceoratory, Chilton, (GB),
Instituto de Astrofisica de Canarias,
MPI für Kernphysik, Heidelberg,
Konkoly-Observatorium, Budapest

ISO Serendipity Survey
M. Stickel, S. Bogun, D. Lemke, U. Klaas, L.V. Toth, U. Herbstmeier in collaboration with:
ISO Science Operations Center, Madrid,
Universität Budapest,
Astrophysikalisches Institut Potsdam,
California Institute of Technology, Pasadena,
Imperial College, London

Brightness Fluctuations of the Zodiacal Light
U. Herbstmeier, P. Sinceraham, D. Lemke, Ch. Leinert, C. Surace, M. Kunkel in collaboration with: Konkoly-Observatorium, Budapest, Ungarn

Disk around Young Stars
S.V.W. Beckwith, M.R. Meyer, T.M. Herbst, M. Robberto.

The Interacting Galaxies Arp 244, NGC 6240 and Arp 220
U. Klaas, M. Haas, in collaboration with:
ISO Science Operations Center, Villafranca, Spanien,
MPI für Kernphysik, Heidelberg

Theoretical Projects

Fragmentation of Molecular Clouds and Star Formation
M.-M. Mac Low, R.S. Klessen, A. Burkert
in collaboration with:
Universität Würzburg,
University of California Observatories

Formation and Evolution of Protostars and Multiple Systems
M.R. Bate, A. Burkert in collaboration with:
University of California Observatories

Dynamics of Spiral Galaxies
P. Patsis in collaboration with:
ESO, Chile,
Universität Athen

Dark Matter in Spiral Galaxies
A. Burkert in collaboration with:
University of California, Berkeley

Evolution of Dwarf Galaxies
A. Burkert in collaboration with:
MPI für Astrophysik, Garching,
Universitad de Barcelona

Substructure of the Globular Cluster System of the Milky Way
A. Burkert in collaboration with:
University of California, Santa Cruz

Superbubbles in Dwarf Galaxies and in the Large Magellanic Cloud
M.-M. Mac Low in collaboration with:
Osservatorio Astrofisico di Arcetri, Florenz,
University of Illinois, Urbana,
University of Michigan, Ann Arbor,
University of Wisconsin, Madison

Collaboration with Industrial Firms

Calar Alto Observatory
British Aerospace/Matra Marconi

ALFA
AOA Inc., Cambridge, Massachusetts,
Bernhard Halle Nachfl., Berlin
Cambridge Innovations, Framingham, Massachusetts,
Coherent Inc., Ashburn, Virginia,
EHROS Inc, Bridgetown, Barbados
FISBA Optik AG, St. Gallen, Schweiz
Hommel-Hercules Werkzeughandel GmbH & Co. KG, Viernheim
Life Science Resources/AstroCam Ltd., Cambridge, (GB)
MIT/Lincoln Lsinceoratory, Lexington, Massachusetts,
NewFocus, Santa Clara, California,
Newport GmbH, Darmstadt
OWIS GmbH, Staufen
Spindler & Hoyer GmbH, Göttingen
THK GmbH, Ratingen
University of Massachusetts, Amherst, Massachusetts,
Xinetics Inc., Ayer, Massachusetts,

MIDI
L.O.T. GmbH, Darmstadt
Physik Instrumente, Waldbronn

Omega Cass
Barr, Westford, Massachusetts,
Carl Zeiss, Jena
EKSMA, Vilnius, Litauen
Infrared Lsinceoratories, Tucson, Arizona,
Janos, Townshend, Vermont,
Präzisionsoptik, Gera

Conica
AP&T, Nürtingen
Barr, Westford, Massachusetts,
Carl Zeiss, Jena
Cryo-Technic, Büttelborn
Janos, Townshend, Vermont,
Leybold, Hanau
Möller, Wedel
Philips, Hamburg
Pörschke, Höchst
Präzisionsoptik, Gera
Queensgate, Barkshire, GB
Richardson Grating, Rochester,
Schenk, Maulbronn
Spindler & Hoyer, Göttingen
Vitron, Jena

MAX Infrared Camera
Infrared Lsinceoratories, Tucson, Arizona,
Janos, Townshend, Vermont,
Mr. Julian, Kalina, Hawaii

Magic Infrared Camera
MKD, Neuhausen

PACS
ANTEC, Kelkheim
IMEC, Leuven

ISO/ISOPHOT
Antec, Kelkheim
Carl Zeiss, Oberkochen
Dornier Satellitensysteme, Friedrichshafen
IMEC, Leuwen, Belgien

CCD Techniques
Dataman, Pliezhausen
Glenair Electric, Oberursel.
Haefele, Schriesheim.
Heraeus, Hanau
New Focus, Santa Clara,
Philips, Eindhoven, Niederlande
Roth, Karlsruhe
SITe Corp., Beaverton, Oregon,
Steward Observatory, Tucson, Arizona,
Tafelmeier, Rosenheim

Instrumentation for Calar Alto Telescopes
Carl Zeiss, Jena
Faulhsinceer Motoren, Schönaich
Kaufmann Präzisions-Optik, Crailsheim-Wittau
Layertec Feinoptik, Mellingen
Proxitronic, Bensheim
Schott Glaswerke, Mainz
Spindler & Heuer, Göttingen

Computers
Additive, Friedrichsdorf
Creaso, Gilching
Draco, Hamburg
Edo, Hockenheim
Laserprint, Darmstadt
ProMedia, Oftersheim
Seicom, Ismaning
SUN, Langen
Transtec, Tübingen

Others
Focus Software, Tucson, Arizona,
Hahn & Kolb, Stuttgart
Korth, Kiel
Melles Griot, Bensheim
Mitutoyo, Leonberg
Würzburger Fotoversand, Würzburg

Mechanics and Electronics
Adam + Hecker, Wiesloch
Almet-AMB, Mannheim
Amphenol-Tuchel Electronics, Heilbronn
AVNET EMG, Braunschweig
Börsig, Neckarsulm
Bubenzer Bremsen, Kirchen-Wehrbach
Bürklin, München
Cadillac-Plastic, Viernheim
Carl Roth, Karlsruhe
Cherry Mikroschalter, Auerbach
Com Pro, Stuttgart
Compumess Electronik, Unterschleissheim
Conrad Electronic, Hirschau
CTS Corp. Microelectronics, Chicago, Illinois,
CTS Microelectronics, West Lafayette, Indiana,
Dalektron, Dreieich
Dannewitz, Linsengericht
Dürkes & Obermayer, Heidelberg
Dyna Systems NCH, Mörfelden-Walldorf
EBJ, Ladenburg
EBV-Electronik, Leonberg
EC Motion, Mönchengladbach
Edsyn Europa, Kreuzwertheim
Eldon, Büttelborn
Elna Transformatoren, Sandhausen
ELV Electronik, Leer
ERNI, Adelberg
eurodis Enatechnik, Quickborn
Euromicron, Mittenaar
EWF, Eppingen
Farnell Electronic Components, Deisenhofen
FCT Electronic, München
Fischer Elektronik, Lüdenscheid
Fritz Faulhsinceer, Schönaich
Gould Nicolet Meßtechnik, Dietzenbach
Hartmann + Braun, Alzenau
Heluksinceel, Hemmingen
Herz, Leister Geräte, Neuwied
Hewlett-Packard Direkt, Böblingen
Holz Electronik, Kirchheim
Hommel-Hercules Werkzeughandel, Viernheim
Horst Göbel, Ludwigshafen
Huber + Suhner, Taufkirchen
IBF Mikroelektronik, Oldenburg
Inkos, Reute/Breisgau
iSystem, Dachau

Jacobi Eloxal, Altlussheim
Jarmyn, Limburg
Kniel, Karlsruhe
Knürr, München
Lambda Electronics, Achern
Lemo Electronik, München
LPKF CAD/CAM Systeme, Garbsen
Macrotron, München
Matsuo Electronics Europe, Eschborn
Maxim Ges. f. elektronische integrierte Bausteine, Planegg
Menges electronic, Dortmund
Metrofunkksinceel-Union, Berlin
MSC Vertriebs-GmbH, Stutensee
MTI, Baden-Baden
Nanotec, Finsing
Nickel Schalt- und Meßgeräte, Villingen-Schwenningen
Niebuhr Optoelectronik, Hamburg
Nies Electronic, Frankfurt
Nova Electronik, Pulheim
Otto Fsinceer, Mannheim
pbe Electronic, Elmshorn
Phytec Meßtechnik, Mainz
Plastipol, Runkel
PSI Tronix, Tulare, California,
Püschel Electronic, Mannheim
R.E.D. Regional-Electronic-Distribution, Rodgau-Jügesheim
Radiall, Rödermark
Rau-Meßtechnik, Kelkheim
Reinhold Halbeck, Offenhausen
Retronic, Ronneburg
Riekert & Sprenger, Wertheim
Rittal-Werk, Herborn
Roland Häfele, Schriesheim
RS Components, Mörfelden-Walldorf
Rufenach Vertriebs-GmbH, Heidelberg
Rutronik, Ispringen
Sasco, Putzbrunn
Scantec, Planegg
Schuricht, Fellbach-Schmiden
SCT Servo Control Technology, Taunusstein
SE Spezial-Electronic, Bückeburg
Spindler & Hoyer, Göttingen
Spoerle Electronic, Dreieich
Synatron, Hallbergmoos
TMS Test- und Meßsysteme, Herxheim/Hayna
Tower Electronic Components, Schriesheim
TreNew Electronic, Pforzheim
TS-Optoelectronic, München
Vero Electronics, Bremen
W. & W. Schenk, Maulbronn
Wikotec, Bramsche
Wilhelm Gassert, Schriesheim
WS CAD Electronik, Berk Kirchen

Teaching Activites

Lectures at the University

H.-J. Röser and M. Scholz (ARI): Introduction to Astronomy and Astrophysics, I

A. Glindemann and Ch. Leinert: High-Resolution Imaging in Astronomy

H.-J- Röser and P. Ulmschneider (Heidelberg University): Introduction to Astronomy and Astrophysics, II

J. Fried and A. Just (ARI): Galaxies

Seminars and Colloquia

D. Lemke, R. Mundt, with J. Ktautter and B. Wolf (State Observatory), and H. Schwan (ARI): Introduction to Astronomy and Astrophysics, III (Seminar)

K. Meisenheimer, with J. Kirk (MPI für Kernphysik): Nonthermal Radiation of Active Galaxies (Seminar)

D. Lemke, K. Meisenheimer, R. Mundt, with H.P. Gail (University), B. Fuchs (ARI), J. Krautter (State Observatory): Introduction to Astronomy and Astrophysics, III (Seminar)

K. Meisenheimer, H.-J. Röser, with J. Kirk (MPI für Kernphysik): Clusters of Galaxies (Advanced Seminar)

Ch. Leinert, F. Arnold, E. Grün (MPI für Kernphysik), W.J. Duschl, W.M. Tscharnuter (University of Heidelberg): Seminar: Kometen

Public Lectures

S.V. Beckwith: Search for Nearby Planets: Olbers-Gesellschaft, Bremen

D. Lemke: The Infrared Observatory ISO: Göttingen, Planetarium and University

D. Lemke: The Cold Universe: High School, Bremen

H. Elsässer: New Ways and Objectives of Research in Astronomy: Nordrhein-Westphalen Academy of Sciences

Meetings

The 11th Calar Alto Colloquium with more than 20 contributions was held at the MPIA on March 12th and 13th.

The German-Spanish Astronomical Centre, in collaboration with the local University, organized the »7.th Week of Astronomy and Astrophysics« in Almeria.

Service in Committees

S.V.W. Beckwith was Acting Director of the LBT Consortium, thus representing the interests of the German community in this project; the Consortium meet in Februay, July and November. He took part in the following international meetings: as Chairman in the meetings of the ESO Science and Technical Committee in April and October, as Board Member in the meeting of the ESO Council in June and December, of the ESO VLTI Governing Committee in July, of the LBT Corporation, of the UKIRT Program Committee im May, of the DARA Council in June and October, and in the MPIA Finding Committee in July and October. He acted as Receiving Editor for the Journal *New Astronomy*.

T. Herbst was invited to take part in the Gemini Review Panel for the Mid-Infrared Imager in Tucson in January. He took part as a member in the meetings of the LBT Science Advisory Committee, the VLT MIDI Team and the LBT Near IR Spectroscopy Working Group.

Ch. Leinert was member of the Organizing Committee of the IAU Commission 21 and served as its President from August 1994 to August 1997.

Ch. Leinert und *R. Mundt* took part as Board Members of the ESO VLTI Science Advisory Committee in a meeting in Garching.

R. Mundt took part as Board Member in two meetings of the Calar Alto Program Committee in Heidelberg and in one meeting in Garching oft the ESO Working Groop »Extrasolar Planets«.

Invited Talks at Conferences

S.V.W. Beckwith: Conference »Science with the NGST«, Washington (USA). Conference »Extrasolar Planets«, Blois (France), Workshop »The Orion Complex Revisited«, Schloß Ringberg, Conference »Origins of Solar Systems«, New Hampshire (USA), Conference »ISO's View on Stellar Evolution«, Noordwijkerhout (Netherlands), Conference »The Young Universe«, Monte Porzio (Italy), Physics Colloquium of the Dortmund University

K. Birkle: Workshop »Seyfert Galaxies«, Asiago (Italy), Workshop »Gamma Ray Astronomy with systems of Cherenkov Telescopes«, Schloß Ringberg

A. Burkert: Workshop »The Orion Complex Revisited«, Schloß Ringberg, Colloquium at the Bochum University. T3E-Workshop at the Computing Centre in Garching

M.-M. Mac-Low: Workshop »The Orion Complex Revisited«, Schloß Ringberg

M. Petr: Workshop »The Orion Complex Revisited«, Schloß Ringberg

Publications

Ábrahám, P., J.A. Acosta-Pulido, U. Klaas, R.J. Laureijs, C. Leinert, D. Lemke, A. Moneti and A. Salama: ISOPHOT-S Measurements of the Zodiacal Light: A Calibration Tool. In: The first ISO workshop on analytical spectroscopy. Proc. Conf. Madrid. ESA SP-419, 119–122 (1997).

Ábrahám, P., Ch. Leinert and D. Lemke: Search for brightness fluctuations in the zodiacal light at 25 µm with ISO. Astronomy and Astrophysics 328, 702–705 (1997).

Bate, M.R.: Accretion during Binary Star Formation I. Ballistic Accretion. Monthly Notices of the Royal Astronomical Society 285 (1), 16–32 (1997).

Bate, M.R.: Disc Formation in Protobinary Systems. In: Star Formation, Near and Far, (Eds.) S.S. Holt, L.G. Mundy. AIP Press, Woodbury, NY 1997. AIP Conference Proceedings 393, 371–374.

Bate, M.R. and I.A. Bonnell: Accretion during Binary Star Formation II. Gaseous Accretion and Disc Formation. Monthly Notices of the Royal Astronomical Society 285 (1), 33–48 (1997).

Bate, M.R. and I.A. Bonnell: The Effects of Accretion during Binary Star Formation. In: Visual Double Stars: Formation, Dynamics and Evolutionary Tracks, (Eds.) J.A. Docobo et al. Kluwer, Dordrecht 1997. Astrophysics and Space Science Library 223, 153–164.

Bate, M.R. and A. Burkert: Resolution Requirements for Smoothed Particle Hydrodynamics Calculations with Self-gravity. Monthly Notices of the Royal Astronomical Society 288 (4), 1060–1072 (1997).

Benítez, N., E. Martínez-González, J.L. Sanz, A. Aguirre and M. Alises: The absorbers towards Q0836+113. Astronomy and Astrophysics 321, 129–133 (1997).

Birkle, K., H. Böhnhardt, G. Richter, L. Jorda, J. Lecacheux and F. Colas: Comet C/1995 01 (Hale-Bopp). IAU Circular No. 6583 (1997).

Birkle, K., U. Thiele and H. Böhnhardt: Comet C/1995 01 (Hale-Bopp). IAU Circular No. 6598, 1 (1997).

Böhm, T. and G.A. Hirth: Forbidden lines in Herbig Ae/Be stars. The [OI] (1F) 6300.31Å and 6363.79Å lines. II. Longslit observations of selected objects. Astronomy and Astrophysics 324, 177–184 (1997).

Bonnell, I.A., M.R. Bate, C.J. Clarke and J.E. Pringle: Accretion and the Stellar Mass Spectrum in Small Clusters. Monthly Notices of the Royal Astronomical Society 285 (1), 201–208 (1997).

Boroson, B., R. McCray, C.O. Clark, J.Slavin, M.-M. Mac Low, Y.-H. Chu and D. van Buren: An Interstellar Conduction Front within a Wolf-Rayet Ring Nebula Observed with the Goddard High Resolution Spectrograph. The Astrophysical Journal 478, 638–647 (1997).

Boselli, A., R.J. Tuffs, G. Gavazzi, H. Hippelein and D. Pierini: Near infrared surface photometry of late-type Virgo cluster galaxies. Astronomy and Astrophysics Supplement Series 121, 507–551 (1997).

Bouvier, J., R. Wichmann, K. Grankin, S. Allain, E. Covino, M. Fernández, E.L. Martín, L. Terranegra, S. Catalano and E. Marilli: COYOTES IV: the rotational periods of low-mass Post-T Tauri stars in Taurus. Astronomy and Astrophysics 318, 495–505 (1997).

Brandner, W., J.M. Alcala, S. Frink and M. Kunkel: An ESO 3.6m/adaptive optics search for young brown dwarfs and giant planets. The Messenger 89, 37–40 (1997).

Burkert, A.: Do Dwarf Spheroidal Galaxies Contain Dark Matter? The Astrophysical Journal Letters 474, 99–102 (1997).

Burkert, A., M.R. Bate and P. Bodenheimer: Protostellar Fragmentation in a Power-Law Density Distribution. Monthly Notices of the Royal Astronomical Society 289 (3), 497–504 (1997).

Burkert, A., D.H. Hartmann and S.A. Majewski: Galactic Chemodynamics 4: The History of the Milky Way and Its Satellite System. Astronomical Society of the Pacific Conference Series Vol. 112, (Eds.) A. Burkert, D.H. Hartmann, S.A. Majewski. Astron. Soc. Pac., San Francisco 1997, 216 pp.

Burkert, A. and P. Ruiz-Lapuente: Dormant Dwarf Spheroidal Galaxies, Deactivated by Type Ia Supernovae. The Astrophysical Journal 480, 297–302 (1997).

Burkert, A. and J. Silk: Dark Baryons and Rotation Curves. Bulletin of the American Astronomical Society 191, 24.05 (1997).

Burkert, A. and J. Silk: Dark Baryons and Rotation Curves. The Astrophysical Journal Letters 488, 55–58 (1997).

Burkert, A. and G.H. Smith: Substructure in the Globular Cluster System of the Milky Way: The Highest Metallicity Clusters. The Astrophysical Journal Letters 474, 15–18 (1997).

Carpenter, J.M., M.R. Meyer, C. Dougados, S.E. Strom and L.A. Hillenbrand: Properties of the Monoceros R2 Stellar Cluster. The Astronomical Journal 114 (1), 198–221 (1997).

Castro-Tirado, A.J., J. Gorosabel, J. Heidt, T. Seitz, E. Thommes, C. Wolf, N. Lund, H. Pedersen, E. Costa, F. Frontera, J. Heise, J. In't Zand, C. Bartolini, A. Guarnieri, A. Masetti, A. Piccioni and E. Palazzi: GRB 970111 and GRB 970228. IAU Circular No. 6598, 2 (1997).

Castro-Tirado, A.J., J. Gorosabel, N. Masetti, C. Bartolini, A. Guarnieri, A. Piccioni, J. Heidt, T. Seitz, E. Thommes, C. Wolf, E. Costa, M. Feroci, F. Frontera, D. Dal Fiume, L. Nicastro, E. Palazzi and N. Lund: The GRB 970111 error box 19-hours after the high energy event. In: The Fourth Compton Symposium Williamsburg, Eds: Ch. Dermer, M. Strickman, J. Kurfess. AIP Conference Series 410, 1516 (1997).

Castro-Tirado, A.J., J. Gorosabel, H. Pedersen, E. Costa, M. Feroci, L. Piro, F. Frontera, E. Palazzi, L. Nicastro, D. Delfiume, N. Benitez, E. Martinez-Gonzalez, J. Heidt, T. Seitz, E. Thommes, C. Wolf, R. Fockenbrock, K. Birkle, J. Greiner, C. Bartolini, A. Guarnieri, N. Masetti, A. Piccioni, M. Mignoli, L. Metcalfe and N. Lund: Optical follow-up observations of GRBs detected by BeppoSAX (I). 4th Huntsville Gamma-Ray Burst Symposium, 15–20 September, 1997.

Castro-Tirado, A.J., J. Gorosabel, D. Thompson, K. Birkle and J. Greiner: GRB 970616. IAU Circular No. 6688, 2 (1997).

Castro-Tirado, A.J., J. Gorosabel, C. Wolf, R. Fockenbrock, E. Martinez-Gonzalez, N. Benitez, J. Greiner, E. Costa, M. Feroci, L. Piro, F. Frontera, E. Palazzi, G. Pizzichini, L. Nicastro, J. In't Zand, C. Bartolini, A. Guarnieri, A. Piccioni, N. Masetti, J. Gallego, J. Zamorano, H. Pedersen and K. Birkle: GRB 970508. IAU Circular 6657, 1 (1997).

Coudé du Foresto, V., S. Ridgway and J.-M. Mariotti: Deriving object visibilities from interferograms obtained with a fiber stellar interferometer. Astronomy and Astrophysics Supplement Series 121, 379–392 (1997).

Dahlem, M., M.G. Petr, M.D. Lehnert, T.M. Heckman and M. Ehle: Evidence for a New »Superwind« Galaxy – NGC 4666. Astronomy and Astrophysics 320, 731–745 (1997).

Doublier, V., G. Comte, A. Petrosian, C. Surace and M. Turatto: Multi-spectral study of a new sample of blue compact dwarf galaxies. I. B and R surface photometry of 23 objects from the Byurakan lists. Astronomy and Astrophysics Supplement Series 124, 405–424 (1997).

Eislöffel, J.: Molecular Hydrogen Emission in Embedded Flows. In: Herbig-Haro Flows and the Birth of Low Mass Stars, (Eds.) B. Reipurth, C. Bertout. IAU Symposium No. 182, Kluwer, Dordrecht 1997, 93–102.

Eislöffel, J. and R. Mundt: Parsec-Scale Jets from Young Stars. The Astronomical Journal 114 (1), 280–287 (1997).

Elsässer, H.: Sichtexpedition auf dem Peloponnes. In: The Earth and the Universe, (Eds.) G. Asteriadis, A. Bantelas, M. E. Contadakis, K. Katsambalos, A. Papadimitriou, I. N. Tziavos. Ziti Editions, Thessaloniki 1997, 73–77.

Elsässer, H.: Neue Wege und Ziele astronomischer Forschung. Nordrhein-Westfälische Akademie der Wissenschaften. Westdeutscher Verlag, Düsseldorf 1997, Vorträge N 426, 1–27.

Fernández, M., J.M. Alcala, E. Covino, L. Terranegra and C. Chavarria: Looking for the spectral fingerprints of some mechanisms responsible of the T Tauri stars variability. In: Low Mass Star Formation – from Infall to Outflow, Poster proceedings of IAU Symposium No. 182 on Herbig-Haro Objects and the Birth of Low Mass Stars. 20–24 January 1997, Chamonix, France, (Eds.) F. Malbet, A. Castets, 269.

Ferraro, F.R., E. Carretta, C.E. Corsi, F. Fusi Pecci, R. Buonanno, B. Paltrinieri and D. Hamilton: The stellar population of the globular cluster M 3. II. CCD photometry of additional 10,000 stars. Astronomy and Astrophysics 320, 757–775 (1997).

Fried, J.W.: Extended emission-line gas in the high luminosity, low redshift QSO E1821+643. Astronomy and Astrophysics Letters 331, 73–76 (1997).

Fried, J.W.: Faint galaxies around quasars at z = 1 and gravitational lensing of distant objects. Astronomy and Astrophysics 319, 365–370 (1997).

Fockenbrock, R., E. Thommes, H. Hippelein, K. Meisenheimer and H.-J. Röser: Object detection and classification in CADIS. In: The Early Universe with the VLT, (Ed.) J. Bergeron. ESO Astrophysics Symposia, Springer, Berlin 1997, 390–391.

Gabriel, C., I. Heinrichsen and U. Klaas: Experience and Lessons learnt by the Development of the ISOPHOT Interactive Analysis PIA. In: The Far Infrared and Submillimeter Universe, Proc. Symp. Grenoble. ESA SP-401, 261 (1997).

García-Segura, G., N. Langer and M.-M. Mac Low: LBV Outbursts: The Effects of Rotation. In: Luminous Blue Variables: Massive Stars in Transition, (Eds.) A. Nota, H. J. G. L. M. Lamers. San Francisco 1997. Astronomical Society of the Pacific Conference Series 120, 332.

Glindemann, A.: Relevant Parameters for Tip-Tilt Systems of Large Telescopes. Publications of the Astronomical Society of the Pacific 109, 682–687 (1997).

Glindemann, A., D. Hamilton, S. Hippler, R.-R. Rohloff and K. Wagner: ALFA – The Laser Guide Star Adaptive Optics System for the Calar Alto 3.5-m Telescope. In: Laser Technology for Laser Guide Star Adaptive Optics Astronomy, (Ed.) N. Hubin. European Southern Observatory, Garching, 1997, 120–125.

Glindemann, A., M.J. McCaughrean, S. Hippler, C. Birk, K. Wagner and R.-R. Rohloff: CHARM – A Tip-Tilt Tertiary System for the Calar Alto 3.5m Telescope. Publications of the Astronomical Society of the Pacific 109, 688–696 (1997).

Glindemann, A. and A. Quirrenbach: Künstlicher Stern über dem Calar Alto. Adaptive Optik mit ALFA am 3.5m-Teleskop. Sterne und Weltraum 36, 950–955 (Teil I) und 1038–1044 (Teil II), (1997).

Haas, M., Ch. Leinert and A. Richichi: On the near-infrared halo of Elias 1. Astronomy and Astrophysics 326, 1076–1080 (1997).

Hawarden, T.G., C.P. Cavedoni, T.C. Chuter, I.A. Look, N.P. Rees, D.G. Pettie, R.J. Bennett, E. Atad, J.W. Harris, C.M. Humphries, B. Mack, E. Pitz, A. Glindemann, S. Hippler, R.-R. Rohloff and K. Wagner: Progress of the UKIRT Upgrades Programme. In: Optical Telescopes of Today and Tomorrow, (Ed.) A.L. Ardeberg. SPIE Vol. 2871, Bellingham 1997, 256–266.

Hawkins, M.R.S., D. Clements, J.W. Fried, A.F. Heavens, P. Véron, E.M. Minty and P. van der Werf: The double quasar Q2138-431: lensing by a dark galaxy? Monthly Notices of the Royal Astronomical Society 291 (4), 811–818 (1997).

Heinrichsen, I., C. Gabriel, P.J. Richards and U. Klaas: The ISO-PHOT Observational Modes and their Pipeline Processing. In: The Far Infrared and Submillimeter Universe. Proc. Symp. Grenoble. ESA SP-401, 273 (1997).

Héraudeau, Ph. and F. Simien: Near-Infrared Surface Photometry of Spiral Galaxies: II Derivation of mass models. Astronomy and Astrophysics 326, 897–907 (1997).

Herbst, T.M., S.V.W. Beckwith and M. Robberto: A New Molecular Hydrogen Outflow in Serpens. In: Low Mass Star Formation – from Infall to Outflow, Poster proceedings of IAU Symposium No. 182 on Herbig-Haro Objects and the Birth of Low Mass Stars. 20–24 January 1997, Chamonix, France, (Eds.) F. Malbet, A. Castets, 135.

Herbst, T.M., S.V.W. Beckwith and M. Robberto: A New Molecular Hydrogen Outflow in Serpens. The Astrophysical Journal Letters 486, 59–62 (1997).

Herbst, T.M., M. Robberto and S.V.W. Beckwith: Molecular and Atomic Shocks in the Near Environment of T Tauri. In: Low Mass Star Formation – from Infall to Outflow, Poster proceedings of IAU Symposium No. 182 on Herbig-Haro Objects and the Birth of Low Mass Stars. 20-24 January 1997, Chamonix, France, (Eds.) F. Malbet, A. Castets. Laboratoire d'Astrophysique, Obs. de Grenoble, Grenoble 1997, p. 215.

Herbst, T.M., M. Robberto and S.V.W. Beckwith: Wind-Disk-Ambient Cloud Interactions in the Near Environment of T Tauri. The Astronomical Journal 114 (2), 744–756 (1997).

Herbstmeier, U.: Future radio and infrared observations of dust in galactic halos. In: The Physics of Galactic Halos, (Eds.) H. Lesch, R.-J. Dettmar, U. Mebold, R. Schlickeiser. Proc. 156th WE-Heraeus Workshop. Akademie Verlag, Berlin 1997, 203.

Herbstmeier, U., P. Ábrahám, R.J. Laureijs, D. Lemke, K. Mattila, C. Leinert and C. Surace: ISOPHOT observations of cirrus. In: Taking ISO to the Limits: Exploring the Faintest Sources in the Infrared, (Eds.) R.J. Laureijs, D. Levine. Proc. Workshop Madrid. ESA Publication (1997), 184–192.

Hirth, G.A., R. Mundt and J. Solf: Spatial and kinematic properties of the forbidden emission line region of T Tauri stars. Astronomy and Astrophysics Supplement Series 126, 436–469 (1997).

Huchtmeier, W.K., U. Hopp and B. Kuhn: HI observations of dwarf galaxies in voids. Astronomy and Astrophysics 319, 67–73 (1997).

Juvela, M., K. Lehtinen, K. Mattila, D. Lemke and L. Haikala: Structure of L 1521B: CO observations of a dense core in Taurus. Astronomy and Astrophysics 317, 898–906 (1997).

Kalas, P.: A candidate dust disk surrounding the binary stellar system BD+31° 643. Nature 386, 52–54 (1997).

Katterloher, R., D. Engemann, M. Fabbricotti, O. Frenzl, L. Hermans, D. Lemke, J. Wolf, E. Czech, E.E. Haller, N. Haegel, Th. Henning, M. Konuma and G. Pilbratt: FIRSA and FIRGA: Development of photoconductor arrays for FIRST, In: The Far Infrared and Submillimeter Universe. Proc. Symp. Grenoble. ESA-SP-401, 393 (1997).

Klaas, U., P. Ábrahám, J.A. Acosta-Pulido, H.O. Castañeda, L. Cornwall, F. Garzón, P. Hammersley, I. Heinrichsen, U. Kinkel, D. Lemke, J. Schubert and M. Wells: ISOPHOT-S: Capabilities and Calibration. In: The first ISO workshop on analytical spectroscopy. Proc. Conf. Madrid. ESA SP-419, 113–118 (1997).

Klaas, U., S. Bogun, U. Herbstmeier, D. Lemke, M. Burgdorf and R. Laureijs: The ISO Serendipity Survey. In: Proc. of a Denis Euroconference Workshop, Puerto de la Cruz, Tenerife, Spain, 1996, (Eds.) F. Garzón, N. Epchtein, A. Omont, B. Burton, P. Persi. Kluwer, Dordrecht, Astrophysics and Space Science Library 210, 45 (1997).

Klaas, U., M. Haas, I. Heinrichsen and B. Schulz: Infrared spectral energy distributions of the interacting galaxies Arp 244, NGC 6240, and Arp 220. Astronomy and Astrophysics Letters 325, 21–24 (1997).

Klessen, R.S.: Fragmentation of Molecular Clouds with GRAPE-SPH, In: Star Formation, Near and Far, (Eds.) S.S. Holt, L.G. Mundy. AIP Conference Proceedings 393, 133–137 (1997).

Klessen, R.S.: GRAPESPH with Fully Periodic Boundaries: Fragmentation of Molecular Clouds. In: 12th Kingston Meeting on Computational Astrophysics, (Eds.) D.A. Clarke, M.J. West. Astronomical Society of the Pacific Conference Series Vol. 123, 169–171 (1997).

Klessen, R.S.: GRAPESPH with Fully Periodic Boundary Conditions: Fragmentation of Molecular Clouds. Monthly Notices of the Royal Astronomical Society 292 (1), 11–18 (1997).

Klessen, R.S. and A. Burkert: Fragmentation in Molecular Clouds: The Initial Phase of a Stellar Cluster. Astronomische Gesellschaft Abstract Series 13, 16 (1997).

Köhler, R.: Multiplicity of T Tauri Stars. Astronomische Gesellschaft Abstract Series 13, 28 (1997).

Koresko, C.D., T.M. Herbst and Ch. Leinert: The infrared companions of T Tauri stars. The Astrophysical Journal 480, 741–753 (1997).

Kroupa, P. and R.S. Klessen: Dwarf Galaxies without Dark Matter: Comparing two Numerical Schemes. Astronomische Gesellschaft Abstract Series 13, 54 (1997).

Kuhn, B., U. Hopp and H. Elsässer: Results of a search for faint galaxies in voids. Astronomy and Astrophysics 318, 405–415 (1997).

Lahulla, J.F., A. Aguirre and J. Hilton: BVRI photometric sequences for nine selected dark globules. Astronomy and Astrophysics Suppl. Ser. 126, 73–80 (1997).

Leech, K.J., H.J. Völk, I. Heinrichsen, H. Hippelein, L. Metcalfe, D. Pierini, C.C. Popescu, R.J. Tuffs and C. Xu: LWS Observations of a Statistical Sample of Late-type Galaxies from the Virgo Cluster. In: The First ISO workshop on analytical spectroscopy. Proc. Conf. Madrid. ESA SP-419, 279 (1997).

Leinert, Ch.: Light of the night sky. In: Reports on Astronomy, Transactions of the IAU, Vol. XXIII A, (Ed.) I. Appenzeller. Kluwer, Dordrecht 1997, 231–256.

Leinert, Ch., T. Henry, A. Glindemann and D.W. McCarthy, Jr.: A search for companions to nearby southern M dwarfs with near-infrared speckle interferometry. Astronomy and Astrophysics 325, 159–166 (1997).

Leinert, Ch., A. Richichi and M. Haas: Binaries among Herbig Ae/Be stars. Astronomy and Astrophysics 318, 472–484 (1997).

Lemke, D.: Die kalte Welt durch ISO sichtbar. Sterne und Weltraum, Spezialausgabe 2/30, 1997.

Lemke, D.: ISOPHOT instrument overview. In: Taking ISO to the Limits: Exploring the Faintest Sources in the Infrared, (Eds.) R.J. Laureijs, D. Levine. Proc. Workshop, Madrid. ESA Publication (1997), 53–67.

Lemke, D.: ISO: The first 10 months of the mission. In: Reviews in Modern Astronomy 10, (Ed.) R.E. Schielicke. Astronomische Gesellschaft (1997), 263–272.

Lemke, D.: Observations with ISOPHOT. In: The Far Infrared and Submillimeter Universe, Proc. Symp., Grenoble. ESA-SP-401, 181–186 (1997).

Mac Low, M.-M., R. Klessen, A. Burkert, M.D. Smith and O. Kessel: Simulations of MHD Turbulence in Molecular Clouds: Decay Timescales and Spatial Structure. Bulletin of the American Astronomical Society 191, 20.02 (1997).

Mac Low, M.-M. and M.D. Smith: Nonlinear Development and Observational Consequences of Wardle C-Shock Instabilities. The Astrophysical Journal 491, 596–614 (1997).

Mac Low, M.-M. and M.D. Smith: Time dependent, multidimensional models of C-Shocks. In: Low Mass Star Formation – from Infall to Outflow, Poster proceedings of IAU Symposium No. 182 on Herbig-Haro Objects and the Birth of Low Mass Stars. 20–24 January 1997, Chamonix, France, (Eds.) F. Malbet, A. Castets, 155.

Mattila, K., D. Lemke, L.K. Haikala, R.J. Laureijs, A. Léger, K. Lehtinen, Ch. Leinert and P.G. Mezger: Spectrophotometry of UIR bands in the diffuse emission of the galactic disk. Astronomy and Astrophysics Letters 315, 353–356 (1996).

McCaughrean, M.J. and Mac Low, M.-M.: The OMC-1 Molecular Hydrogen Outflow as a Fragmented Stellar Wind Bubble. The Astronomical Journal 113, 391–400 (1997).

Meisenheimer, K., S. Beckwith, R. Fockenbrock, J. Fried, H. Hippelein, U. Hopp, Ch. Leinert, H.-J. Röser, E. Thommes and Ch. Wolf: The Calar Alto Deep Imaging Survey. In: The Early Universe with the VLT, (Ed.) J. Bergeron. ESO Astrophysics Symposia, Springer, Berlin 1997, 165–172.

Meisenheimer, K., M.G. Yates and H.-J. Röser: The synchrotron spectra of radio hot spots II. Infrared imaging. Astronomy and Astrophysics 325, 57–73 (1997).

Meyer, M.R., S.V.W. Beckwith, T.M. Herbst and M. Robberto: The Transitional Pre-Main-Sequence Object DI Tauri: Evidence for a Substellar Companion and Rapid Disk Evolution. The Astrophysical Journal Letters 489, 173–178 (1997).

Meyer, M.R., S.V.W. Beckwith and A. Natta: The structure of disks and envelopes around young stars: new results from ISO. In: Low Mass Star Formation – from Infall to Outflow, Poster proceedings of IAU Symposium No. 182 on Herbig-Haro Objects and the Birth of Low Mass Stars. 20–24 January 1997, Chamonix, France, (Eds.) F. Malbet, A. Castets, 224.

Neeser, M.J., K. Meisenheimer and H. Hippelein: A Detailed Study of the Complex Line Emission Regions in the Radio Galaxy 3C 34. The Astrophysical Journal 491, 522–535 (1997).

Neumann, M., K. Meisenheimer and H.-J. Röser: Near-infrared photometry of the jet 3C 273. Astronomy and Astrophysics 326, 69–76 (1997).

Neumann, M., K. Meisenheimer, H.-J. Röser and H.H. Fink: ROSAT-HRI observations of the jet in M87. Astronomy and Astrophysics 318, 383–389 (1997).

O'Dell, C.R.: Herbig-Haro Objects in the Orion Nebula Region. In: Herbig-Haro Flows and the Birth of Low Mass Stars, (Eds.) B. Reipurth, C. Bertout. IAU Symposium No. 182, Kluwer Dordrecht 1997, 39–46.

O'Dell, C.R. and S.V.W. Beckwith: Young Stars and their Surroundings. Science 276, 1355–1359 (1997).

Paresce, F., D. Mourard, T. Bedding, J. Beletic, C. Haniff, Ch. Leinert, F. Malbet, J.-M. Mariotti, D. Mozurkevich, R. Mundt, P. Petitjean, A. Quirrenbach, T. Reinheimer, A. Richichi, A. Rottgering, O. von der Lühe and R. Waters [ISAC-; Interferometry Science Advisory Committee]: A new start for the VLTI. Messenger 83, 14–21 (1996).

Patrashin, M., B. Fouks, U. Grözinger, D. Lemke and J. Wolf: Residual conductivity of stressed Ge:Ga photoconductors after low-dose gamma irradiation. Journal of Applied Physics 82, 1450–1453 (1997).

Patsis, P.A.: The relation between existing resonances and morphology in disk galaxies. In: Proc. of the 2nd HEL.A.S. Conference, (Eds.) M. Contadakis et al., 346–349 (1997).

Patsis, P.A., E. Athanassoula and A.C. Quillen: Orbits in the bar of NGC 4314. The Astrophysical Journal 483, 731–744 (1997).

Patsis, P.A., C. Efthymiopoulos, G. Contopoulos and N. Voglis: Dynamical spectra of barred galaxies. Astronomy and Astrophysics 326, 493–500 (1997).

Patsis, P.A., P. Grosbøl and N. Hiotelis: Interarm features in gaseous models of spiral galaxies. Astronomy and Astrophysics 323, 762–774 (1997).

Perley, R.A., H.-J. Röser and K. Meisenheimer: The radio galaxy Pictor A – a study with the VLA. Astronomy and Astrophysics 328, 12–32 (1997).

Pesce, J.E., C.M. Urry, L. Maraschi, A. Treves, P. Grandi, R.I. Kollgaard, E. Pian, P.S. Smith, H.D. Aller, M.F. Aller, A.J. Barth, D.A.H. Buckley, E. Covino, A.V. Filippenko, E.J. Hooper, M.D. Joner, L. Kedziora-Chudczer, D. Kilkenny, L.B.G. Knee, M. Kunkel, A.C. Layden, A.M. Magalhães, F. Marang, V. E. Margoniner, C. Palma, A. Pereyra, C.V. Rodrigues, A. Schutte, M.L. Sitko, M. Tornikoski, J. van der Walt, F. van Wyk, P.A. Whitelock and S.J. Wolk: Multiwavelength Monitoring of the BL Lacertae Object PKS 2155–304 in 1994 May. I. The Ground-based Campaign. The Astrophysical Journal 486, 770–783 (1997).

Pharasyn, A., F. Simien and Ph. Héraudeau: On the fundamental plane of spiral galaxies. In: Dark and visible matter in galaxies, (Eds.) M. Persic, P. Salucci. Proc. Conf. Sesto, Italy, 1996. Astronomical Society of the Pacific Conference Series Vol. 117, 180–184 (1997).
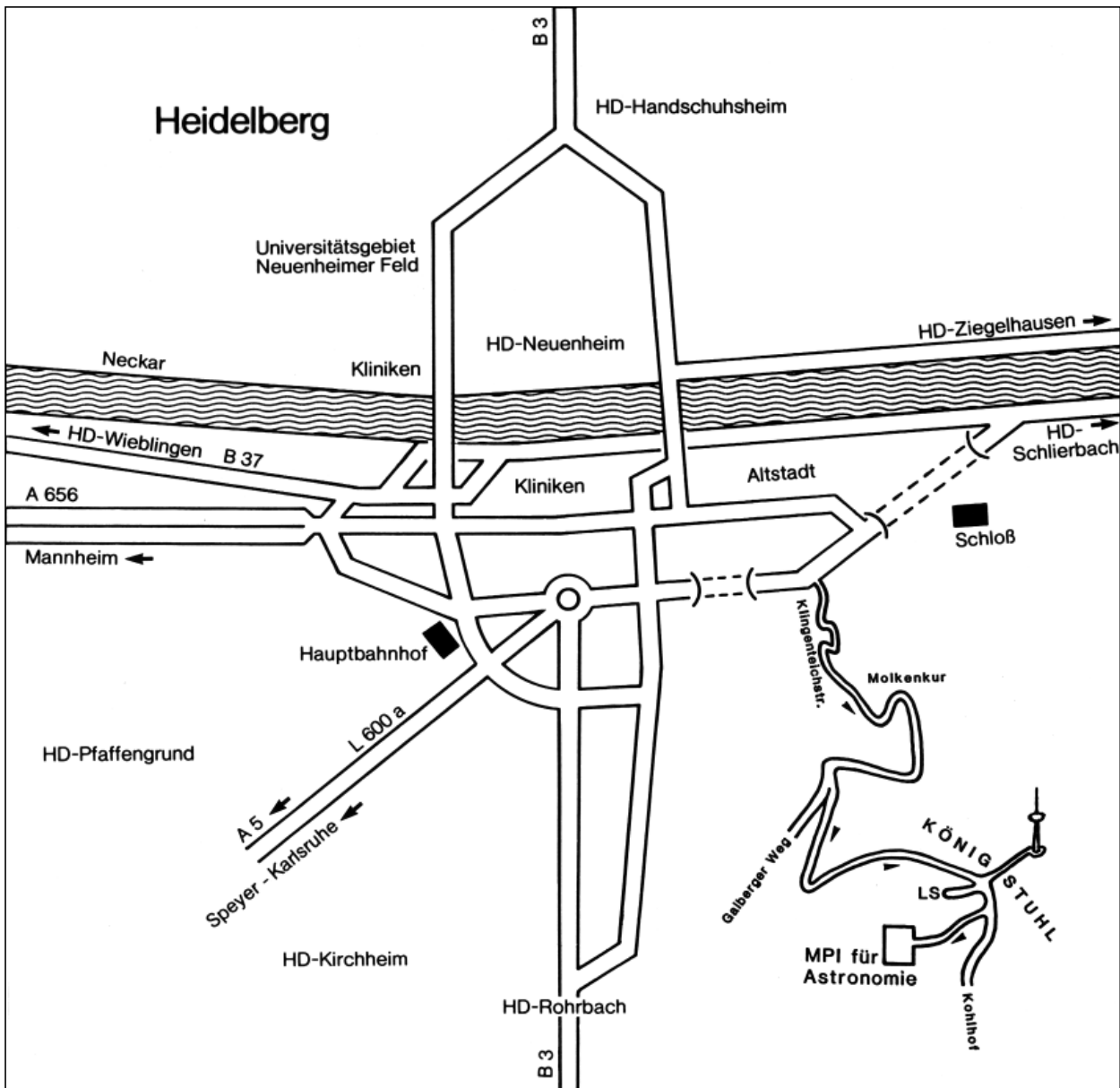
Popescu, C.C., U. Hopp and H. Elsässer: Results of a search for emission-line galaxies towards nearby voids. The spatial distribution. Astronomy and Astrophysics 325, 881–892 (1997).

Popescu, C.C., P. Rafanelli, S. Benetti, U. Hopp, K. Birkle and H. Elsässer: SN 1995ah: the first supernova observed in a blue compact dwarf galaxy. Astronomy and Astrophysics 326, 982–987 (1997).

Radovich, M., P. Rafanelli, K. Birkle and G. M. Richter: Spectroscopic analysis of the nuclear and circumnuclear regions of the Seyfert 2 galaxy NGC 7130. Astronomische Nachrichten 318 (4), 229–236 (1997).

Rafanelli, P., L. Piro, M. Radovich, A. Rifatto, T. Boller, K. Birkle, U. Thiele, R. Assendorp and G. Richter: Soft X-ray emission luminosity of Seyfert 1 galaxies in pairs. Memorie della Societa' Astronomica Italiana 68 (1), 257–258 (1997).

Ray, T.P., T.W.B. Muxlow, D.J. Axon, A. Brown, D. Corcoran, J.E. Dyson and R. Mundt: Evidence for Magnetic Fiels in the Outflow from T Tau S. In: Herbig-Haro Flows and the Birth of Low Mass Stars, (Eds.) B. Reipurth, C. Bertout. IAU Symposium No. 182, Kluwer Dordrecht 1997, 475–480.

Ray, T.P., T.W.B. Muxlow, D.J. Axon, A. Brown, D. Corcoran, J. Dyson and R. Mundt: Large-scale magnetic fields in the outflow from the young stellar object T Tauri S. Nature 385, 415–417 (1997).

Rees, N.P. and S. Hippler: Progress on the UKIRT upgrades program. In: Telescope Control Systems II. (Ed.) H. Lewis. SPIE Proc. Vol. 3112, Bellingham 1997, 2–8.

Reimers, D., F. Toussaint, H.-J. Hagen, H. Hippelein and K. Meisenheimer: Two X-ray clusters close to line of sight of the luminous QSO HS1700+6416. Astronomy and Astrophysics 326, 489–492 (1997).

Richichi, A., G. Calamai, Ch. Leinert and B. Stecklum: New binary stars discovered by lunar occultations III. Astronomy and Astrophysics 322, 202–208 (1997).

Robberto, M., T. Herbst, S.V.W. Beckwith, C. Birk and P. Bizenberger: Thermal IR Imaging with MAX: Pushing the Limit of Single-Dish Ground Based Observations. In: Science with the VLT Interferometer, (Ed.) P. Paresce. Springer, Berlin 1997, 391.

Röser, H.-J., K. Meisenheimer, M. Neumann, R.G. Conway, R.J. Davis and R.A. Perley: The Jet of the Quasar 3C 273 at High Resolution. Reviews in Modern Astronomy Vol. 10, Springer, Berlin 1997, 253–261.

Rubin, R.H., R.J. Dufour, G.J. Ferland, P.G. Martin, C. O'Dell, J.A. Baldwin, J.J. Hester, D.K. Walter and Z. Wen: [Fe IV] in the Orion Nebula. The Astrophysical Journal Letters 474, 131–134 (1997).

Schmidt, K.-H., P. Böhm and H. Elsässer: On the emptiness of voids. Astronomische Nachrichten 318 (2), 81–87 (1997).

Small, T.A.,W.L.W. Sargent and D. Hamilton: The Norris Survey of the Corona Borealis Supercluster. I. Observations and Catalog Construction. The Astrophysical Journal Supplement Series 111, 1–72 (1997).

Small, T.A.,W.L.W. Sargent and D. Hamilton: The Norris Survey of the Corona Borealis Supercluster. II. Galaxy Evolution with Redshift and Environment. The Astrophysical Journal 487, 512–528 (1997).

Smith, K.W., I.A. Bonnell and M.R. Bate: The Effect of Accretion on Young Hierarchical Triple Systems. In: Visual Double Stars: Formation, Dynamics and Evolutionary Tracks, (Eds.) J.A. Docobo et al. Kluwer, Dordrecht 1997. Astrophysics and Space Science Library 223, 145–151.

Smith, K.W., I.A. Bonnell and M.R. Bate: The Stability of Accreting Triples. Monthly Notices of the Royal Astronomical Society 288 (4), 1041–1048 (1997).

Smith, M.D. and M.-M. Mac Low: The Formation of C-Shocks: Structure and Signatures. Astronomy and Astrophysics 326, 801–810 (1997).

Stickel, M., D. Lemke, M. Haas, K. Mattila and L.K. Haikala: Far infrared emission of intracluster dust in the Coma cluster. In: Untangling Coma Berenices: A New Vision of an Old Cluster, (Eds.) A. Mazure, F. Casoli, F. Durret, D. Gerbal. Proc. Conf. Marseilles. World Scientific Publishing Co. Ltd. 1997, 183.

Stickel, M., D. Lemke, K. Mattila, L.K. Haikala and M. Haas: Far-Infrared Emission of Intracluster Dust in the Coma Galaxy Cluster. Astronomy and Astrophysics 329, 55–60 (1997).

Surace C. and G. Comte: Survey of a sample of starburst galaxies – The emission line objects. Revista Mexicana de Astronomia y Astrofisica 6, 102 (1997).

Taam, R.E., E.L. Sandquist, X. Chen, P. Bodenheimer and A. Burkert: 3-D Hydrodynamics Simulations of Envelope Ejection in Common Envelope Binaries. Bulletin of the American Astronomical Society 191, 44.04 (1997).

Thommes, E.: Entdeckung einer alten Galaxie im jungen Universum. Sterne und Weltraum 36, 431–432 (1997).

Thommes, E., R. Fockenbrock, H. Hippelein, K. Meisenheimer and H.-J. Röser: Faint emission line galaxies detected in CADIS. In: The Early Universe with the VLT, (Ed.) J. Bergeron. ESO Astrophysics Symposia, Springer, Berlin 1997, 173–176.

Thommes, E., K. Meisenheimer, R. Fockenbrock, H. Hippelein and H.-J. Röser: Search for Primeval Galaxies with the Calar Alto Deep Imaging Survey: First Results. Reviews in Modern Astronomy Vol. 10, Springer Berlin 1997, 297–321.

Tóth, L.V. and M. Kun: New Water Maser in L 1251. Information Bulletin on Variable Stars 4492, 1–4 (1997).

Wehrse, R., Ph. Rosenau, A. Suvernev, J. Liebert and Ch. Leinert: ISOPHOT-S spectra and the temperature distribution in M dwarfs, In: The First ISO Workshop on Analytical Spectroscopy. Proc. Confer. Madrid. ESA SP-419, 309–310 (1997).

Woitas, J.: Detection of 43 New Bright Variable Stars by the Tycho Instrument of the Hipparcos Satellite. Information Bulletin on Variable Stars 4444, 1 (1997).

Woitas, J.: Röntgenemission von Protosternen. Sterne und Weltraum 36, 830–831 (1997).

Wolf, J., R. Katterloher, D. Lemke, U. Grözinger, L. Hermans, O. Frenzl, D. Engemann, J. Beeman and M. Fabricotti: Submm- and Far Infrared Space Instruments. In: Proc. 30th ESLAB Symposium, Noordwijk, The Netherlands, ESA SP-388, 25–28 (1997).

Diploma Theses

Kasper, M. E.: Das astronomische Seeing. Theorie, Methodik und Messungen. Universität Heidelberg 1997.

von Kuhlmann, B.: Inbetriebnahme und Leistungstest des Fokalreduktors MOSCA für das 3.5-Meter-Teleskop auf dem Calar Alto. Universität Heidelberg 1997.

Doctoral Theses

Kania, U.: IRAS 20024+3330: Ein Vorhauptreihenstern hoher Leuchtkraft als Anreger der ausgedehnten, nichtthermischen Radioquelle G70.7+1.2. Universität Heidelberg 1997.

Köhler, R.: Doppelsternhäufigkeit unter röntgenselektierten T Tauri-Sternen. Universität Heidelberg 1997.

Müller, T.: Asteroiden als photometrische Eichquellen für den fernen Infrarotbereich. Universität Heidelberg 1997.

Reuther, K.-M.: Suche nach roten QSO. Universität Heidelberg 1997.

Schubert, J.: Die Eichung des Infrarot-Gitterspektrometers im Satelliten-Experiment ISOPHOT und die Korrektur der Transienten seiner Detektoren. Universität Heidelberg 1997.

Heidelberg – City map